

Title	Novel Approaches for the Synthesis of Graft and Alternating Copolymers through Simultaneous Copolymerization by Different Mechanisms
Author(s)	樋口, 元樹
Citation	大阪大学, 2020, 博士論文
Version Type	VoR
URL	https://doi.org/10.18910/76402
rights	
Note	

Osaka University Knowledge Archive : OUKA

<https://ir.library.osaka-u.ac.jp/>

Osaka University

**Novel Approaches for the Synthesis of Graft and Alternating
Copolymers through Simultaneous Copolymerization
by Different Mechanisms**

A Doctoral Thesis
by
Motoki Higuchi

Submitted to
the Graduate School of Science,
Osaka University

February 2020

Acknowledgments

This thesis research was performed at the Department of Macromolecular Science, Graduate School of Science, Osaka University under the direction of Professor Sadahito Aoshima from 2014 to 2020.

First of all, the author would like to express his deepest and sincere gratitude to Professor Sadahito Aoshima for his numerous advices, enthusiastic discussion and for always being supportive throughout the author's laboratory life. The author has been impressed by his insightful suggestions, a great idea, and enthusiasm on science. The author is also deeply grateful to Professor Shokyoku Kanaoka for his sincere guidance and warm encouragement, and Associate Professor Arihiro Kanazawa for his stimulating discussion, deep knowledge, and enormous help.

The author would like to express his deep appreciation to Professor Akihito Hashizume and Professor Hiroyasu Yamaguchi for kindly reviewing this thesis and fruitful comments.

The author also thanks Dr. Yasuto Todokoro and Dr. Naoya Inazumi for NMR spectroscopic measurements, and Dr. Akihito Ito for mass spectroscopy.

The author is deeply indebted to Professor Yoshio Okamoto (Nagoya University; Harbin Engineering University), Professor Mitsuo Sawamoto (Kyoto University; Chubu University), Professor Yoshitsugu Hirokawa (The University of Shiga Prefecture), Professor Masao Tanihara (Nara Institute of Science and Technology), Professor Eiji Yashima (Nagoya University), Professor Masami Kamigaito (Nagoya University), Professor Kotaro Satoh (Tokyo Institute of Technology), Professor Makoto Ouchi (Kyoto University), and all "ORION" members for active discussions and good interactions.

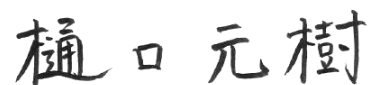
The author thanks to all the members who supported and shared productive time with him in the Aoshima group. Specifically, the author is grateful to Dr. Kira B. Landenberger (Lecturer, Kyoto University), Dr. Hayato Yoshimitsu, Dr. Mayuka Yamada, Dr. Koichiro Takii, Dr. Ryohei Saitoh, Dr. Tomoya Yoshizaki, Dr. Norifumi Yokoyama, Dr. Suzuka Matsumoto, Dr. Sensho Kigoshi, Dr. Daichi Yokota, Mr. Hiroshi Oda, Ms. Chihiro Suemitsu, Ms. Natsuki Okada, Ms. Marie Kawamura, Mr. Tatsuya Suzuki, Mr. Yukinori Togo, Mr. Yoshiki Tode, Ms. Mai Hijikata, Mr. Takashi Sasahara, Ms. Tomoka Shirouchi, Ms. Yukiko Seki, Mr. Kota Fujiwara, Ms. Fumina Koga, Mr. Tadashi Naito, Mr. Tsuyoshi Nishikawa, Mr. Yoshiki Tatsuno, Mr. Shintaro Araoka, Ms. Haruka Nishimura, Mr. Daisuke Hotta, Mr. Kazutoshi Mishima, Mr. Hironobu Watanabe, Mr. Ryusei Kato, Mr. Keisuke Hayashi, Mr. Kazuya Maruyama, Ms. Maki Mimura, Ms. Haruna Kagasaki, Mr. Tomohito Asakawa, Ms. Rui Haraguchi, Ms. Kano Hyoi, Mr. Takuya Yamamoto, Ms. Tomo

Yoshiki, Mr. Masamichi Inoue, Ms. Yui Kawamura, Ms. Sae Taniguchi, Mr. Shunya Hasegawa, Mr. Yuya Asada, Mr. Yuya Kinoshita, Mr. Jun-ichi Azuma, Mr. Mikiya Umemoto, Mr. Tomoki Nara, and Mr. Ryosuke Hada for sharing his pleasant student life. The author is also obliged to Ms. Misato Nishiuchi, Ms. Mariko Okamoto, and Ms. Naomi Imai for their thoughtful assistance in laboratory life.

The author is grateful to the Japan Society for the Promotion of Sciences (JSPS) for JSPS Research Fellowship for Young Scientists (DC2) and a Grant-in-Aid for JSPS Fellowship (18J11009) from April 2018 to March 2020.

Finally, the author would like to express a great appreciation to his father Yutaka Higuchi, his mother Misako Higuchi, his sisters Hikari Higuchi and Chiharu Higuchi, his fiancée Yurika Miyamae, and all his relatives for their constant care and considerable encouragement.

February 2020



Motoki Higuchi

Department of Macromolecular Science
Graduate School of Science
Osaka University

Contents

Chapter 1	General Introduction	1
Part I Synthesis of Graft Copolymers via Concurrent Cationic Vinyl-Addition Polymerization, Coordination Ring-Opening Polymerization, and AGE Reactions		
Chapter 2	Concurrent Cationic Vinyl-Addition and Coordination Ring-Opening Copolymerization via Orthogonal Propagation and Transient Merging at the Propagating Chain End	15
Chapter 3	Design of Graft Architecture via Simultaneous Kinetic Control of Cationic Vinyl-Addition Polymerization of Vinyl Ethers, Coordination Ring-Opening Polymerization of Cyclic Esters, and Merging at the Propagating Chain End . . .	29
Part II Synthesis of Alternating Copolymers via Concurrent Unzipping and Scrambling Reactions in Cationic Ring-Opening Copolymerization		
Chapter 4	Tandem Unzipping and Scrambling Reactions for the Synthesis of Alternating Copolymers by the Cationic Ring-Opening Copolymerization of a Cyclic Acetal and a Cyclic Ester	49
Chapter 5	Equilibrium Monomer Concentration-Dependent Sequence Control of Copolymer Chains via Temperature Changes in Cationic Ring-Opening Copolymerization of Cyclic Acetals and Cyclic Esters	67
Chapter 6	Summary	81
List of Publications	83

General Introduction

1. Background

1.1 Design of Copolymer Structures –Unlimited Potential/Limitation in Synthesis

Copolymers have unlimited potential to exhibit advantageous properties and functions that homopolymers and homopolymer blends do not possess. The distinct features of copolymers originate from their specific high-order structures, which are constructed based on the information contained in their primary structures. For example, proteins self-assemble to specific three-dimensional folded structures in vivo based on perfectly controlled monomer sequences from twenty types of amino acids, exhibiting sophisticated functions. Among synthetic polymers, amphiphilic block copolymers can form polymer micelles in solution¹ or microphase separations in the bulk,^{2,3} a characteristic utilized by many emerging technologies, including microelectronics and biomedicines. Accordingly, the expansion of accessible synthetic copolymers with highly controlled structures is expected to provide a new class of materials with sophisticated functions comparable to the functions of biopolymers.

Thanks to the development of living/controlled polymerization techniques, the control of molecular weight (MW), molecular weight distribution (MWD), and the end-group structures of polymers has become feasible to a large extent (Figure 1).⁴⁻²¹ In addition, by utilizing living polymerization techniques, various kinds of strategies for designing specific copolymer sequences and topologies have been proposed; however, the synthesis of these special structures still faces many challenges in terms of the preciseness, versatility, and facility of synthesis. The precise control of the copolymer sequence and topology is of great importance because those factors have large impacts on the self-assembly behavior and the resulting properties. Further improvement of polymer synthesis techniques is highly demanded.

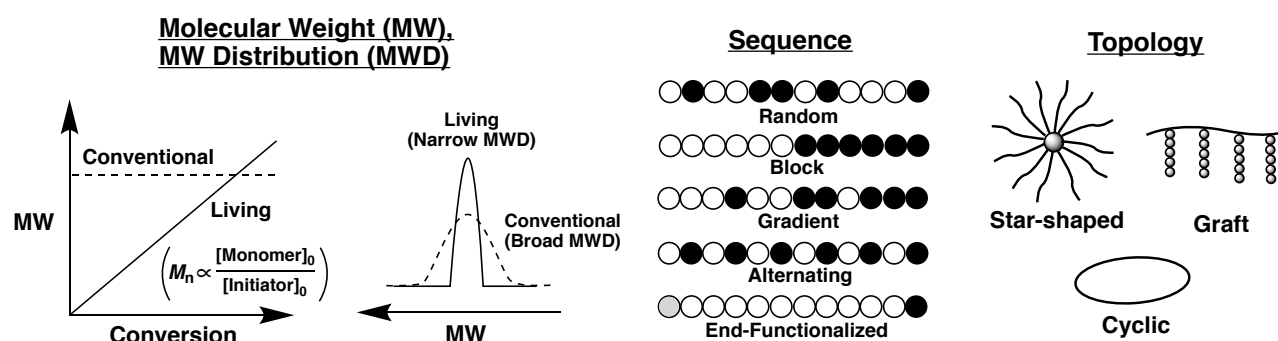


Figure 1. Polymers obtainable via the living/controlled polymerization.

1.1-1 Sequence control

Various approaches have been explored for the synthesis of sequence-regulated polymers, which are mainly categorized into the following three groups (Figure 2A–C).²² (A) Step-by-step monomer addition to the chain end (iterative method) is the most reliable strategy.^{23–25} In this method, a copolymer with desired sequences can be obtained, as exemplified by the Merrifield peptide synthesis,²⁵ although considerable amounts of time and effort are required for the synthesis of polymers with long chains. (B) Polymerization of a monomer that includes a specific sequence of multiple monomer units is also a promising method, whereas only a specific sequence can be obtained from a designed monomer, the synthesis of which is generally cumbersome.^{26–31} For example, a series of sequence-incorporated monomers, which are synthesized via iterative single vinyl monomer addition, are polymerized via step-growth radical polymerization to yield several patterns of sequence-regulated copolymers, such as ABC-, ABCD-, and ABBAC-type sequences.^{29–31} (C) Polymerization of monomers with specific reactivities is the most practical approach.^{32–36} However, available monomer combinations and achievable sequences are very limited because extremely high selectivity is required in propagation reactions. As demonstrated above, each method has inherent advantages and disadvantages, and accessible sequence patterns from certain monomer pairs are actually very limited. It is imperative to develop a new methodology for the synthesis of copolymers with a much wider variety of well-defined sequences.

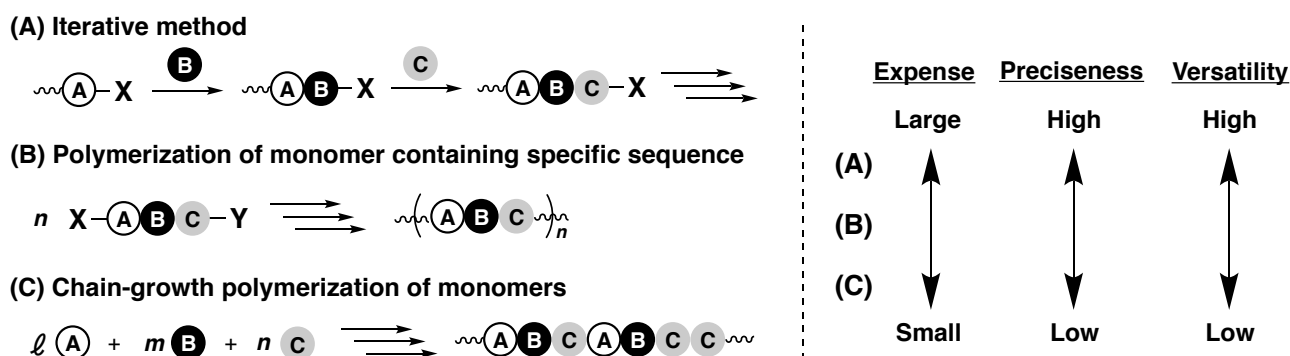


Figure 2. Various approaches for the synthesis of sequence-controlled copolymers and the trade-off relationships between the expense, preciseness, and versatility.

1.1-2 Topology control of graft copolymer

The topology of polymers, such as linear, cyclic, star-shaped, graft, hyperbranched, and more complex structures, significantly affects their solubility, crystallinity, and mechanical and viscoelastic properties.^{37–39} Moreover, polymer topology is responsible for the formation of various kinds of complex high-order structures and nano-objects through specific self-assembly behavior.⁴⁰ Among polymers with various topologies, graft copolymers, which consist of multiple branched polymer chains attached to a linear backbone, have been extensively studied as a model compound of branched structures, which has revealed various distinct properties and functions.^{41–44} For example, in many cases, graft copolymers can form micelles with a smaller aggregation number than that of linear block copolymers.^{45,46} In addition, the characteristic constraint structures of graft copolymers are often efficient for changing surface properties, which is exploited in many commercial

applications, such as surface modifiers,⁴⁷ compatibilizers,⁴⁸ and dispersion agents.⁴⁹ Because subtle differences in the primary structures, including the length, numbers, and interval of graft chains, are responsible for their properties and functions, strict control of those factors is crucial.

The synthesis of graft copolymers has been conducted via a variety of procedures.⁴⁴ However, as in the case of sequence-regulated copolymer synthesis, each method has inherent drawbacks in terms of the preciseness, versatility, and facility of the synthesis. Initial studies on the synthesis of graft copolymers mainly utilized chain transfer reactions of propagating species, although only ill-defined graft architectures could be obtained by this method. For example, cationic polymerization of styrene in the presence of poly(*p*-methoxystyrene) yielded a graft copolymer via the Friedel-Crafts reaction of the growing carbocation and the aromatic ring of poly(*p*-methoxystyrene).⁵⁰ Since the discovery of living/controlled polymerization, extensive investigations have been made to design well-defined graft copolymer architectures.^{51,52} These methods generally fall into the following three groups based on the order of the preparation of backbones and branches: (A) a backbone having multiple functional groups is first produced, from which a second polymerization is initiated to form graft chains (grafting-from), (B) a polymer having a polymerizable group at the chain end is prepared first, followed by the subsequent (co)polymerization of the macromonomer (grafting-through), and (C) separately produced backbones and graft chains are attached via postpolymerization reactions (grafting-onto). Although these methods are used, precise control of the positions and the number of branches is difficult to achieve. In contrast, Paraskeva and Hadjichristidis⁵³ performed the synthesis of an “exact graft copolymer”, in which the MW and MWD of the backbone and branched chains and the number and interval between the branched chains are strictly controlled by combining living anionic polymerization and repetitive polymer coupling reactions. This strategy requires increasing the number of reaction steps as the number of branches increases. Owing to the development of graft copolymer synthesis techniques, the influence of graft architectures on the property and morphology have been gradually understood.⁵⁴ For deeper understanding, however, we need more effective strategies that provide a wide variety of well-defined graft copolymers.

1.2 Polymerization mechanisms

Various types of repetitive reactions have been applied to construct polymers from monomers.⁵⁵ Depending on reaction types (mechanisms), polymerization characteristics vary in terms of kinetics, available monomer scope, effective reaction conditions, and possibility of structure control. The fundamentals of individual mechanisms have been largely established through numerous efforts by polymer scientists.

All polymerization reactions are classified as either chain-growth or step-growth polymerization. In step-growth polymerization, all the molecules present (monomer, oligomer, and polymer) can react with any other molecules. Thus, the MWD value is generally large (ultimately approaches M_w/M_n of 2.0 in theory), and high reaction conversion is necessary to achieve high MWs. Monomers with multiple functional groups, such as the combination of adipic acid and hexamethylene diamine (AA/BB-type) or the single use of 4-acetoxy benzoic acid (AB-type), are polymerized in step-growth mechanisms. By contrast, in chain-growth polymerization, propagation reactions occur only via the reaction of monomers and reactive growing ends, and a polymer chain continues to grow until the growing end is deactivated via chain-transfer and/or termination reactions. Thus, higher-MW products can be formed in the early stages of reactions. A special case of chain-growth polymerization in which irreversible chain transfer and termination reaction do not occur is

defined as living polymerization, as explained in the following section. Vinyl and cyclic monomers, such as propylene, styrene, epoxides, and cyclic esters, are polymerized in chain-growth mechanisms.

Even in chain-growth polymerization, vinyl-addition polymerization of vinyl monomers and ring-opening polymerization (ROP) of cyclic monomers are quite different in terms of reaction kinetics, reaction thermodynamics, the kinds of side reactions, and the structure of reactive species. In a propagation reaction of vinyl-addition polymerization, in general, a marked change in the Gibbs free energy (ΔG) is involved through the formation of two sigma bond by the breaking of a double bond. Thus, the reverse reaction of propagation (depropagation) is negligible in many cases. In sharp contrast, depropagation tends to occur in ROP because the major driving force of the propagation reaction is the release of ring-strain, which is generally not as large, particularly when relatively stable monomers with five- or six-membered rings are used.⁵⁶ Accordingly, quantitative monomer consumption is difficult to achieve, especially at high reaction temperatures. As another feature of ROP, reactions of a chain end with intra- and intermolecular polymer chains can occur, resulting in the formation of a macrocyclic polymer and the redistribution of polymer chains, respectively. This is because the chemical structure of a cyclic monomer is not distinguishable from that of the polymer chain.

When certain monomers are polymerized via a common mechanism, copolymerization can be achieved in one shot, often accompanying crossover reactions. By contrast, for the synthesis of a copolymer consisting of different types of monomers that are polymerized via different mechanisms, stepwise reactions are required. For instance, Register and coworkers⁵⁷ produced a block copolymer from different kinds of monomers by preparing a polystyrene with a formyl group at the chain end via living anionic polymerization, which was used as a macroterminator for ring-opening metathesis polymerization of norbornene. In such cases, only block-type copolymer structures can be obtained. These difficulties in synthesizing copolymers from different types of monomers significantly limit the accessible copolymer structures.

1.3 Tandem Reactions

A tandem reaction is an environmentally friendly and time-saving reaction process composed of two or more sequentially or simultaneously occurring reactions in the same batch. For a successful tandem reaction, the catalyst and/or an intermediate of a reaction must be prevented from interfering with the other reactions.⁵⁸ As another interesting point of tandem reactions, a reaction intermediate, generated by the first reaction, can be exploited for other reactions.⁵⁹ This process involving “nonorthogonal reactions” has great potential to produce a compound that has never been produced in conventional stepwise reactions.

Tandem reactions are also employed for polymerization reactions (Figure 3).^{60–67} Trollsas and coworkers⁶⁰ demonstrated that a block copolymer consisting of different types of monomers was obtained in one shot via the concurrent living coordination ROP of ϵ -caprolactone (CL) and nitroxide-mediated radical polymerization (NMP) of styrene by using a bifunctional initiator with initiating sites for both polymerizations (Figure 3A). More recently, nonorthogonal-type tandem polymerizations have attracted increasing attention because copolymers with multiblock or more complicated sequences can be obtained from different types of monomers [Figure 3B(*i*)]. For example, concurrent cationic vinyl-addition polymerization of vinyl ethers (VEs) and ROP of oxiranes proceeded via two-way crossover reactions, generating copolymers with a variety of sequences.⁶⁵ In this case, the copolymer sequence is determined based on the monomer reactivity ratios, as in the conventional copolymerization by the same mechanism. Nonorthogonal tandem copolymerization with different intermediates is also very interesting because the kinetics of each polymerization can be tuned

independently by changing the polymerization conditions, leading to versatile sequence patterns [Figure 3B(ii)]. Kamigaito and coworkers^{66,67} generated a series of copolymer sequences from a certain combination of VEs and acrylates or vinyl esters via concurrent cationic and radical copolymerization. This copolymerization was feasible by using common reversible addition-fragmentation chain transfer (RAFT) agents, such as dithioesters and trithiocarbonates, that generate both radical and cationic propagating species. Despite the potential of nonorthogonal tandem polymerizations that produce copolymers with conventionally inaccessible structures, reports on these types of polymerization are very limited, presumably because of the difficulty in designing such a system. However, these potentials encouraged the author to develop novel tandem polymerization systems.

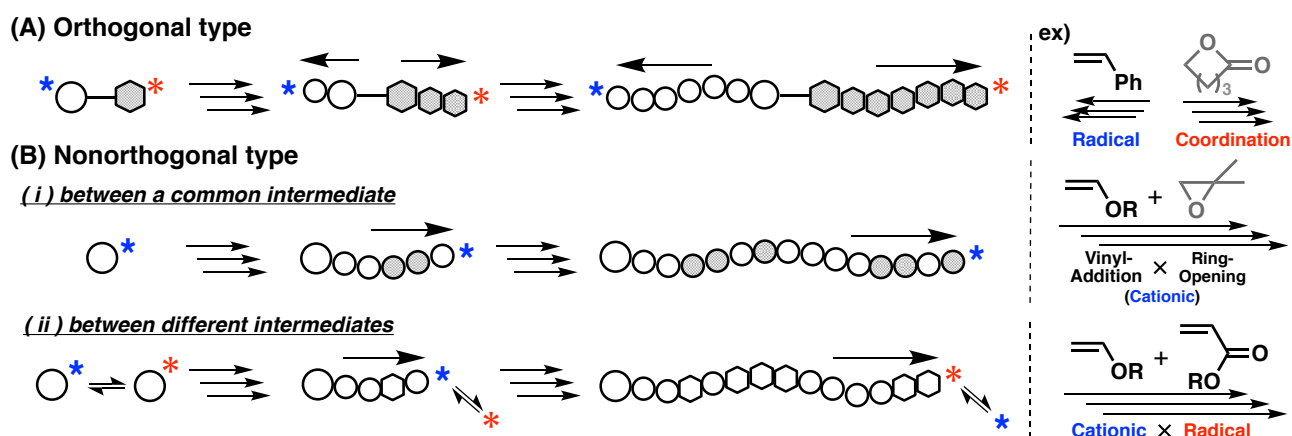


Figure 3. Tandem polymerization reactions between (A) two orthogonal polymerizations and (B) two nonorthogonal polymerizations with (i) a common intermediate and (ii) different intermediates.

1.4 Living Cationic Polymerization

Living polymerization is a specific case of chain-growth polymerization involving only initiation and propagation reactions during polymerization.⁴⁻²¹ Thus, living polymerization is effective for controlling the MW, MWD, comonomer composition, and chain-end structures, which enables synthesis of specially designed polymers, such as block, graft, and star-shaped polymers, in a controlled manner (Figure 1). Living polymerization was first reported by Szwarc in 1956 for the anionic polymerization of styrene.⁶⁸ After this breakthrough, living polymerization was continuously achieved by other mechanisms, such as cationic ROP,⁶⁹ coordination polymerization,⁷⁰ and ring-opening metathesis polymerization,^{71,72} which proceed via relatively stable active species.

Living polymerization with relatively unstable intermediates, such as carbocations and radicals, was allowed by the introduction of dormant species into a growing chain end. The first living cationic polymerization was discovered in 1984 for the polymerization of isobutyl VE with the HI/I₂ initiating system.⁷³ A fast equilibrium between the dormant and active species was also indispensable for obtaining polymers with a narrow MWD. Following these principles, various kinds of living radical and cationic polymerization systems have been developed, all of which are categorized into the following three groups from a kinetics viewpoint: (1) dissociation-combination mechanism, such as NMP and cationic polymerization with HI/*n*Bu₄NI^{74,75} and CF₃SO₃H/thioether⁷⁶ initiating systems, (2) atom transfer mechanism, such as atom transfer

radical polymerization (ATRP)⁹ and cationic polymerization catalyzed by metal halides,⁸ and (3) degenerative chain transfer mechanism, such as RAFT polymerization.^{12,13} Among these mechanisms, the atom transfer mechanism, which utilizes atom transfer reactions between a growing end and a metal catalyst, is highly attractive for developing unprecedented smart polymerization systems, considering the variety of specific reactions controlled by metal catalysts.

Recently, Aoshima and coworkers⁷⁷⁻⁸² developed living cationic polymerization of VEs and styrene derivatives using a series of metal catalysts in conjunction with weak Lewis bases, such as esters and ethers. In this “base-assisting” system, Lewis bases are responsible for stabilization of the growing carbocation and adjustment of the Lewis acidity via interaction with the metal catalysts (Figure 4). Systematic studies have revealed that the extent of the latter contribution differs significantly depending on the metal catalysts used. For example, TiCl₄ strongly interacted with the carbonyl oxygen of ethyl acetate due to its “oxophilic” nature, resulting in much slower polymerization than that without additives, while the polymerization rate hardly changed when ZnCl₂ was used with or without ethyl acetate.⁸¹ The difference in the affinity of metal catalysts toward different anionic species, such as halogen anions and alkoxide groups, is also important. In this case, the resulting two or more kinds of dormant species need to be evenly activated to achieve a narrow MWD. For example, a specific kind of metal species, such as zirconium and titanium, abstract chloride and alkoxide anions evenly from the propagating end of poly(VE) with carbon-chlorine bonds and acetal moieties, respectively, which indicates that those catalysts have an appropriate balance between chlorophilicity and oxophilicity.⁸² These specific features of metal catalysts have a great potential to construct unconventional smart polymerization systems.

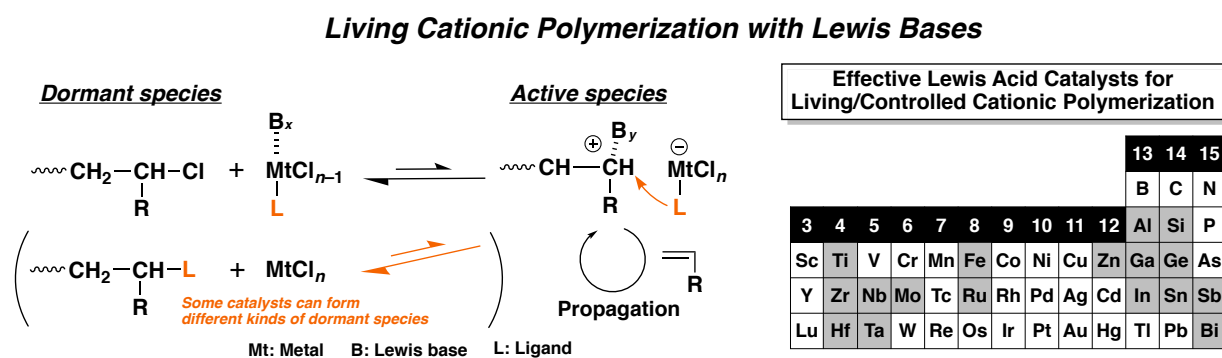


Figure 4. Living cationic polymerization of VEs with various initiating systems.

2. Objective and outline of this thesis

As demonstrated in the background section, conventional copolymer design methods utilizing living polymerization techniques have several kinds of intrinsic limits, whereas more flexible approaches will be feasible considering the reaction diversity of organic chemistry. The objective of this thesis is to develop novel strategies for constructing copolymers with versatile sequences and architectures via nonorthogonal tandem polymerizations (Figure 5). To this end, a key reaction that affords flexible molecular constructs is desired. The acetal exchange reaction is a suitable candidate for such a purpose because of the two kinds of reaction directions (for example, OR^2 or OR^3 in Figure 5) and the dynamic reaction nature, which will lead to many molecular construction patterns. First, the author focuses on acetals that are generated at the propagating end of poly(VE) as a dormant species. These acetals are formed by the reaction of an alkoxy ligand on a metal catalyst and a VE-derived carbocation. Thus, when the VE-derived alkoxy group of the acetal is abstracted by a metal catalyst, the resulting cationic species is composed of the ligand-derived alkoxy group. This process is referred to as alkoxy group exchange (AGE) reactions, which are the key for copolymerization via unprecedented mechanisms. Next, dynamic acetal exchange reactions in the main chain of a linear copolymer (scrambling) are utilized for the design of copolymer sequences. Although scrambling reactions generally induce statistical sequence distributions, a specific sequence can be achieved by combining with depolymerization of cyclic acetals.

Novel Approaches for the Synthesis of Copolymers with Versatile Architectures/Sequences

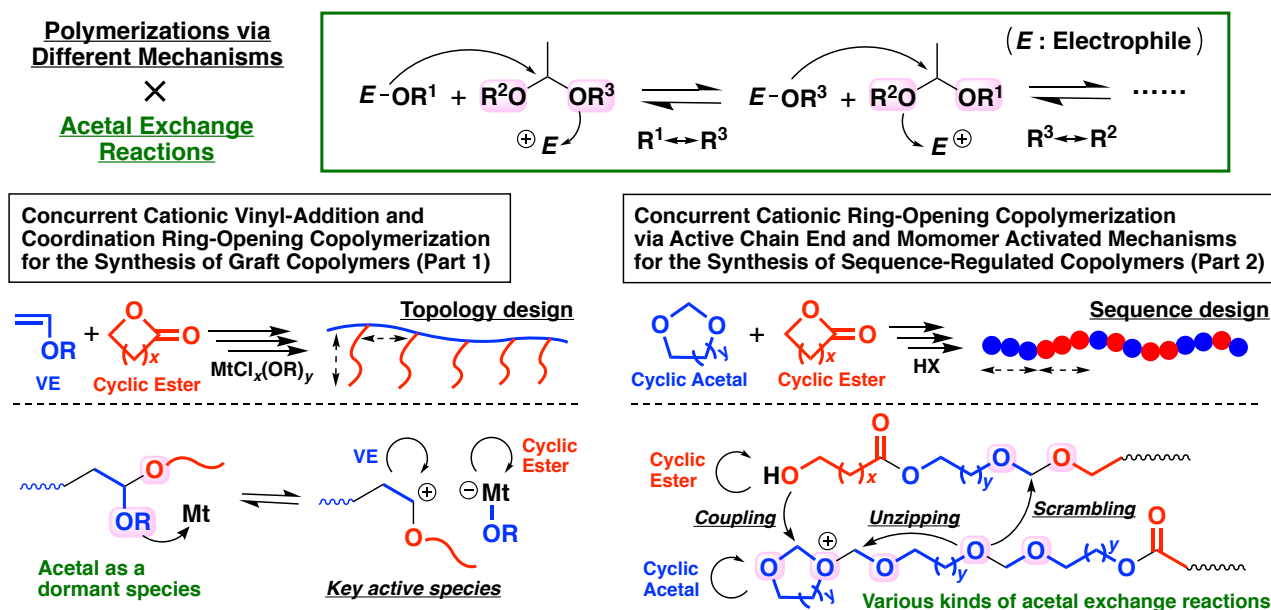


Figure 5. Objective and outline of this thesis.

This thesis consists of two parts: Part 1 (Chapters 2 and 3) describes a novel approach for the synthesis of graft copolymers by simultaneously occurring cationic vinyl-addition polymerization of VEs, coordination ring-opening polymerization of cyclic esters, and the AGE reactions. In Part 2 (Chapters 4 and 5), control of copolymer sequences is investigated by utilizing scrambling and unzipping reactions of acetal units in the main chain during cationic ring-opening copolymerization of cyclic acetals and cyclic esters.

In Chapter 2, concurrent cationic vinyl-addition polymerization of ethyl VE (EVE) and coordination ROP of CL are conducted using a mixture of HfCl_4 and $\text{Hf}(\text{O}i\text{Bu})_4$ as catalysts, yielding graft copolymers consisting of a poly(EVE) backbone and poly(CL) branched chains (Figure 6). A propagating poly(CL) chain is incorporated into a poly(EVE) propagating end through the AGE reactions. Thus, the poly(CL) chain becomes a branched chain by the subsequent addition of an EVE monomer. An appropriate molar ratio of HfCl_4 and $\text{Hf}(\text{O}i\text{Bu})_4$ was indispensable for the simultaneous consumption of both monomers at comparable rates.

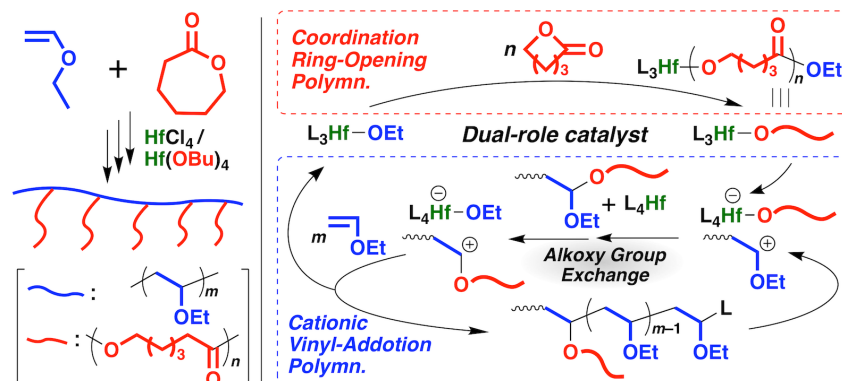


Figure 6. Graft copolymer synthesis via orthogonal propagation and transient merging at propagating ends in the concurrent cationic vinyl-addition and coordination ring-opening copolymerization.

Chapter 3 describes the creation of a guideline for the synthesis of graft copolymers with various architectures via the mechanism developed in Chapter 2. In this mechanism, the grafting density and the grafting length are determined by the relative rates of the propagation of VEs, propagation of cyclic esters, and the AGE reactions (Figure 7). The critical factors that affect the rate of the two different propagations and the AGE reactions are revealed through a systematic investigation of polymerization conditions. Based on these factors, a principle for the design of graft copolymers is established. Notably, a copolymer with very high grafting density is obtained when 2-methoxyethyl VE and CL are used as monomers and a mixture of TiCl_4 and $\text{Ti}(\text{O}i\text{Pr})_4$ is used as the catalyst due to the frequent occurrence of the AGE reactions. Moreover, the obtained graft copolymer is effective for the fine dispersion of TiO_2 in toluene.

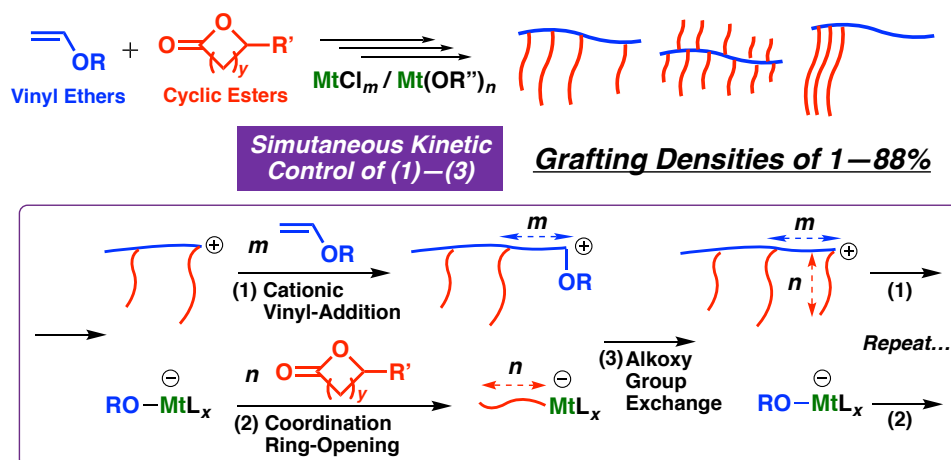


Figure 7. Design of graft architectures via simultaneous kinetic control of cationic vinyl-addition polymerization, coordination ring-opening polymerization, and the AGE reactions.

Chapter 4 addresses the cationic ring-opening copolymerization of 2-methyl-1,3-dioxepane (MDOP), which is formed via the isomerization of 4-hydroxybutyl VE (HBVE) in the initial stages of polymerization, and CL using EtSO_3H as a catalyst. MDOP is successfully copolymerized with CL even below the equilibrium monomer concentration of MDOP. Various kinds of copolymer sequences were obtained by tuning the initial monomer concentrations. Moreover, unprecedented sequence transformation from a copolymer with no CL homosequences to an alternating copolymer is achieved by removing the MDOP monomers from the system using a vacuum pump (Figure 8). Concurrently proceeding unzipping and scrambling of acetal moieties were the key for the unique sequence transformation.

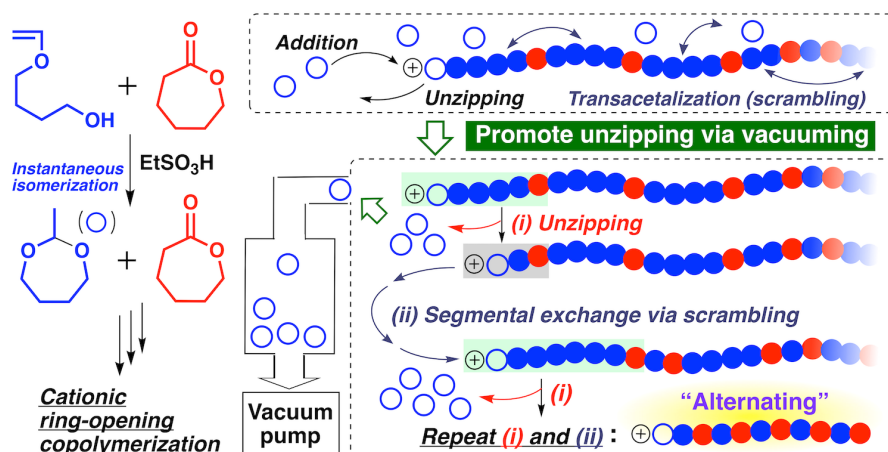


Figure 8. Sequence transformation from a copolymer with no CL homosequences to an “alternating” copolymer via concerted unzipping and scrambling reactions of acetal units.

In Chapter 5, the author attempts the sequence transformation developed in Chapter 4 by changing the reaction temperature without removing cyclic acetal monomers from the system, instead of using a vacuum pump (Figure 9). To achieve this goal, an additional requirement is imposed; i.e., frequent crossover reactions from cyclic ester to cyclic acetal are desired. Systematic investigations on the kinds of monomers and catalysts revealed that the combination of HBVE, δ -valerolactone, and EtSO_3H can satisfy the requirement. Using these monomers and catalysts, an alternating-like copolymer is generated via sequence transformation upon heating from 30 °C to 100 °C.

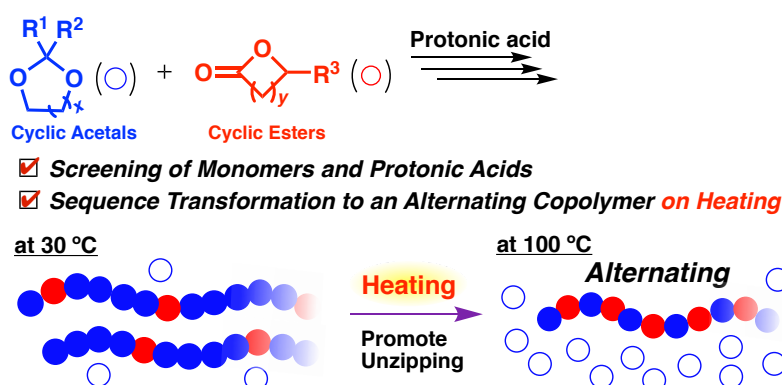


Figure 9. Screening of monomers and protonic acids in the cationic ring-opening copolymerization of cyclic acetals with cyclic esters and the sequence transformation to an alternating copolymer on heating.

References.

1. Riess, G. *Prog. Polym. Sci.* **2003**, *28*, 1107.
2. Leibler, L. *Macromolecules* **1980**, *13*, 1602.
3. Bates, F. S.; Fredrickson, G. H. *Phys. Today* **1999**, *52*, 32.
4. Hadjichristidis, N.; Pitsikalis, M.; Pispas, S.; Iatrou, *Chem. Rev.* **2001**, *101*, 3747.
5. Hirao, A.; Goseki, R.; Ishizone, T. *Macromolecules* **2014**, *47*, 1883.
6. Penczek, S.; Cypriak, M.; Duca, A.; Kubisa, P.; Slomkowski, S. *Prog. Polym. Sci.* **2007**, *32*, 30.
7. Otsu, T. *J. Polym. Sci., Part A: Polym. Chem.* **2000**, *38*, 2121.
8. Aoshima, S.; Kanaoka, S. *Chem. Rev.* **2009**, *109*, 5245.
9. Ouchi, M.; Terashima, T.; Sawamoto, M. *Chem. Rev.* **2009**, *109*, 4963.
10. Matyjaszewski, K. *Macromolecules* **2012**, *45*, 4015.
11. Hawker, C. J.; Bosman, A. W.; Harth, E. *Chem. Rev.* **2001**, *101*, 3661.
12. Moad, G.; Rizzardo, E.; Thang, S. H. *Polymer* **2008**, *49*, 1079.
13. Kamigaito, M.; Satoh, K.; Uchiyama, M. *J. Polym. Sci., Part A, Polym. Chem.* **57**, 243.
14. Yamago, S. *Chem. Rev.* **2009**, *109*, 5051.
15. Goto, A.; Hirai, N.; Wakada, T.; Nagasawa, K.; Tsujii, Y.; Fukuda, T. *Macromolecules* **2008**, *41*, 6261.
16. Bielawski, C. W.; Grubbs, R. H. *Prog. Polym. Sci.* **2007**, *32*, 1.
17. Webster, O. W. *J. Polym. Sci., Part A: Polym. Chem.* **2000**, *38*, 2855.
18. Webster, O. W. *Science*, **1991**, *251*, 887.
19. Yokozawa, T.; Yokoyama, A. *Chem. Rev.* **2009**, *109*, 5595.
20. Rosen, B. M.; Percec, V. *Chem. Rev.* **2009**, *109*, 5069.
21. Domski, G. J.; Rose, J. M.; Coates, G. W.; Bolig, A. D.; Brookhart, M. *Prog. Polym. Sci.* **2007**, *32*, 30.
22. Lutz, J.-F.; Ouchi, M.; Liu, D. R.; Sawamoto, M. *Science* **2013**, *341*, 1238149.
23. Solleder, S. C.; Schneider, R. V.; Lutz, J.-F. *Macromol. Chem. Phys.* **2015**, *216*, 1498.
24. Hill, S. A.; Gerke, C.; Hartmann, L. *Chem. Asian J.* **2018**, *13*, 3611.
25. Merrifield, R. B. *J. Am. Chem. Soc.* **1963**, *85*, 2149.
26. Cho, I.; Hwang, K. M. *J. Polym. Sci., Part A: Polym. Chem.* **1993**, *31*, 1079.
27. Zhang, J.; Matta, M. E.; Hillmyer, M. A. *ACS Macro Lett.* **2012**, *1*, 1383.
28. Espeel, P.; Carette, L. L.; Bury, K.; Capenberghs, M.; Martins, J. C.; Du Prez, F. E.; Madder, A. *Angew. Chem. Int. Ed.* **2013**, *52*, 13621.
29. Satoh, K.; Mizutani, M.; Kamigaito, M. *Chem. Commun.* **2007**, 1260.
30. Satoh, K.; Ozawa, S.; Mizutani, M.; Nagai, K.; Kamigaito, M. *Nat. Commun.* **2010**, *1*, 6.
31. Satoh, K.; Ishizuka, K.; Hamada, T.; Handa, M.; Abe, T.; Ozawa, S.; Miyajima, M.; Kamigaito, M. *Macromolecules*, **2019**, *52*, 3327.
32. Rzaev, Z. M. O. *Prog. Polym. Sci.* **2000**, *25*, 163.
33. Satoh, K.; Matsuda, M.; Nagai, K.; Kamigaito, M. *J. Am. Chem. Soc.* **2010**, *132*, 10003.
34. Klumperman, B. *Polym. Chem.* **2010**, *1*, 558.
35. Lutz, J.-F.; Schmidt, B. V. K. J.; Pfeifer, S. *Macromol. Rapid Commun.* **2011**, *32*, 127.
36. Kanazawa, A.; Aoshima, S.; *ACS Macro Lett.* **2015**, *4*, 783.

37. Tezuka, Y.; Hideaki, O. *Prog. Polym. Sci.* **2002**, *27*, 1069.
38. Müller, A. H. E.; Wooley, K. L. In *Polymer Science: A Comprehensive Reference*; Matyjaszewski, K., Möller, M. Eds.; Elsevier B.V.: Amsterdam, **2012**; Vol. 6.01.
39. Polymeropoulos, G.; Zapsas, G.; Ntetsikas, K.; Bilalis, P.; Gnanou, Y.; Hadjichristidis, N. *Macromolecules* **2017**, *50*, 1253.
40. Cauët, S. I.; Lee, N. S.; Lin, K. L.; Wooley, K. L. In *Polymer Science: A Comprehensive Reference*; Matyjaszewski, K., Möller, M. Eds.; Elsevier B.V.: Amsterdam, **2012**; Vol. 6.20.
41. Feng, C.; Li, Y.; Yang, D.; Hu, J.; Zhang, Z.; Huang, X. *Chem. Soc. Rev.* **2011**, *40*, 1282.
42. Hadjichristidis, M.; Pitsikalis, M.; Iatrou, H.; Driva, P.; Chatzichristi, M.; Sakellariou, G. In *Encyclopedia of Polymer Science and Technology*; Seidel, A. Ed.; John Wiley; New York, **2010**.
43. Uhrig, D.; Mays, J. *Polym. Chem.* **2011**, *2*, 69.
44. Lutz, P. L.; Peruch, F. In *Polymer Science: A Comprehensive Reference*; Matyjaszewski, K., Möller, M. Eds.; Elsevier B.V.: Amsterdam, **2012**; Vol. 6.14
45. Pispas, S.; Hadjichristidis, N.; Mays, J. W. *Macromolecules* **1996**, *29*, 7387.
46. Pitsikalis, M.; Woodward, J.; Mays, J. W.; Hadjichristidis, N. *Macromolecules* **1997**, *30*, 5384.
47. Koning, C.; Van Duin, M.; Pagnouille, C.; Jerome, R. *Prog. Polym. Sci.* **1998**, *23*, 707.
48. Klimkevicius, V.; Graule, T.; Makuska, R. *Langmuir* **2015**, *31*, 2074.
49. Ramakrishna, S. N.; Morgese, G.; Zenobi-Wong, M.; Benetti, E. M. *Macromolecules* **2019**, *52*, 1632.
50. Haas, H. C.; Kamath, P. M.; Schuler, N. W. *J. Polym. Sci.* **1957**, *24*, 85.
51. Börner, H. G.; Matyjaszewski, K. *Macromol. Symp.* **2002**, *177*, 1.
52. Hadjichristidis, N.; Iatrou, H.; Pitsikalis, M.; Mays, J. *Prog. Polym. Sci.* **2006**, *31*, 1068.
53. Paraskeva, S.; Hadjichristidis, N.; *J. Polym. Sci Part A: Polym. Chem.* **2000**, *38*, 931.
54. Takano, A.; Kondo, K.; Ueno, M.; Ito, K.; Kawahara, S.; Isono, Y.; Suzuki, J.; Matsushita, Y. *Polym. J.* **2007**, *33*, 732.
55. Hillmyer, M. A. In *Polymer Science: A Comprehensive Reference*; Matyjaszewski, K., Möller, M. Eds.; Elsevier B.V.: Amsterdam, **2012**; Vol. 1.03.
56. Penczek, S.; Kaluzynski, K. In *Polymer Science: A Comprehensive Reference*; Matyjaszewski, K., Möller, M. Eds.; Elsevier B.V.: Amsterdam, **2012**; Vol. 4.02
57. Notestein, J. M.; Lee, L.-B. W.; Register, R. A. *Macromolecules* **2002**, *35*, 1985.
58. Demmark, S. E.; Thorarensen, A. *Chem Rev.* **1996**, *96*, 137.
59. Wasilke, J.; Obrey, S. J.; Baker, R. T.; Bazan, G. C. *Chem. Rev.* **2005**, *105*, 1001.
60. Mecerreyes, D.; Moineau, G.; Dubois, P.; Jérôme, R.; Hedrick, L. J.; Hawker, J. C.; Malmström, E. E.; Trollsas, M. *Angew. Chem. Int. Ed.* **1998**, *37*, 1275.
61. Bielawski, C. W.; Louie, J.; Grubbs, R. H. *J. Am. Chem. Soc.* **2000**, *122*, 12872.
62. de Freitas, A. G.; Trindade, S. G.; Murano, P. I.; Schmidt, V.; Satti, A. J.; Villar, M. A.; Ciolino, A. E.; Giacomelli, C. *Macromol. Chem. Phys.* **2013**, *214*, 2336.
63. Simionescu, C. I.; Grigoras, M.; Bicu, E.; Onofrei, G. *Polym. Bull.* **1985**, *14*, 79.
64. Yang, H.; Xu, J.; Pispas, S.; Zhang, G. *Macromolecules* **2012**, *45*, 3312.
65. Kanazawa, A.; Kanaoka, S.; Aoshima, S. *J. Am. Chem. Soc.* **2013**, *135*, 9330.

66. Aoshima, H.; Uchiyama, M.; Satoh, K.; Kamigaito, M. *Angew. Chem. Int. Ed.* **2014**, *53*, 10932.
67. Satoh, K.; Hashimoto, H.; Kumagai, S.; Aoshima, H.; Uchiyama, M.; Ishibashi, R.; Fujiki, Y.; Kamigaito, M. *Polym. Chem.* **2017**, *8*, 5002.
68. Szwarc, M. *Nature* **1956**, *178*, 1168.
69. Dreyfuss, M. P.; Dreyfuss, P. *Polymer* **1965**, *6*, 93.
70. Doi, Y.; Ueki, S.; Keii, T. *Macromolecules* **1979**, *12*, 814.
71. Gilliom, L. R.; Grubbs, R. H. *J. Am. Chem. Soc.* **1986**, *108*, 733.
72. Wallace, K. C.; Schrock, R. R. *Macromolecules* **1987**, *20*, 448.
73. Miyamoto, M.; Sawamoto, M.; Higashimura, T. *Macromolecules* **1984**, *17*, 265.
74. Nuyken, O.; Kröner, H.; *Makromol. Chem.* **1990**, *191*, 1.
75. Cramail, H.; Deffieux, A.; Nuyken, O. *Makromol. Chem., Rapid Commun.* **1993**, *14*, 17.
76. Cho, C. G.; Feit, B. A.; Webster, O. W. *Macromolecules* **1990**, *23*, 1918.
77. Aoshima, S.; Higashimura, T. *Polym. Bull.* **1986**, *15*, 417.
78. Kanazawa, A.; Kanaoka, S.; Aoshima, S. *Macromolecules* **2009**, *4*, 3965.
79. Kanazawa, A.; Shibutani, S.; Yoshinari, N.; Konno, T.; Kanaoka, S.; Aoshima, S. *Macromolecules* **2012**, *43*, 468.
80. Saitoh, R.; Kanazawa, A.; Kanaoka, S.; Aoshima, S. *Polym. J.* **2016**, *48*, 933.
81. Kanazawa, A.; Kanaoka, S.; Aoshima, S. *Macromolecules* **2010**, *43*, 2739.
82. Kanazawa, A.; Kanaoka, S.; Aoshima, S. *J. Polym. Sci., Part A: Polym. Chem.* **2010**, *48*, 2509.

Part I

Synthesis of Graft Copolymers via Concurrent Cationic Vinyl Addition Polymerization, Coordination Ring-Opening Polymerization, and AGE Reactions

Chapter 2

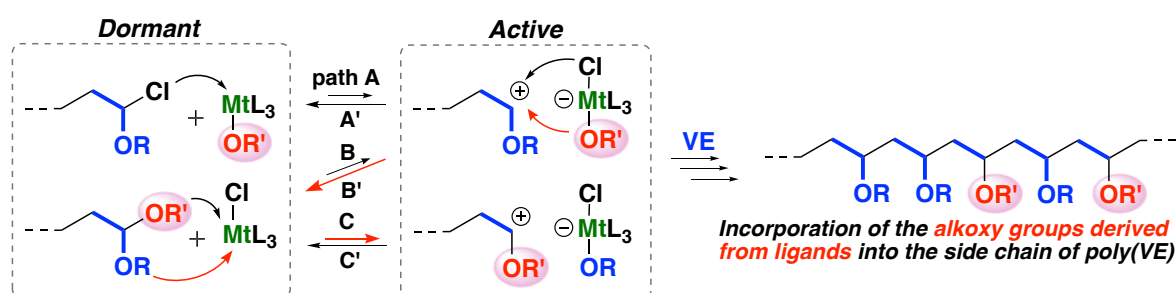
Concurrent Cationic Vinyl-Addition and Coordination Ring-Opening Copolymerization via Orthogonal Propagation and Transient Merging at the Propagating Chain End

Introduction

Simultaneous copolymerization via different mechanisms or intermediates has great potential to produce copolymers with novel properties in one step from conventionally incompatible monomers. To accomplish these types of reactions,¹⁻⁶ each polymerization must proceed without significantly interfering with the other reactions. For example, reversible addition-fragmentation chain transfer polymerization of styrene and ring-opening polymerization (ROP) of ϵ -caprolactone (CL) simultaneously proceeded to yield a block copolymer using a bifunctional initiator that generates propagating species for the two orthogonal polymerization reactions.¹ Concurrent polymerization that proceeds via common propagating ends or dormant species is also attractive because copolymers with diverse structures that cannot be synthesized via completely orthogonal reactions are produced from typically incompatible monomers. These copolymerization reactions that proceed via different mechanisms generally require an astute strategy to generate efficient crossover propagation reactions.^{7,8}

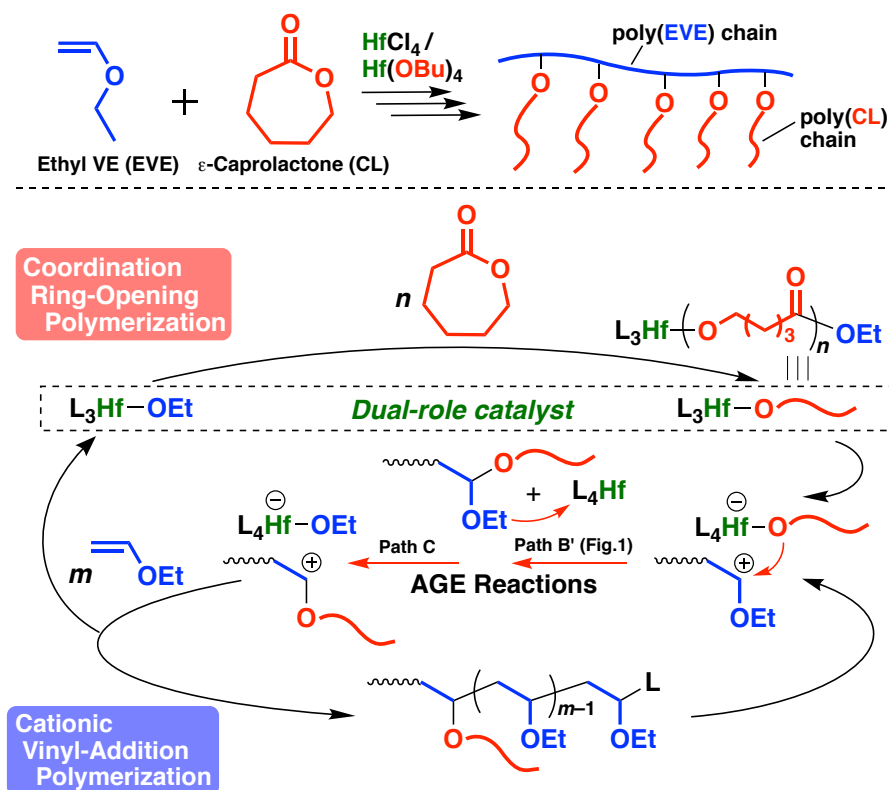
A reversible equilibrium between the dormant and active species plays a central role in most living chain-growth polymerization reactions.^{9,10} In living cationic polymerization of vinyl monomers, the concentration of the propagating carbocationic species is kept extremely low via reversible deactivation with anionic species such as halogen anions.¹⁰ Recently, Aoshima and coworkers¹¹ reported that in the systematic study on the cationic polymerization of vinyl ether (VE) using alcohols as a cationogen, the alcohol-derived alkoxy group was incorporated into the side chains of the resulting poly(VE)s via alkoxy group exchange (AGE) reactions in the dormant-active equilibrium (Scheme 1). In this system, the metal chloroalkoxide catalysts, generated in situ by the reaction of alcohols and metal chlorides, provide the active species with the chloride anion (path A' in Scheme 1) or the alkoxide anion (path B'), producing two types of dormant species. The acetal end generated via path B' contains two alkoxy groups; hence, the alcohol-derived alkoxy group is incorporated into the side chain of the poly(VE)s through the abstraction of the VE-derived alkoxy group (path C) and the subsequent propagation reactions. Metal catalysts with an optimum balance between chlorophilicity and oxophilicity were indispensable for enabling the unique mechanisms.

Scheme 1. Propagation reaction of VE using $MtCl_x(OR')_y$ catalysts via AGE mechanisms (L: chloride or alkoxide group)



In this study, the author seeks to develop a new type of concurrent copolymerization reaction consisting of the simultaneous cationic vinyl-addition polymerization of VE and the coordination ROP of cyclic esters. Because the ROP of cyclic esters using metal alkoxide catalysts proceeds via the generation of the growing alkoxide ends attached to the central metal,¹² a metal chloroalkoxide that exhibits catalytic activity for both cationic vinyl-addition polymerization and ROP enables copolymerization via unique pathways (Scheme 2). Specifically, given that both propagation reactions proceed orthogonally to each other under the same conditions, exchange reactions between the alkoxy group of a polyester chain end and the alkoxy group derived from a VE side chain will occur occasionally at the acetal moiety of the propagating ends via the AGE mechanism (paths B' and C). Repetitive propagation and AGE reactions are expected to generate a graft copolymer via the incorporation of several polyester chains into the side chains of the backbone poly(VE) chain.

Scheme 2. Copolymerization of EVE and CL using $\text{HfCl}_4/\text{Hf}(\text{O}i\text{Bu})_4$ catalysts via AGE mechanisms (L: chloride or alkoxide group)



Experimental Section

Materials.

Isopropyl vinyl ether (IPVE; Wako; 97.0+%) and ethyl vinyl ether (EVE; TCI; >98.0%) were washed with 10% aqueous sodium hydroxide solution and then water, and then distilled twice over calcium hydride. Ethyl acetate (Wako; >99.5%) was distilled twice over calcium hydride. ϵ -Caprolactone (CL; TCI; >99.0%) was distilled twice over calcium hydride under reduced pressure. Dichloromethane (Wako; 99.0%), toluene (Wako; 99.5%), and hexane (Wako; 96.0%) were dried by passage through solvent purification columns (Glass Contour). Commercially available HfCl_4 (Aldrich; 99.9%) was used without further purification. Commercially available $\text{Hf}(\text{O}i\text{Bu})_4$ (Aldrich; 99%) was used without further purification after preparing its stock solutions in dichloromethane or toluene. All chemicals except for dichloromethane, toluene, and HfCl_4 were stored in brown ampules under dry nitrogen.

Polymerization Procedure.

The following is a typical polymerization procedure. A glass tube equipped with a three-way stopcock was dried using a heat gun (Ishizaki; PJ-206A; the blow temperature ~ 450 °C) under dry nitrogen. HfCl_4 was added into the tube in a N_2 -filled glove box (DBO-1B; MIWA MFG Co., Ltd.). To this tube, a $\text{Hf}(\text{O}i\text{Bu})_4$ solution in dichloromethane was added using a dry syringe. The mixture of HfCl_4 and $\text{Hf}(\text{O}i\text{Bu})_4$ in dichloromethane was stirred at 30 °C until it turned into a transparent solution (~ 30 min). Dichloromethane and hexane were added successively into the tube using dry syringes. The polymerization was started by the successive addition of EVE and CL at 30 °C. After a predetermined time, the reaction was terminated with methanol containing a small amount of an aqueous ammonia solution. The quenched mixture was washed with water. The volatiles were then removed under reduced pressure to yield a colorless polymer. The monomer conversion was determined by gas chromatography (column packing material: PEG-20M-Uniport B; GL Sciences Inc.) using hexane as an internal standard.

Alkali Hydrolysis.

The alkali hydrolysis of the polymers was conducted with 2.0 M NaOH aq in 1,2-dimethoxyethane at 30 °C for 23 h (sample: ~ 1 wt%). The quenched mixture was diluted with dichloromethane and then washed with water. The volatiles were removed under reduced pressure.

Acid Hydrolysis.

The acid hydrolysis of the polymer was conducted with 1.0 M HCl aq in 1,2-dimethoxyethane at room temperature for 3 h (sample: ~ 1 wt%). The quenched mixture was diluted with dichloromethane and then washed with water. The volatiles were removed under reduced pressure.

Characterization.

The MWD of the polymers was measured by gel permeation chromatography (GPC) in chloroform at 40 °C with polystyrene gel columns [TSKgel GMH_{HR}-M $\times 2$ (exclusion limit molecular weight = 4×10^6 ; bead size = 5 μm ; column size = 7.8 mm I.D. \times 300 mm); flow rate = 1.0 mL/min] connected to a Tosoh DP-8020 pump, a CO-8020 column oven, a UV-8020 ultraviolet detector, and an RI-8020 refractive-index detector.

The number-average molecular weight (M_n) and polydispersity ratio [weight-average molecular weight/number-average molecular weight (M_w/M_n)] were calculated from the chromatographs with respect to 16 polystyrene standards (Tosoh; $M_n = 5.0 \times 10^2$ — 1.09×10^6 , $M_w/M_n \leq 1.2$). The absolute weight-average molecular weight and the exponent a of the Mark–Houwink–Sakurada equation were determined using GPC system comprising a pump (Viscotek VE 1122), two polystyrene gel columns [TSKgel GMH_{HR}-M \times 2, flow rate = 0.7 mL min^{-1}], and a Viscotek TDA 305 triple detector [refractive index, laser light scattering ($\lambda = 670 \text{ nm}$, 90° and 7° ; RALS and LALS), and differential pressure viscometer]. The GPC equipment was calibrated using a standard polystyrene sample with a known dn/dc value. The dn/dc value of the sample was determined via the analysis of the RI signal (the dn/dc value of the graft copolymer composed of EVE and CL was 0.064 in THF). The data were analyzed using an OmniSEC software (Viscotek). NMR spectra were recorded using a JEOL JNM-ECA 500 spectrometer (500.16 MHz for ^1H). MALDI-TOF-MS spectra were recorded using a SHIMADZU/KRATOS AXIMA-CFR spectrometer (linear mode; voltage: 20 kV; pressure: $<1.9 \times 10^{-3} \text{ Pa}$) with dithranol as the matrix and sodium trifluoroacetate as the ion source. A solution (2–3 μL) containing a polymer, the matrix, and the ion source (polymer/matrix/ion source = 1 mg/8 mg/1 mg in 1 mL of THF) was cast onto a stainless steel sample plate (Shimadzu Biotech, DE1580TA) and loaded into the spectrometer. ESI-MS spectra were recorded using an LTQ Orbitrap XL Spectrometer (Thermo Scientific). Polymer solutions in dichloromethane/methanol (1/1 v/v) were used for the analysis.

Results and Discussion

The author designed an initiating system using a mixture of HfCl_4 and $\text{Hf}(\text{OBU})_4$ as catalysts for the copolymerization of ethyl VE (EVE) and CL. Hafnium compounds were chosen because hafnium chloroalkoxides are effective for controlled cationic polymerization via the AGE reactions due to an appropriate balance between oxophilicity and chlorophilicity¹¹ and because hafnium catalysts with alkoxy ligands catalyze the living coordination ROP of CL.¹³ Most importantly, an appropriate balance of the chloride and alkoxide contents was found to be essential for the simultaneous consumption of both monomers.

First, reactions using either HfCl_4 or $\text{Hf}(\text{OBU})_4$ in dichloromethane at 30°C resulted in homopolymerization of either monomer (entries 3 and 4 in Table 1). Only EVE was consumed when HfCl_4 was used, while only CL was consumed using $\text{Hf}(\text{OBU})_4$. The reaction using a mixture of these catalysts, however, allowed for the consumption of both monomers. In particular, both monomers were consumed at similar rates with an appropriate ratio of both catalysts (entries 1 and 2). The product polymer had a unimodal molecular weight (MW) distribution (Figure 1A). Moreover, the peak shifted to the high molecular weight region as the total monomer conversion increased, indicating the generation of long-lived species. Hafnium species $\text{HfCl}_x(\text{OR})_{4-x}$, generated in situ from HfCl_4 and $\text{Hf}(\text{OBU})_4$ in a manner similar to that of the Ti and Zr counterparts,¹⁴ were likely responsible for catalyzing the copolymerization. The occurrence of the ligand exchange reaction between the butoxide and chloride groups was suggested by the ^1H NMR spectrum, in which the peaks for $\text{Hf}(\text{OBU})_4$ shifted downfield by mixing with HfCl_4 (peaks 1–4 in Figure 2). The catalytic activity of the $\text{HfCl}_x(\text{OR})_{4-x}$ species for both polymerization reactions appeared to be moderated compared to the original tetrachloride and tetrabutoxide.¹⁵

Table 1. Concurrent cationic vinyl-addition and coordination ring-opening copolymerization of VE and CL^a

entry	VE	HfCl ₄ (mM)	Hf(OBu) ₄ (mM)	time	conv. ^b (%)		$M_n \times 10^{-3}$ ^c	M_w/M_n ^c	grafting density (per 100 VE units) ^d
					VE	CL			
1	EVE	12	10	77 h	27	57	5.8	2.16	9
2	EVE	12	10	191 h	95	92	14.1	1.81	10
3	EVE	20	–	4.5 min	99	0	6.0	2.73	–
4	EVE	–	20	60 h	0	100	3.4	1.15	–
5	IPVE	12	8.0	70 h	67	44	3.2	2.66	< 1 ^e

^a[VE]₀ = 1.52 M (entries 1–4) or 0.75 M (entry 5), [CL]₀ = 1.52 M (entries 1–4) or 0.76 M (entry 5), in dichloromethane (entries 1–4) or in toluene (entry 5) at 30 °C. ^bDetermined by gas chromatography. ^cDetermined by GPC (polystyrene standards). ^dEstimated by ¹H NMR. ^eExcept for the linkage of poly(IPVE) and poly(CL) chains at the ω-end of the poly(IPVE) chain.

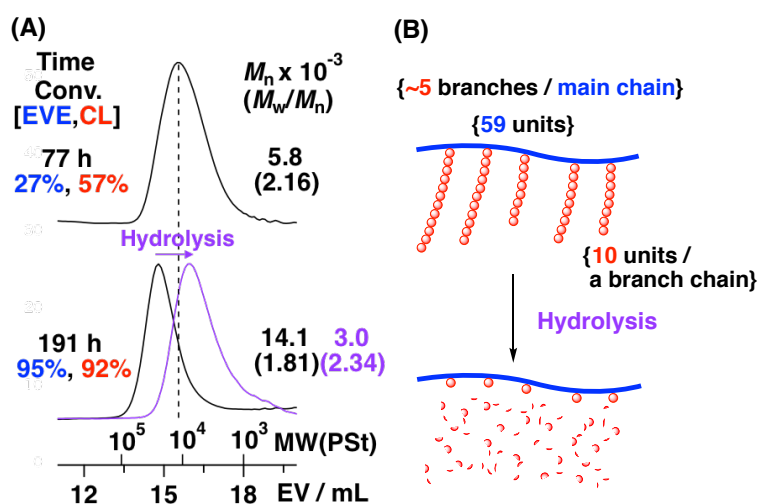


Figure 1. (A) MWD curves for poly(EVE-co-CL) (black; Table 1, entries 1 and 2) and its alkali hydrolysis product (purple). (B) Illustrations of the obtained graft copolymer (entry 2) and its alkali hydrolysis product.

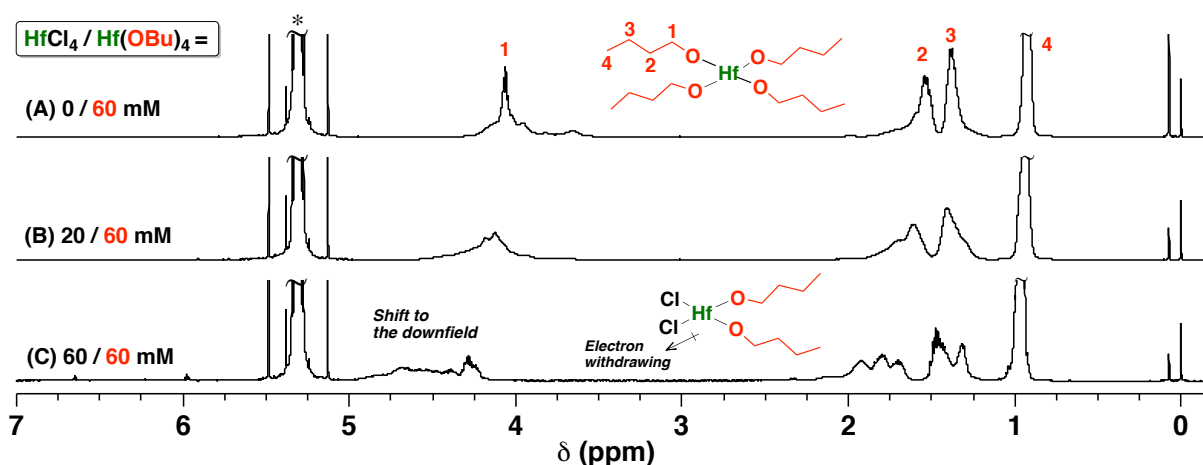


Figure 2. ¹H NMR spectra of (A) Hf(OBu)₄ (60 mM), (B) and (C) a mixture of HfCl₄ and Hf(OBu)₄ catalysts {[HfCl₄]/[Hf(OBu)₄] = (B) 20/60 mM and (C) 60/60 mM}; in CDCl₃ at 30 °C; * dichloromethane.

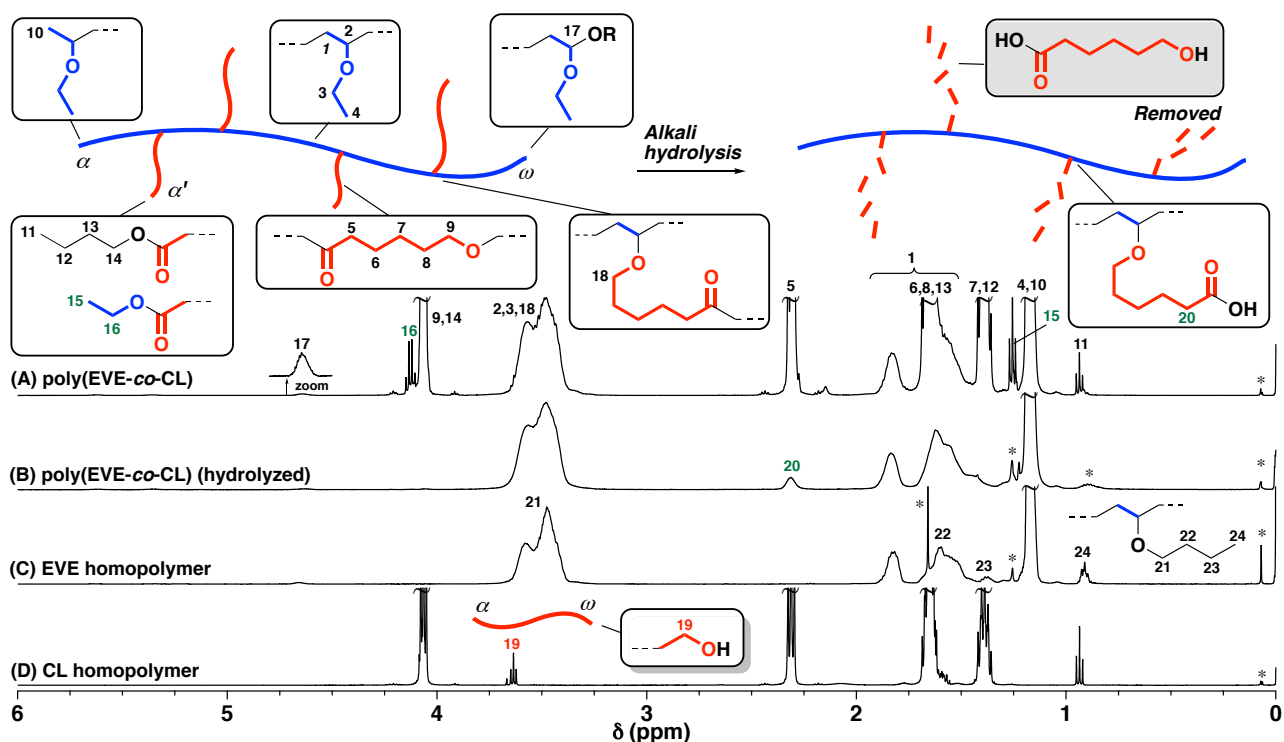


Figure 3. ^1H NMR spectra of (A) poly(EVE-co-CL) (entry 2 in Table 1), (B) poly(EVE-co-CL) after alkali hydrolysis, (C) EVE homopolymer $\{[\text{EVE}]_0 = 0.76 \text{ M}, [\text{HfCl}_4]_0 = 14 \text{ mM}, [\text{Hf}(\text{O}i\text{Bu})_4]_0 = 6.0 \text{ mM}, [\text{EtOAc}] = 1.4 \text{ M}, \text{ in dichloromethane at } 0^\circ\text{C}, M_n(\text{GPC}) = 6.4 \times 10^3\}$, and (D) CL homopolymer $\{[\text{CL}]_0 = 0.81 \text{ M}, [\text{HfCl}_4]_0 = 22 \text{ mM}, [\text{Hf}(\text{O}i\text{Bu})_4]_0 = 11 \text{ mM}, \text{ in toluene at } 30^\circ\text{C}, M_n(\text{GPC}) = 2.4 \times 10^3\}$; in CDCl_3 at 30°C ; * grease, vaseline, and water.

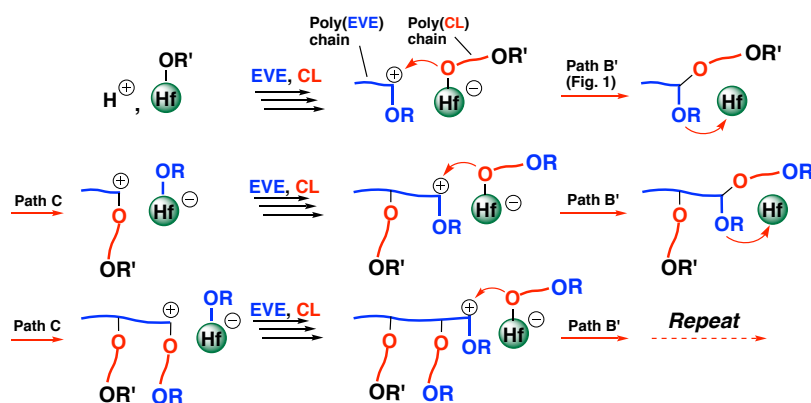
^1H NMR analyses of the obtained polymers confirmed that the copolymerization successfully proceeded via the AGE mechanism to yield graft copolymers consisting of a poly(EVE) main chain and several poly(CL) side chains (Figure 3). The structure of the product was elucidated from several key structures, such as the absence of a hydroxy group at the ω -end of a poly(CL) chain, the presence of ethoxy groups at the α -end of poly(CL) chains, and residual CL-derived structures after alkali hydrolysis, as explained below. The grafting density and grafting length of VE and CL homosequences were determined by simultaneous equations of integral ratios. In the spectrum of the copolymerization product (Figure 3A), there was no peak assigned to the hydroxy group-adjacent methylene protons of the ω -end of a CL homopolymer at 3.6–3.7 ppm (peak 19 in Figure 3D), indicating the incorporation of the poly(CL) growing chains into the side chains of poly(EVE). In addition, the generation of the EVE-derived ethoxy groups at the α -end of poly(CL) (peaks 15 and 16) indicated the occurrence of the initiation reaction of CL polymerization from the Hf-OEt bonds generated via the AGE reactions. The average structure of the copolymer, deduced from the integral ratios of peaks 11, 15, and 4 to the peak for the ω -end of poly(EVE) (peak 17), was composed of 59 units of EVE in the main chain and approximately 5 branch chains with 10 units of CL in each branch (Figure 1B). The molecular weight estimated from this structure, approximately 10×10^3 , was comparable to the value from GPC [14.1×10^3 by polystyrene calibration and 13.7×10^3 by a system equipped with refractive index, light scattering, and

viscosity detectors (the dn/dc value of the product was 0.064 in THF)]. The Mark-Houwink-Sakurada constant, determined by the GPC analysis via light scattering and viscometric detections, was 0.54.

Cleavage of the ester linkages of the poly(CL) segments by alkali hydrolysis also provided evidence for the generation of graft copolymers. Peaks for the protons adjacent to the ester moiety (peaks 9, 14, and 16 in Figure 3A) completely disappeared after hydrolysis, as shown in the ^1H NMR spectrum (Figure 3B). In contrast, a small peak assigned to the methylene group adjacent to the carbonyl group of a CL unit (peak 20) remained, suggesting that the original copolymer structure consisted of a poly(EVE) backbone and poly(CL) side chains. In addition, the MW distribution curve of the original copolymer shifted to the lower MW region after hydrolysis while maintaining a unimodal shape (Figure 1, purple). The M_n value of the degradation product was 3.0×10^3 , which is consistent with the value expected from the remaining poly(EVE) chain (59 units; $MW \sim 4 \times 10^3$).

From these results, the polymerization mechanisms are rationally explained as follows. The ROP of CL is initiated through the coordination of CL to the Hf center and the insertion of CL into the Hf-oxygen bond through the ring-opening reaction. The propagation reaction of CL smoothly proceeds in a manner similar to that of the initiation reaction.^{12,13} The cationic polymerization of EVE appeared to occur via the initiation reaction from a proton derived from adventitious water or alcohol impurities, although the details are currently unclear.¹⁶ The propagation reaction of EVE subsequently proceeds via the dormant-active equilibrium involving both the carbon-chlorine and carbon-alkoxy dormant ends, as explained above (Scheme 1). During these orthogonal reactions, the incorporation of poly(CL) chains into a poly(EVE) chain transiently occurs through the following sequential procedures: the addition reaction of a poly(CL) chain into the carbocation at the growing ends of poly(EVE) to form an acetal moiety (path B' in Scheme 3), the abstraction of the EVE-derived ethoxy group from the acetal end by the Hf catalyst (path C), and the addition reaction of EVE to the resulting carbocation. In addition, new poly(CL) chains are continuously generated via the initiation reaction from the resulting Hf-OEt catalyst, which was also confirmed by the incorporation of the ethoxy group into the chain end of poly(CL) segments (peaks 15 and 16 in Figure 3). The graft copolymers are produced by the repetition of these reactions. These mechanisms were also supported by the copolymerization via the addition of the EVE monomer into the reaction solution of living ROP of CL at the later stage of the polymerization (Figures 4 and 5). In this method, a graft copolymer with several poly(CL) side chains having uniform length was obtained.

Scheme 3. Illustrative drawing of the copolymerization of EVE and CL via the AGE mechanisms



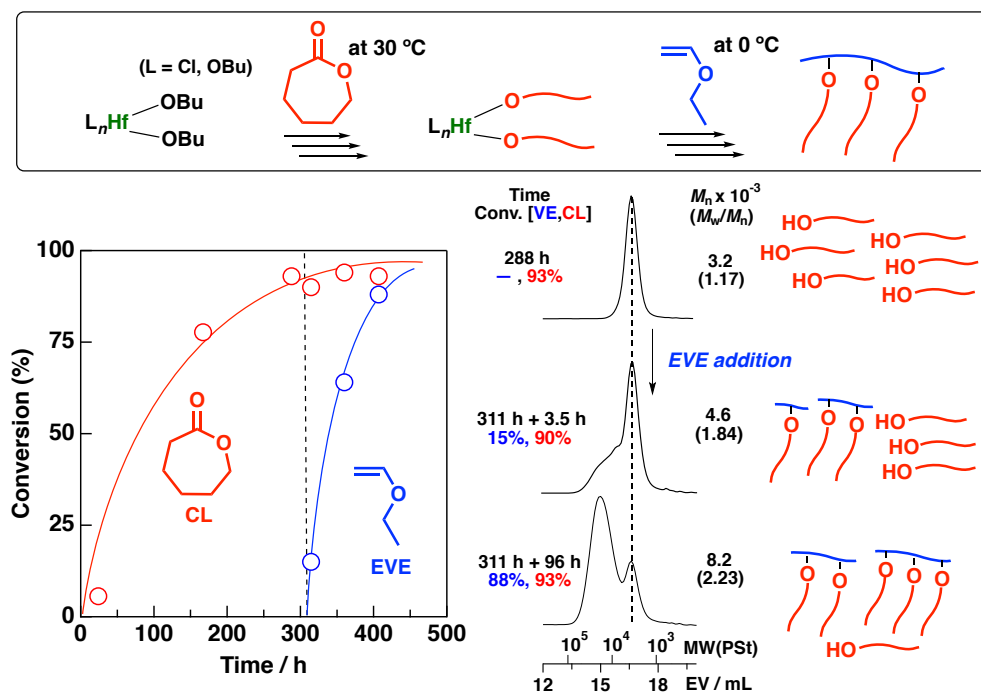


Figure 4. Time–conversion plots for the copolymerization via the addition of EVE and MW distribution curves of the CL homopolymer and poly(EVE-*co*-CL)s obtained. {[EVE]_{added} = 0.76 M, [CL]₀ = 0.70 M, [HfCl₄]₀ = 13 mM, [Hf(OBu)₄]₀ = 8.6 mM, in dichloromethane at 30 °C (for CL polymerization) and 0 °C (cooled just before the EVE addition)}.

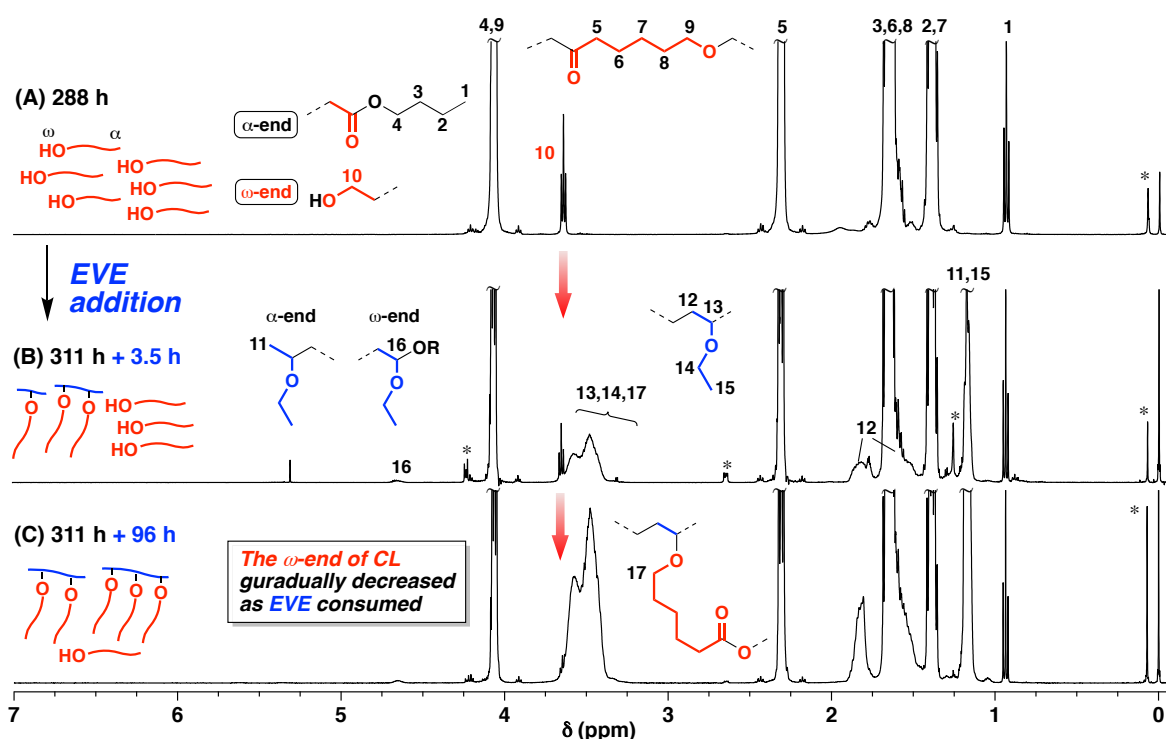


Figure 5. ¹H NMR spectra of (A) CL homopolymer and (B) and (C) poly(EVE-*co*-CL)s obtained in the copolymerization via the addition of EVE; in CDCl₃ at 30 °C; *grease, vaseline, and residual CL monomer.

Considering these mechanisms, the selectivity in abstracting alkoxy groups at the acetal chain ends is responsible for the grafting density. This selectivity appears to depend on the stability of the resulting carbocation and/or the affinity between a metal catalyst and alkoxy groups. In fact, the use of isopropyl VE (IPVE), a VE with a secondary alkoxy group, instead of EVE resulted in the negligible generation of graft copolymers (entry 5 in Table 1). The AGE mechanism rarely operated (Figure S2) to mainly produce the CL homopolymer and diblock copolymer, which was suggested from the calculation of ^1H NMR integrals and analyses via the acid hydrolysis of the product (Figures 6 and 7). The selective abstraction of the poly(CL) chain from the acetal moiety consisting of the isopropoxy group and the poly(CL) chain (Scheme 4) is consistent with several reports on the Lewis acid-catalyzed activation of acetals containing primary and secondary alkoxy groups.¹⁷ Thus, a higher grafting efficiency will be attained using appropriate monomers, which is described in the following chapter. In addition, a metal catalyst that exhibits sufficient affinity to alkoxy groups is indispensable for efficient copolymerization; hence, the reaction using catalysts with various central metals is also examined in the following chapter.

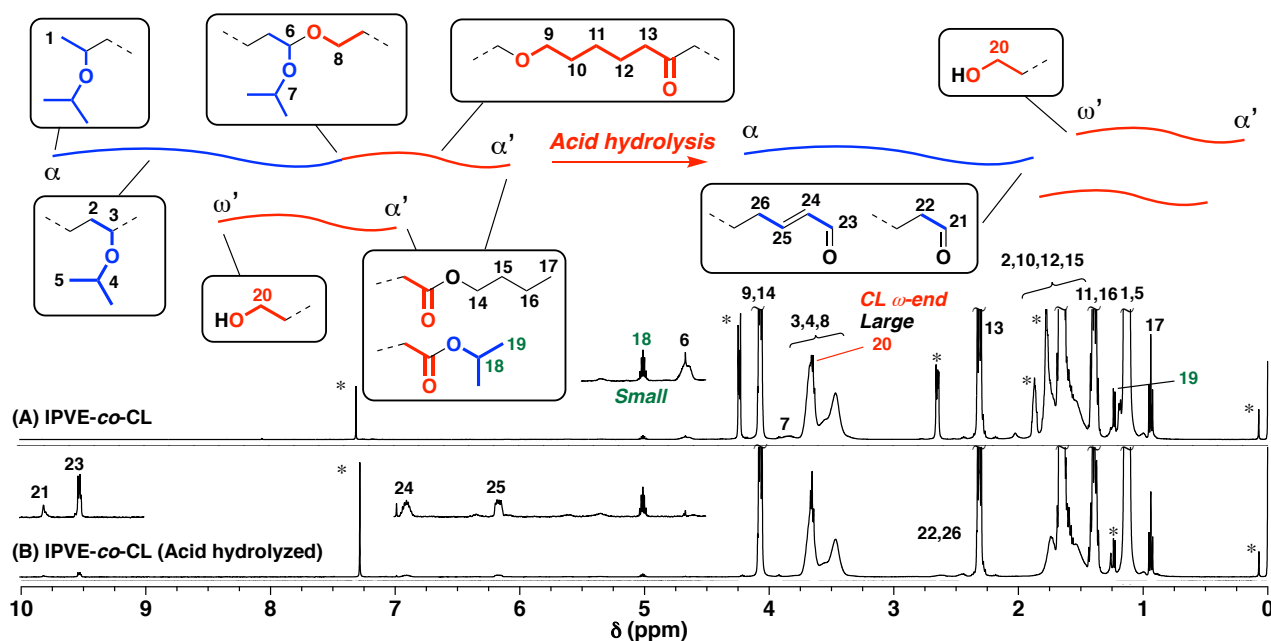


Figure 6. ^1H NMR spectra of (A) poly(IPVE-co-CL) (entry 5 in Table 1) and (B) poly(IPVE-co-CL) after acid hydrolysis.

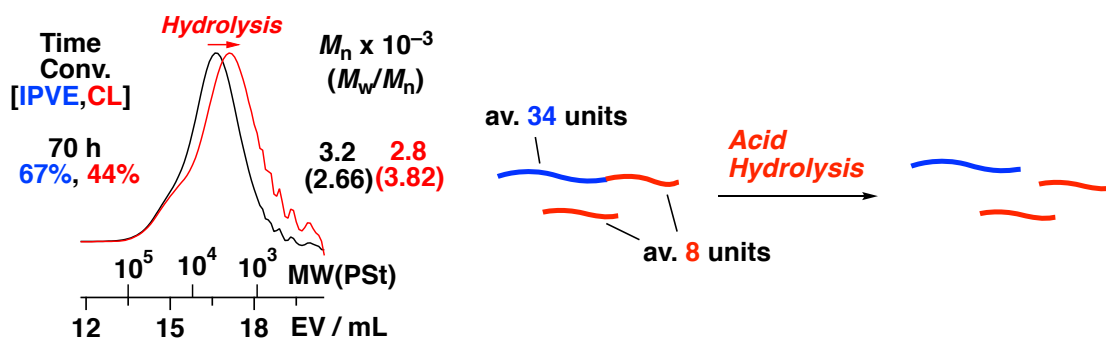
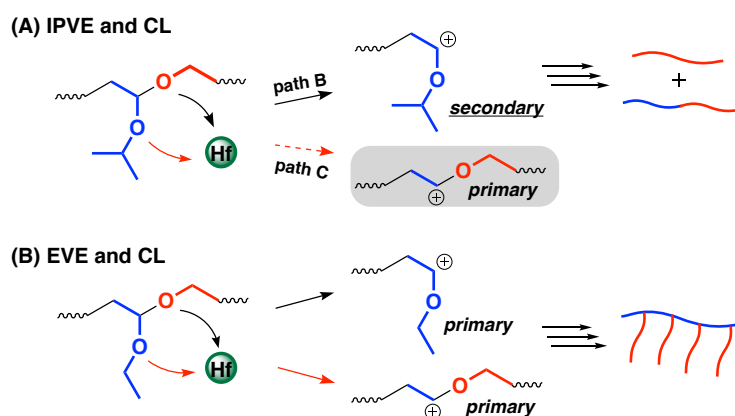


Figure 7. MWD curves of poly(IPVE-co-CL)s before and after acid hydrolysis (entry 5 in Table 1).

Scheme 4. Selectivity in abstracting an alkoxy group from an acetal-type dormant species derived from (A) IPVE and (B) EVE



Conclusion

In conclusion, the copolymerization of VEs and CL was achieved via the AGE mechanisms using a mixture of HfCl_4 and $\text{Hf}(\text{O}i\text{Bu})_4$ as a dual-role catalyst. Most importantly, both the cationic vinyl-addition and the ring-opening polymerization reactions orthogonally proceeded without interfering with the other reactions, while the different types of propagating chains transiently merged to yield graft copolymers consisting of a poly(VE) main chain with several poly(CL) side chains. An appropriate ratio of HfCl_4 and $\text{Hf}(\text{O}i\text{Bu})_4$ was essential for the propagation reactions of both monomers at similar rates. Further optimization of the polymerization conditions, including catalyst design, will allow for precise control over the frequency of the AGE reactions and the MWs of the backbone and branch chains. The characteristic strategy demonstrated in this chapter will be applied to the synthesis of graft copolymers and other highly branched copolymers from a wide variety of commercially available VEs and cyclic esters.

References and Notes

- de Freitas, A. G.; Trindade, S. G.; Murano, P. I.; Schmidt, V.; Satti, A. J.; Villar, M. A.; Ciolino, A. E.; Giacomelli, C. *Macromol. Chem. Phys.* **2013**, *214*, 2336.
- Bielawski, C. W.; Louie, J.; Grubbs, R. H. *J. Am. Chem. Soc.* **2000**, *122*, 12872.
- Mecerreyes, D.; Moineau, G.; Dubois, P.; Jérôme, R.; Hedrick, J. L.; Hawker, C. J.; Malmström, E. E.; Trollsas, M. *Angew. Chem. Int. Ed.* **1998**, *37*, 1274.
- Le Hellaye, M.; Lefay, C.; Davis, T. P.; Stenzel, M. H.; Barner-Kowollik, C. *J. Polym. Sci., Part A* **2008**, *46*, 3058.
- Zhou, J.; Villarroya, S.; Wang, W.; Wyatt, M. F.; Duxbury, C. J.; Thurecht, K. J.; Howdle, S. M. *Macromolecules* **2006**, *39*, 5352.
- Bernaerts, K. V.; Du Prez, F. E. *Prog. Polym. Sci.* **2006**, *31*, 671.
- Aoshima, H.; Uchiyama, M.; Satoh, K.; Kamigaito, M. *Angew. Chem. Int. Ed.* **2014**, *53*, 10932.

8. (a) Kanazawa, A.; Kanaoka, S.; Aoshima, S. *J. Am. Chem. Soc.* **2013**, *135*, 9330. (b) Kanazawa, A.; Aoshima, S. *Polym. J.* **2016**, *48*, 679.
9. Fukuda, T.; Goto, A. In *Polymer Science: A Comprehensive Reference*; Matyjaszewski, K., Möller, M., Eds.; Elsevier B.V.: Amsterdam, 2012; Vol. 3.05.
10. (a) Sawamoto, M. *Prog. Polym. Sci.* **1991**, *16*, 111. (b) Kennedy, J. P.; Ivan, Hanser: New York, 1992. (c) Faust, R. In *Polymaer Science: A Comprehensive Reference*; Matyjaszewski, K., Möller, M., Eds.; Elsevier B.V.: Amsterdam, 2012; Vol. 3.15. (d) Aoshima, S.; Kanaoka, S. *Chem. Rev.* **2009**, *109*, 5245. (e) Puskas, J. E.; Kaszas, G. *Prog. Polym. Sci.* **2000**, *25*, 403.
11. (a) Kanazawa, A.; Kanaoka, S.; Aoshima, S. *Macromolecules* **2010**, *43*, 2739. (b) Kanazawa, A.; Kanaoka, S.; Aoshima, S. *J. Polym. Sci., Part A: Polym. Chem.* **2010**, *48*, 2509.
12. (a) Penczek, S.; Cypryk, M.; Duda, A.; Kubisa, P.; Slomkowski, S. *Prog. Polym. Sci.* **2007**, *32*, 247. (b) Labet, M.; Thielemans, W. *Chem. Soc. Rev.* **2009**, *38*, 3484.
13. (a) Hsieh, K. C.; Lee, W. Y.; Hsueh, L. F.; Lee, H. M.; Huang, J. H. *Eur. J. Inorg. Chem.* **2006**, *11*, 2306. (b) Liang, L.; Lin S.; Chien, C. Chen, M. *Dalton Trans.* **2013**, *42*, 9286. (c) Chmura, A. J.; Davidson, M. G.; Jones, M. D.; Lunn, M. D.; Mahon, M. F.; Johnson, A. F.; Khunkamchoo, P.; Roberts, S. L.; Wong, S. F. *Macromolecules* **2006**, *39*, 7250.
14. (a) Kamigaito, M.; Sawamoto, M.; Higashimura, T. *Macromolecules* **1995**, *28*, 5671. (b) Bradley, D. C.; Halim, F. M.; Mehrotra, R. C.; Wardlaw, W. J. *Chem. Soc.* **1952**, 4609. (c) Bradley, D. C.; Hancock, D. C.; Wasdlaw, W. J. *Chem. Soc.* **1952**, 2773.
15. Cationic homopolymerization of EVE using $\text{HfCl}_x/(\text{OBU})_{4-x}$ in the presence of ethyl acetate proceeded much slower (90% conversion in 70 h at $[\text{HfCl}_4]_0/[\text{Hf}(\text{OBU})_4]_0 = 14 \text{ mM}/6 \text{ mM}$) compared to that using HfCl_4 alone (97% in 11 min at $[\text{HfCl}_4]_0 = 20 \text{ mM}$) due to the decrease in the Lewis acidity through the replacement of chlorine atoms to alkoxy groups. The polymerization rate of CL with $\text{HfCl}_4/\text{Hf}(\text{OBU})_4$ (entries 1 and 2) was approximately one-third of that with $\text{Hf}(\text{OBU})_4$ (entry 4) likely due to the difference in the abilities to coordinate a CL monomer and to involve the alkoxy group in the propagation reaction.
16. Another possibility is the initiation reaction through the addition of a VE monomer to the central metal; however, this mechanism appears unlikely from a control experiment using methan(ol-*d*) as a quencher (Figure S1 in the Supporting Information)
17. (a) Silverman, R.; Edington, C.; Elliott, J. D.; Johnson, W. S. *J. Org. Chem.* **1987**, *52*, 180. (b) Denmark, S. E.; Willson, T. M.; Almstead, N. G. *J. Am. Chem. Soc.* **1989**, *111*, 9258. (c) Kobayashi, S.; Arai, K.; Yamakawa, T.; Chen, Y.; Salter, M. M.; Yamashita, Y. *Adv. Synth. Catal.* **2011**, *353*, 1927. (d) Kinugasa, M.; Harada, T.; Egusa, T.; Fujita, K.; Oku, A. *Bull. Chem. Soc. Jpn.* **1996**, *69*, 3639.

Supporting Information

Cationic homopolymerization of EVE using $\text{HfCl}_4/\text{Hf}(\text{OEt})_4$ as catalysts was quenched with CH_3OH or CH_3OD to examine the possibility of the initiation via the addition reaction of an EVE monomer to the central metal (Scheme S1). In that case, the Hf-C bonds at the α -end of the poly(EVE) chain should be converted to H-C or D-C bonds by the proton or the deuterium atom derived from CH_3OH or CH_3OD , respectively. The ESI-MS spectra of the products (Figure S1A and S1B), however, did not show differences in the m/z values of the peaks, indicating that deuterium atoms were not introduced into polymer chains. The m/z values of the peaks agreed with the mass values of the structures having a proton-derived α -end. Therefore, the initiation reaction most likely occurred not from the central metal but from protons derived from protic impurities such as adventitious water and alcohols remained in the metal alkoxide.

Scheme S1. Termination reactions of the cationic polymerization of EVE catalyzed by $\text{HfCl}_4/\text{Hf}(\text{OEt})_4$ using CH_3OH or CH_3OD as a quencher

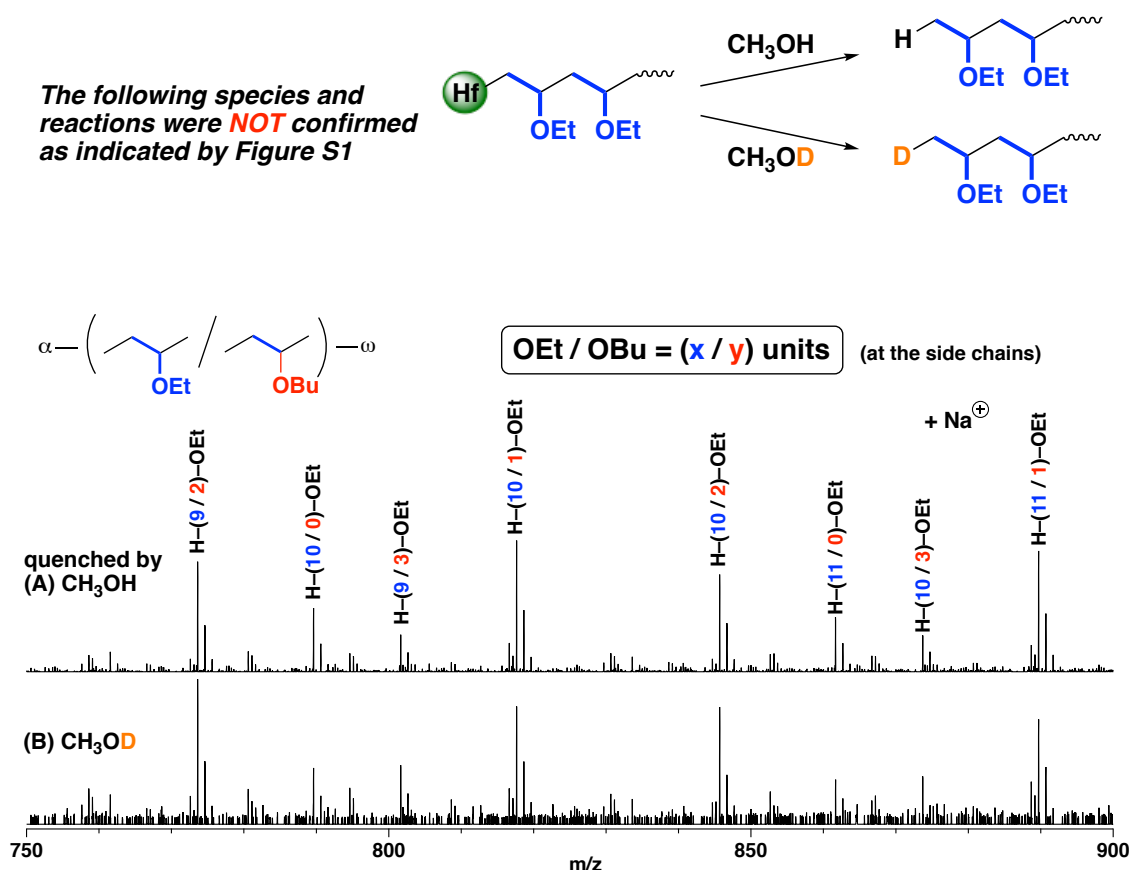


Figure S1. ESI-MS spectra of EVE homopolymers quenched by (A) CH_3OH or (B) CH_3OD {polymerization conditions: $[\text{EVE}]_0 = 0.76 \text{ M}$, $[\text{HfCl}_4]_0 = 14 \text{ mM}$, $[\text{Hf}(\text{OEt})_4]_0 = 6.0 \text{ mM}$, $[\text{EtOAc}] = 1.4 \text{ M}$ in dichloromethane at $0 \text{ }^\circ\text{C}$. $M_n(\text{GPC}) = 6.4 \times 10^3$ }.

Cationic homopolymerization of IPVE and EVE using $\text{HfCl}_4/\text{Hf}(\text{OBu})_4$ as catalysts was conducted to examine the AGE reactions. The MS spectrum of the obtained poly(IPVE) (Figure S2A) consisted of two series of peaks. The m/z values of the main peaks agreed with the mass values of the polymer chains generated without the AGE reaction, whereas the m/z values of the minor series were consistent with the fact that one butoxy group was introduced into the side chain. The result indicates that the AGE mechanism negligibly operated during the IPVE polymerization (at most once/propagating chain). In addition, the MS analysis demonstrated that most of the ω -ends were not the carbon–methoxy bonds derived from methanol quencher but the carbon–butoxy bonds derived from the catalyst, which suggests that the propagating ends generated during the polymerization reaction mainly existed in the form of acetal. Thus, IPVE homopolymer appeared to be negligibly generated in the copolymerization of IPVE and CL due to the linkage between the poly(IPVE) and poly(CL) chains through the acetal moiety. In contrast to the case of IPVE, the MS spectrum of the obtained poly(EVE) (Figure S2B) exhibited many series of peaks. The m/z value of these peaks agreed with the structures of poly(EVE) having several butoxy groups at the side chains and ω -ends, indicating that the AGE reactions frequently occurred during the polymerization reaction. These results, arisen from the selectivity in abstracting alkoxy groups, support the differences in the products obtained via the copolymerization of CL and IPVE or EVE (Scheme 4).

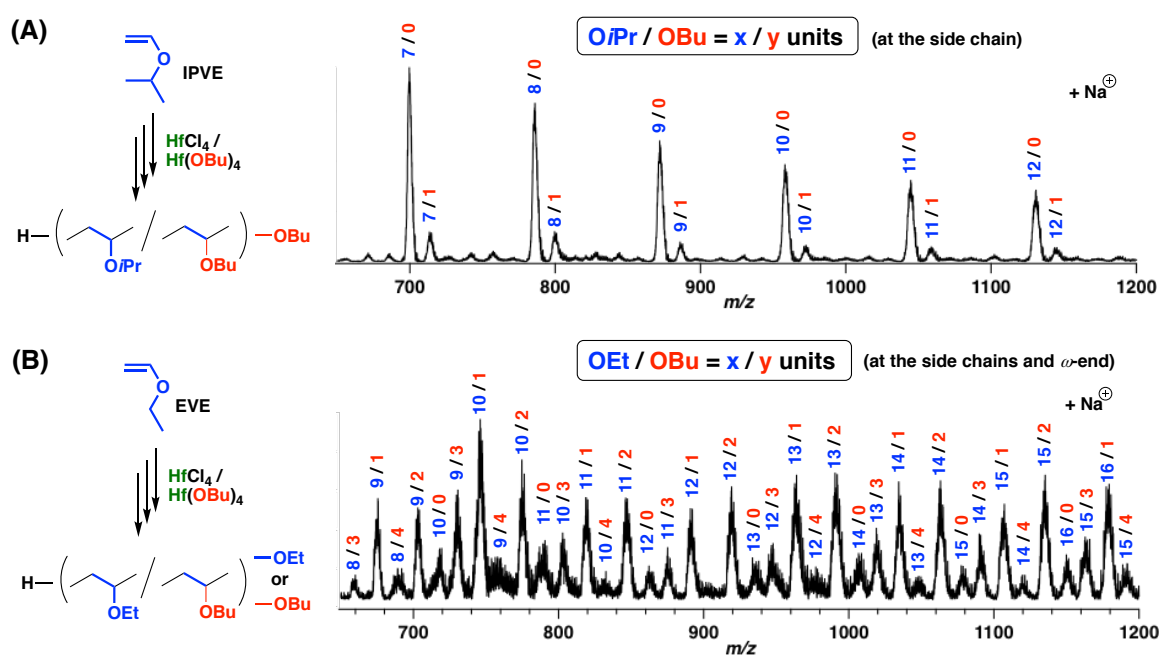


Figure S2. MALDI-TOF-MS spectra of (A) IPVE and (B) EVE homopolymers obtained with the mixture of HfCl_4 and $\text{Hf}(\text{OBu})_4$ catalysts {polymerization conditions: (A) $[\text{IPVE}]_0 = 0.75$ M, $[\text{HfCl}_4]_0 = 12$ mM, $[\text{Hf}(\text{OBu})_4]_0 = 8.0$ mM, $[\text{EtOAc}] = 1.2$ M in toluene at 0°C . $M_n(\text{GPC}) = 8.6 \times 10^3$; (B) see Figure S1}.

Design of Graft Architectures via Simultaneous Kinetic Control of Cationic Vinyl-Addition Polymerization of Vinyl Ethers, Coordination Ring-Opening Polymerization of Cyclic Esters, and Merging at the Propagating Chain End

Introduction

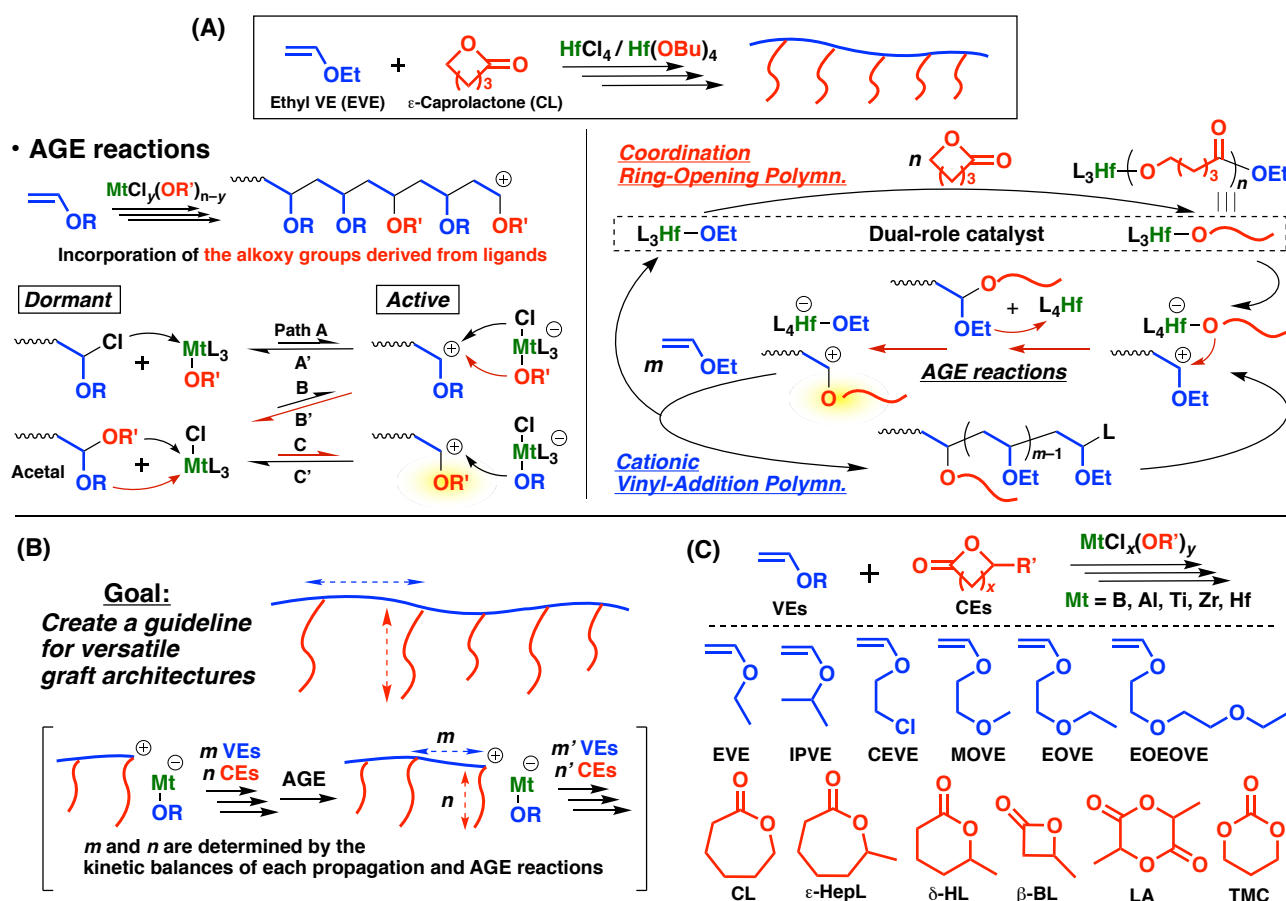
Graft copolymers, which constitute an important class of branched polymers, have been extensively used in many applications, such as lithography, adhesives, compatibilizing agents, and coating materials, by exploiting the specific properties originating from their topological features.¹⁻³ The primary structure of a graft copolymer, which has a decisive effect on the morphology and properties of the copolymer, is described by many parameters, including chemical nature, molecular weight (MW), molecular weight distribution (MWD), and the number, location, and length of graft chains. Based on living/controlled polymerization techniques, structural design of graft copolymers has become feasible via the following three approaches: “grafting-from”, “grafting-through”, and “grafting-onto” methods. These three methods, however, require multistep reactions involving cumbersome isolation and purification steps.

Simultaneous copolymerization via different mechanisms is an effective method for the facile synthesis of copolymers from different types of monomers.⁴⁻¹² For example, Trollsas and coworkers⁴ simultaneously (but orthogonally) conducted the living coordination ring-opening polymerization of ϵ -caprolactone (CL) and the nitroxide-mediated radical polymerization of styrene from a bifunctional initiator with initiating sites for both polymerizations, resulting in a diblock copolymer in one shot. More versatile copolymer structures can be designed by simultaneous copolymerization of different mechanisms that proceed in a nonorthogonal manner.⁷⁻¹² For example, copolymers with a wide range of comonomer sequence distributions were obtained by the simultaneous living radical polymerization of acrylates or vinyl esters and cationic polymerization of vinyl ethers (VEs) involving multiple crossover reactions in both directions. Radical and cationic propagating species are generated from a common growing end that has a structure of reversible addition-fragmentation chain transfer agents, such as dithioesters and trithiocarbonates.^{10,11} In this copolymerization, the comonomer sequence distributions were designed by simultaneously tuning the kinetics of the two different propagation reactions and the interconversion of the active species based on the polymerization conditions, such as the amount and/or kinds of radical initiators and Lewis acid catalysts.

In Chapter 2, the author developed a novel method for the synthesis of graft copolymers via simultaneous cationic vinyl-addition polymerization of ethyl vinyl ether (EVE) and coordination ring-opening polymerization of CL using a mixture of HfCl_4 and $\text{Hf}(\text{O}i\text{Bu})_4$ as catalysts by utilizing alkoxy group exchange (AGE) reactions (Scheme 1A).¹² In this chapter, the author aims to create a guideline for synthesizing a variety of graft architectures via the above-described mechanisms (Scheme 1B). Importantly, the grafting density (the number of graft chains per 100 VE units) and the grafting length [the degree of polymerization (DP_n) of Cyclic Ester (CE)] of a copolymer produced by these mechanisms are most likely determined by the kinetic balance of each propagation and the AGE reaction (Scheme 1B, below). For example, the distance between adjacent graft chains, which is inversely proportional to the grafting density, corresponds to the number of VE monomers that reacted between the two AGE events; hence, the average branch spacing is determined by the

rate of VE propagation compared to that of the AGE reactions. Similarly, the grafting length is the number of CE monomers that reacted from an alkoxy ligand until the AGE reactions occur, which is related to the rate of CE propagation against that of the AGE reactions. These insights suggest that if the kinetics of these three reactions are controlled simultaneously, a variety of graft architectures can be designed. In particular, the development of a system that enables frequent AGE reactions will dramatically increase the variety of structures of accessible polymers, including a copolymer with a very high grafting density. Accordingly, the author investigated the effects of polymerization conditions, such as the kinds and/or concentrations of monomers and catalysts, on the kinetics of the two different propagation reactions and the AGE reaction, with a special focus on designing the reaction conditions that cause frequent AGE reactions (Scheme 1C).

Scheme 1. (A) Concurrent cationic vinyl-addition and coordination ring-opening copolymerization of EVE and CL using $\text{HfCl}_4/\text{Hf}(\text{O}i\text{Bu})_4$ as catalysts, alkoxy group exchange (AGE) reactions, and mechanisms for graft copolymer formation via AGE reactions, (B) the goal of this chapter, and (C) monomers and catalysts employed



Experimental Section

Materials.

2-Chloroethyl VE (CEVE; TCI; >97%) was washed with a 10% aqueous sodium hydroxide solution and then water, dried overnight over sodium sulfate, and distilled twice over calcium hydride under reduced pressure. 2-Methoxyethyl VE (MOVE; Maruzen Petrochemical) and 2-ethoxyethyl VE (EOVE; Maruzen Petrochemical) were distilled twice over calcium hydride. 2-(2-Ethoxy)ethoxyethyl VE (EOEOVE; Maruzen Petrochemical), δ -hexanolactone (δ -HL; TCI; >99.0%) and β -butyrolactone (β -BL; TCI; >95.0%) were distilled twice over calcium hydride under reduced pressure. L-Lactide (LA; TCI; >98%) was recrystallized from 1,4-dioxane and then toluene before being dried for more than 3 h prior to use. Trimethylene carbonate (TMC; TCI; >98.0%) was recrystallized from toluene. $\text{Et}_{1.5}\text{AlCl}_{1.5}$ (Nippon Aluminum Alkyls; 1.0 M solution in toluene) and TiCl_4 (Aldrich; 1.0 M solution in toluene or dichloromethane) were used as received. Commercially available $\text{Ti}(\text{OiPr})_4$ (Aldrich; 97%), BF_3OEt_2 (TCI; >98.0%), $\text{B}(\text{OiPr})_3$ (Aldrich; >98%), and 2-propanol (Nacalai Tesque; >99.5%) were used without further purification after preparing a stock solution in dichloromethane or toluene. ZrCl_4 and $\text{Zr}(\text{OEt})_4$ were used without further purification. The adduct of IBVE with HCl (IBVE-HCl) was prepared from the addition reaction of IBVE with HCl according to the reported method.¹³ Perylene (L3910HD; Pigment Red 178 99%, BaSO_4 1%; BASF Japan), Cu phthalocyanine (SFG-8; 75% Pigment Blue 15:4, 20% aluminum benzoate, 5% BaSO_4 ; Toyochem), FeOOH (HY-100; 95.4% FeOOH , 4.6% $\text{Al}(\text{OH})_3$; Titan Kogyo), quinacridone (7093-Y; 95% Pigment Violet 19, 5% other; DIC Corporation), and TiO_2 (CR-97; 94% TiO_2 , 4% Al_2O_3 , 1% ZrO , 1% SnO ; Ishihara Sangyo Kaisha) were supplied by Nippon Paint Co., Ltd. and used as received. Other materials were prepared and used as described in Chapter 2.

Polymerization Procedure.

Polymerization was conducted in a manner similar to that described in Chapter 1.

Synthesis of ϵ -Heptanolactone (ϵ -HepL)

ϵ -HepL was synthesized by the Baeyer-Villiger oxidation reaction of 2-methylcyclohexanone (TCI; >96.0%) using monoperoxyphthalic acid magnesium salt hexahydrate (TCI; >65.0%) as a catalyst in dichloromethane.¹⁴ After the oxidation reaction, the reaction mixtures were neutralized with aqueous NaHCO_3 and then washed with water and brine. The organic layer was dried over sodium sulfate, and the solvents were evaporated under reduced pressure. The concentrated solution was distilled twice (calcium hydride was used in the second distillation) under reduced pressure to yield the monomer. Colorless liquid. $^1\text{H NMR}$ (CDCl_3 , 30 °C): δ 4.44 (1H, m), 2.16 (2H, m), 1.51–2.00 (6H, m), 1.38 (3H, d).

Transesterification.

Transesterification was conducted under a dry nitrogen atmosphere in a glass tube equipped with a three-way stopcock. The purified copolymer (21 mg) was dissolved in ethyl acetate (EtOAc ; 4.7 mL), and then transesterification was started by the addition of a 200 mM $\text{Ti}(\text{OiPr})_4$ solution in toluene (1.2 mL) at 70 °C. After 17 h, the reaction was quenched by diluting the reaction mixture with dichloromethane, and then the

mixture was washed with water to remove the resulting salt. The volatiles were removed under reduced pressure at 60 °C to yield the transesterification products.

Characterization.

The thermal properties of the polymers were examined using a Shimadzu DSC-60 Plus differential scanning calorimeter. The particle size was measured by dynamic light scattering (DLS; Otsuka Electronics FPAR-1000HG, $\lambda = 632.8$ nm, scattering angle = 90 °). The MWD and ^1H NMR spectra were measured in a manner similar to that described in Chapter 2.

Results and Discussion

I. Copolymerization of Various VEs and CEs Using a Variety of Metal Haloalkoxides: Investigations of the Effects of Monomers and Catalysts on the Kinetics of the Two Different Polymerization Reactions and the AGE Reaction.

For the occurrence of the AGE reaction in cationic polymerization, acetal structures need to be generated and participate in the dormant-active equilibrium at the propagating ends. When the carbon–chlorine ends are also generated at the propagating ends, both the chloride (halide) anion (paths A and A' in Scheme 1A) and the alkoxy groups (paths B, B', C, and C') have to be abstracted from the carbon–chlorine and acetal ends, respectively, by a Lewis acid catalyst. Thus, the affinity of metal catalysts for alkoxide groups and chloride anions is an important factor for the kinetics of AGE reactions. Indeed, the author's group previously reported that AGE reactions proceeded when metal catalysts with an appropriate balance of oxophilicity and chlorophilicity were used.¹⁵ In addition, the rates of activation and deactivation reactions in the dormant-active equilibrium are known to be affected by the catalyst species. These points motivated the author to examine the effects of catalysts possessing different central metals on the copolymerization behavior.

I-1. Effects of Catalysts (Central Metals)

Copolymerization of EVE and CL was performed using several kinds of metal halide–metal alkoxide (or alcohol) mixtures (Table 1). Simultaneous consumption of both monomers was achieved with all the catalysts employed except for $\text{BF}_3\text{OEt}/\text{B}(\text{O}i\text{Pr})_3$ (entry 10 in Table 1). Importantly, the rates of both polymerizations were tunable by changing the molar ratio of the catalyst mixtures, as schematically demonstrated in Figure 1B. For example, only EVE was polymerized by HfCl_4 alone (entry 3) even in the presence of both EVE and CL, while only CL was polymerized by $\text{Hf}(\text{O}i\text{Pr})_4$ alone (entry 4). When a mixture of HfCl_4 and $\text{Hf}(\text{O}i\text{Pr})_4$ was used, both monomers were consumed simultaneously. In addition, the consumption rates of both monomers depended on the molar ratio of the catalysts (entries 1 and 2). The rate of cationic polymerization with the mixed catalysts was lower than the rate with the metal chlorides alone, which suggested that the Lewis acidity of the central metal decreased due to the substitution of electron-donating alkoxy ligands for electron-withdrawing chloride ligands.¹⁶ The ^1H NMR spectrum of the mixture of TiCl_4 and $\text{Ti}(\text{O}i\text{Pr})_4$ supported the occurrence of ligand exchange (Figure S1 in the Supporting Information).

Table 1. Copolymerization of EVE and CL with various metal haloalkoxides^a

entry	metal halides	(mM)	metal alkoxides	(mM)	time	conv. (%) ^b		$M_n \times 10^{-3}$ ^c	M_w/M_n ^c	grafting density ^d
						EVE	CL			
1	HfCl ₄	12	Hf(OBu) ₄	8.0	80 h	96	44	3.1	2.40	15
2		12		12	90 h	68	52	2.5	2.26	17
3		20		0	5 min	99	0	6.0	2.75	-
4		0		20	60 h	0	95	3.4	1.15	-
5 ^e	ZrCl ₄	12	Zr(OEt) ₄	8.0	283 h	55	53	3.0	3.16	19
6	TiCl ₄	16	Ti(OiPr) ₄	6.0	127 h	95	91	4.7	2.32	10
7		14		6.0	90 h	58	87	3.9	2.10	11
8		12		6.0	55 h	11	72	3.4	1.43	13
9	Et _{1.5} AlCl _{1.5}	10	<i>i</i> PrOH	10	70 h	76	90	8.2	10.9	~2
10	BF ₃ OEt ₂	10	B(OiPr) ₃	10	6 min	96	0	5.3	2.56	-

^a[EVE]₀ = 0.59 M, [CL]₀ = 0.60 M in toluene at 20 °C (entries 6–10) or [EVE]₀ = [CL]₀ = 0.76 M (entries 1, 2, and 5) or 1.52 M (entries 3 and 4) in CH₂Cl₂ at 30 °C. ^bDetermined by ¹H NMR analysis. ^cDetermined by GPC (polystyrene standards). ^dEstimated by ¹H NMR. ^eThe slow reaction with ZrCl₄/Zr(OEt)₄ was likely due to the low solubility.

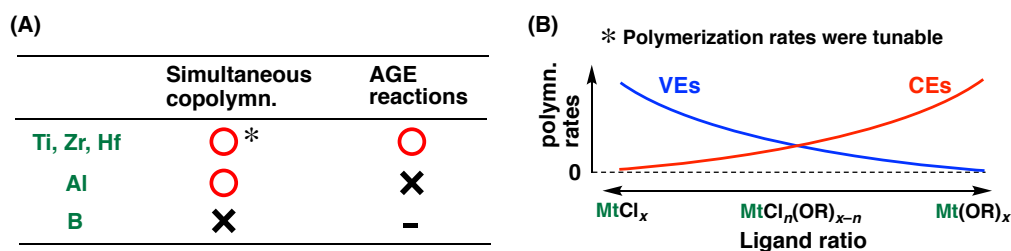


Figure 1. (A) Effective central metals for the graft copolymerization and (B) tuning of polymerization rates based on the molar ratio of alkoxy and chlorine ligands (a schematic diagram).

Successful formation of a graft copolymer was demonstrated when TiCl₄/Ti(OiPr)₄ were used as a catalyst (entry 6 in Table 1). Both EVE and CL were consumed at comparable rates by fine tuning the catalyst molar ratios (entries 6–8). The MWD curve of the product had a bimodal shape (Figure 2, black). In the ¹H NMR spectrum, the peaks attributed to the ethoxy group at the α'-end of the poly(CL) chains [peaks 15 and 16 in Figure 3(i)] were clearly confirmed, which suggested the occurrence of the AGE reactions. In addition, the peak derived from the ω'-end of the CL homopolymer (peak 18) was much smaller than the peaks attributed to the α'-ends (peaks 13–16), which indicated the formation of a copolymer with a small amount of CL homopolymer. The existence of the CL homopolymer suggests that the AGE reactions did not occur frequently compared to the CL propagation. Simultaneous equations using the peaks of the α- and ω-ends and repeating units of both poly(EVE) and poly(CL) revealed that the copolymer was composed of 52 units of EVE in the main chain and approximately five branch chains consisting of 10 CL units in each branch (Figure 2). A graft copolymer was also generated with ZrCl₄/Zr(OEt)₄ (entry 5) but not with Et_{1.5}AlCl_{1.5}/*i*PrOH due to negligible

AGE reactions (Figure 1A). The grafting densities of the products obtained with different catalysts were comparable [$Zr(19) > Hf(15) > Ti(10)$], which indicated that the effects of these catalysts on the rate of the AGE reactions were limited under the employed conditions.

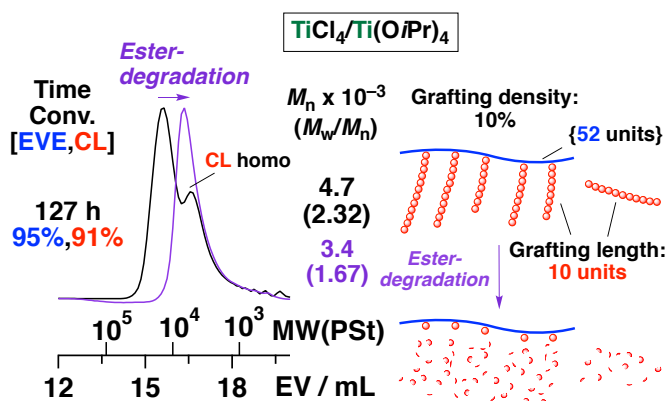


Figure 2. MWD curves of the product obtained by the copolymerization of EVE and CL catalyzed by $TiCl_4/Ti(OiPr)_4$ (black; entry 6 in Table 1) and the transesterification product (purple); transesterification: 25 mM $Ti(OiPr)_4$ in $EtOAc/CH_2Cl_2$ (8/1 v/v; 0.3 wt% polymer) at 70 °C for 21 h.

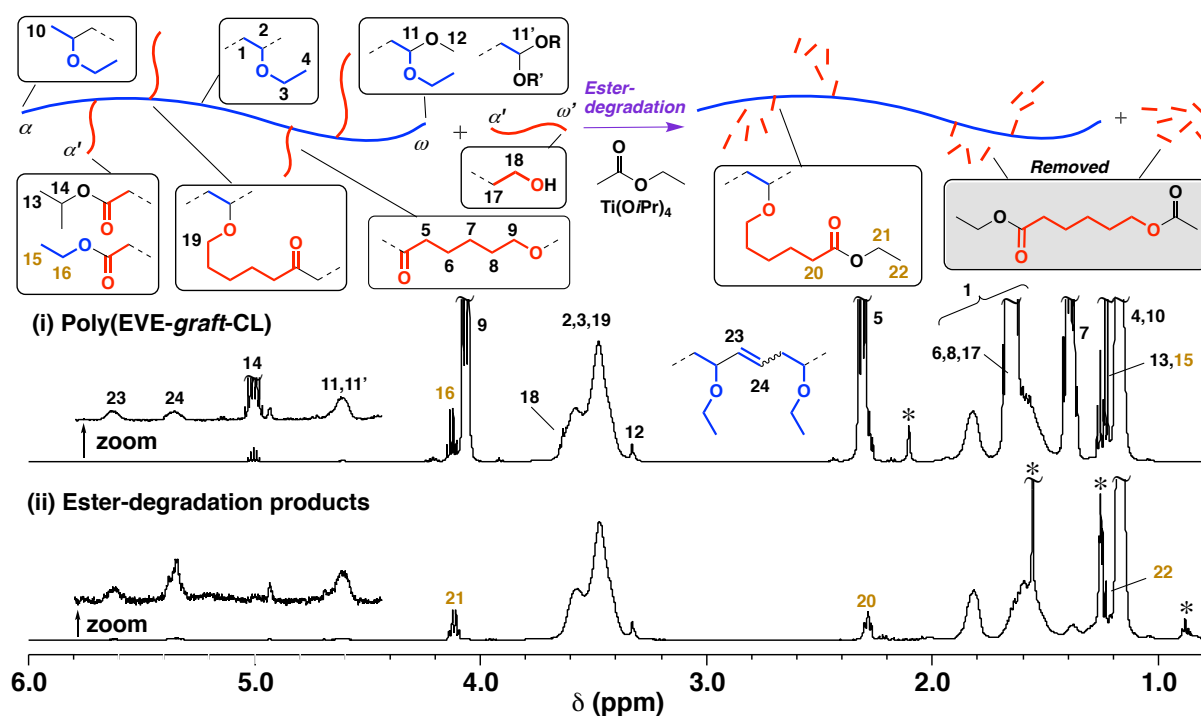


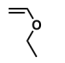
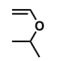
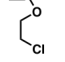
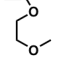
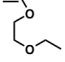
Figure 3. (i) 1H NMR spectra of the product obtained by the copolymerization of EVE and CL catalyzed by $TiCl_4/Ti(OiPr)_4$ (entry 6 in Table 1) and (ii) the transesterification product; transesterification: 25 mM $Ti(OiPr)_4$ in $EtOAc/CH_2Cl_2$ (8/1 v/v; 0.3 wt% polymer) at 70 °C for 21 h; *vaseline, acetone, and water.

Transesterification of the product polymer with ethyl acetate by $\text{Ti}(\text{OiPr})_4$ corroborated the formation of a graft copolymer. The ^1H NMR spectrum of the transesterification product did not include the peak derived from CL homosequences [Figure 3(ii), peak 9], indicating that the degradation proceeded quantitatively. In addition, the degradation product from CL homosequences (Figure 3, filled with gray) was completely removed during purification, as confirmed by the absence of an acetyl group-derived peak at approximately 2.0 ppm. Accordingly, the resulting ester-derived peaks (peaks 20, 21, and 22) most likely originated from the ester moieties of the CL-derived unit that is attached to the main chain, as illustrated in Figure 3. The integrals of these peaks were consistent with the values expected from the above-estimated graft structures. The clear shift of the main peak in the MWD curve to the low-MW region after transesterification also supported the formation of the graft copolymer (Figure 2). In addition, the MWD of the transesterification product was not broad, which indicated that the cationic polymerization of EVE proceeded in a relatively controlled manner.¹⁷

I-2. *Effects of Vinyl Ethers*

Next, several kinds of VEs were copolymerized with CL using $\text{HfCl}_4/\text{Hf}(\text{O}i\text{Bu})_4$ as a catalyst to examine the effects of the alkoxy side chains of VEs on the polymerization kinetics (Table 2). All the VEs tested were consumed at rates comparable to the consumption rate of CL when the molar ratio of catalysts and/or solvent polarity were appropriately tuned according to the reactivity of each monomer. The grafting densities of the copolymers were significantly influenced by the kinds of VEs (Figure 4A, green circles). For example, isopropyl VE (IPVE) produced not a graft copolymer but a mixture of a diblock copolymer and both IPVE and CL homopolymers (entry 2 in Table 2), as reported in Chapter 2, which indicated that the IPVE-derived isopropoxy group on the acetal-type dormant species was not abstracted (path C in Scheme 1B did not proceed). EVE, MOVE, and EOVE gave copolymers having similar grafting densities (entries 1, 4, and 5). Notably, a copolymer obtained with CEVE had a grafting density twice as large as that of a copolymer obtained with EVE, which suggested frequent occurrence of the AGE reaction.

Table 2. Copolymerization of various VEs and CL using $\text{HfCl}_4/\text{Hf}(\text{O}i\text{Bu})_4$ as catalysts^a

entry	VEs	$\text{HfCl}_4/\text{Hf}(\text{O}i\text{Bu})_4$ (mM)	time (h)	conv. (%) ^b		$M_n \times 10^{-3}$ ^c	M_w/M_n ^c	grafting length ^d	grafting density ^d
				VEs	CL				
1	 EVE	12/8.0	80	96	44	3.1	2.40	2.8	15
2	 IPVE	12/8.0	70	67	44	3.2	2.66	8.1	~1
3	 CEVE	12/10	309	58	95	5.4	1.62	4.1	40
4	 MOVE	12/10	60	73	73	4.0	2.06	5.1	20
5	 EOVE	12/8.0	86	95	25	3.8	1.80	3.0	17

^a $[\text{VEs}]_0 = 0.75\text{--}0.77$ M, $[\text{CL}]_0 = 0.76$ M in CH_2Cl_2 (entries 1 and 3–5) or toluene (entry 2) at 30 °C. ^bDetermined by ^1H NMR analysis. ^cDetermined by GPC (polystyrene standards). ^dEstimated by ^1H NMR.

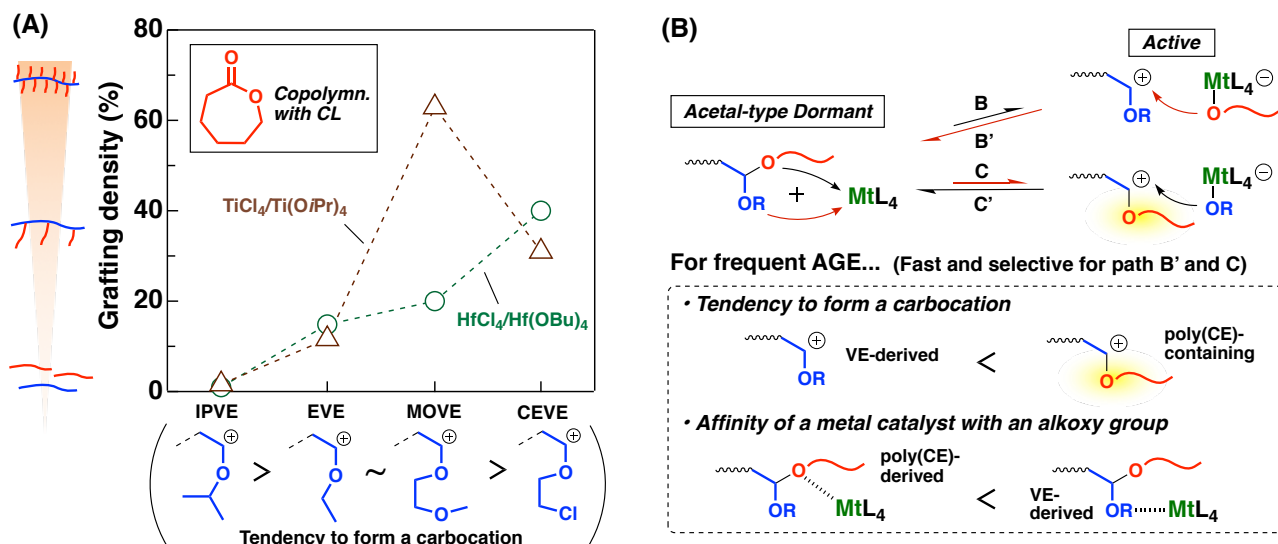


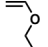
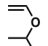
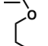
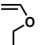
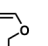
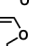
Figure 4. (A) The grafting densities of the products obtained by the copolymerization of various VEs and CL using HfCl₄/Hf(OBu)₄ or TiCl₄/Ti(OiPr)₄ as catalysts and (B) key factors determining the frequency of AGE reactions.

The difference in grafting density among different kinds of VEs was reasonably explained based on the mechanisms of the AGE reactions. A high grafting density was achieved when paths B' and C in Figure 4B proceeded rapidly and selectively. Considering the abstraction of either of the alkoxy groups from an acetal end (path B or path C), the tendency to form a carbocation is likely responsible for the selectivity. Specifically, the less a VE-derived (original) carbocation tends to form, the more path C proceeds selectively, thereby producing a copolymer with a high grafting density. This expectation was consistent with the actual results. For example, IPVE, which likely has a greater tendency to form a carbocation than the other VEs used due to the secondary alkyl side chain, did not generate graft chains, while CEVE, a carbocation from which is not favored due to the electron-withdrawing nature of the side chain, produced a high-density graft copolymer. As another factor, the affinity between metal catalysts and alkoxy groups is likely responsible for the selectivity. For example, when a VE-derived alkoxy group has a strong affinity for the metal catalysts, path C will be much more favored than path B. IPVE has a sterically hindered alkoxy oxygen, which is another possible cause of the negligible abstraction of the isopropoxy group by the catalysts.¹⁸

Surprisingly, a copolymer with a grafting density of 66% was produced when MOVE and CL were copolymerized with TiCl₄/Ti(OiPr)₄ (entry 4 in Table 3). This copolymer had a short grafting length and a notably narrow MWD (Figure 5A), which stemmed from the frequent AGE reactions. By contrast, the grafting densities of the products obtained with IPVE, EVE, and CEVE catalyzed by TiCl₄/Ti(OiPr)₄ were almost the same as those catalyzed by HfCl₄/Hf(OBu)₄ (entries 1, 2, and 3 in Table 3; Figure 4, brown triangles). From these results, the exceptionally high grafting density of the copolymer with MOVE is attributed to a specific interaction between the titanium metal of the catalysts and the side chain of MOVE (Figure 5B), which led to a fast and selective reaction along path C (Figure 4B). Indeed, the strong affinity of TiCl₄ for 1,2-dimethoxyethane, which has a similar structure to the side chain of MOVE, was suggested in a past study by experimental and computational results.¹⁹ Furthermore, copolymers with very high grafting densities were

obtained even when EOVE (61%) or EOEOVE (57%) was employed instead of MOVE, which demonstrated the importance of the ethylenedioxy structure (entries 5 and 6 in Table 3).

Table 3. Copolymerization of various VEs and CL using $\text{TiCl}_4/\text{Ti}(\text{OiPr})_4$ as catalysts^a

entry	VEs	$\text{TiCl}_4/\text{Ti}(\text{OiPr})_4$ (mM)	time (h)	conv. (%) ^b		$M_n \times 10^{-3}$ ^c	M_w/M_n ^c	grafting length ^d	grafting density ^d	
				VEs	CL					
1		EVE	16/6.0	127	95	91	4.7	2.32	9.6	10
2		IPVE	12/6.0	99	80	95	7.0	2.66	18	~1
3		CEVE	18/6.0	170	41	71	2.2	5.42	7.6	31
4		MOVE	16/6.0	65	73	94	6.4	1.41	2.3	66
5		EOVE	16/6.0	87	51	89	7.1	1.38	3.1	61
6		EOEOVE	16/6.0	339	80	66	2.6	1.48	2.0	57

^a $[\text{VEs}]_0 = 0.59\text{--}0.63$ M, $[\text{CL}]_0 = 0.60$ M in CH_2Cl_2 (entries 3) or toluene (entries 1, 2, and 4–6) at 20 °C. ^bDetermined by ^1H NMR analysis. ^cDetermined by GPC (polystyrene standards). ^dEstimated by ^1H NMR.

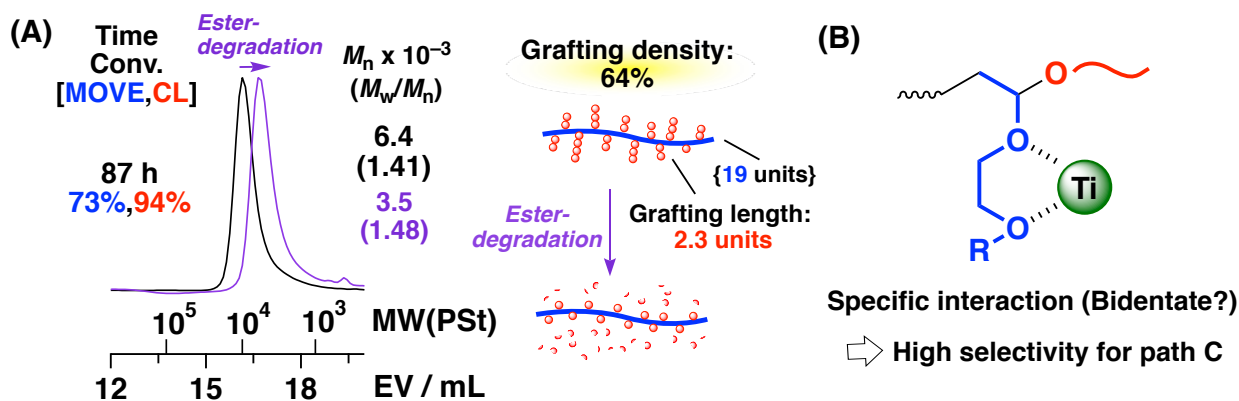
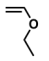
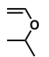
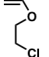
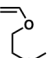


Figure 5. (A) MWD curves of the product obtained by the copolymerization of MOVE and CL catalyzed by $\text{TiCl}_4/\text{Ti}(\text{OiPr})_4$ (black; entry 4 in Table 3) and the transesterification product (purple); transesterification: 25 mM $\text{Ti}(\text{OiPr})_4$ in $\text{EtOAc}/\text{CH}_2\text{Cl}_2$ (8/1 v/v) (0.3 wt% polymer) at 70 °C for 21 h. (B) A specific interaction between an ethylenedioxy group and a titanium catalyst.

I-3. Effects of Cyclic Esters

Copolymerization of ϵ -heptanolactone (ϵ -HepL), which generates a branched alkoxy propagating end, and various VEs was conducted with Ti catalysts to examine the effect of the CE-derived alkoxy group on the copolymerization kinetics (Table 4; Figure 6). The introduction of a branched structure to the CE-derived alkoxy group is expected to enhance the grafting density because the selectivity for path C likely increases upon activation of the dormant acetal, as in the case of the copolymerization of IPVE with CL. Indeed, the copolymerization of IPVE with ϵ -HepL produced a graft copolymer (entry 2 in Table 4), unlike the case with CL, which suggested an increase in the selectivity for path C. However, the grafting density was not enhanced in the copolymerization of ϵ -HepL with EVE and even decreased in the copolymerization with MOVE and CEVE (entries 1, 3, and 4). These results are possibly explained by the decrease in the rate of path B', which is the reaction of a carbocation and a CE-derived alkoxy ligand, due to steric hindrance. The trade-off of these two factors was most likely a result of the introduction of the branched structure.

Table 4. Copolymerization of various VEs and ϵ -HepL using $\text{TiCl}_4/\text{Ti}(\text{O}i\text{Pr})_4$ as catalysts^a

entry	VEs	$\text{TiCl}_4/\text{Ti}(\text{O}i\text{Pr})_4$ (mM)	time (h)	conv. (%) ^b		$M_n \times 10^{-3}$ ^c	M_w/M_n ^c	grafting length ^d	grafting density ^d
				VEs	ϵ -HepL				
1	 EVE	16/6.0	246	77	87	3.8	1.86	6.7	12
2	 IPVE	10/6.0	165	52	85	3.7	1.57	9.7	8.0
3	 CEVE	17/6.0	407	53	81	1.3	1.94	5.8	25
4	 MOVE	14/6.0	250	40	87	2.6	1.81	5.1	38

^a $[\text{VEs}]_0 = 0.59\text{--}0.60$ M, $[\epsilon\text{-HepL}]_0 = 0.60$ M in CH_2Cl_2 (entry 3) or toluene (entries 1, 2, and 4) at 20 °C. ^bDetermined by ^1H NMR analysis. ^cDetermined by GPC (polystyrene standards). ^dEstimated by ^1H NMR.

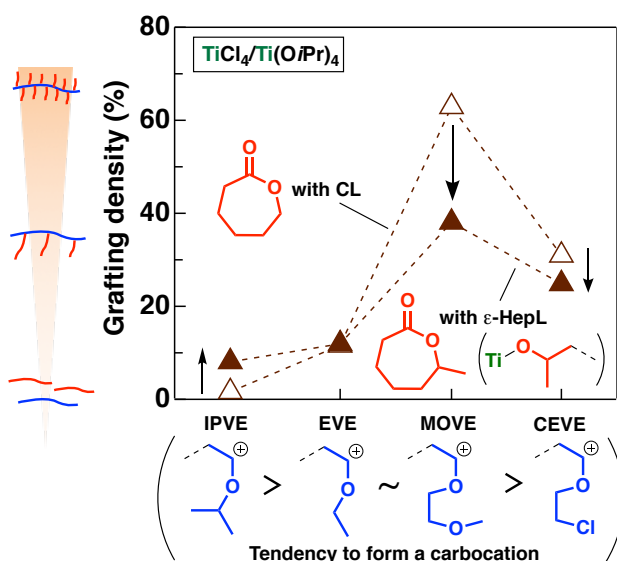


Figure 6. The grafting densities of the products obtained by the copolymerization of various VEs with CL or ϵ -HepL catalyzed by $\text{TiCl}_4/\text{Ti}(\text{O}i\text{Pr})_4$ (data shown with open symbols are the same as the data shown in Figure 4A).

Copolymerization of EVE with other cyclic esters (Scheme 1C) was also performed with $\text{TiCl}_4/\text{Ti}(\text{OiPr})_4$ catalysts. The copolymerization with δ -hexanolactone (δ -HexL), a six-membered CE with a methyl group on the ester-adjacent carbon, proceeded slowly to yield a graft copolymer. However, the grafting density was similar to that with ϵ -HepL. β -Butyrolactone (β -BL), a four-membered CE with a methyl group, was not consumed at all. The copolymerization with L-Lactide (LA) accompanied the AGE reactions; however, the MW of the obtained copolymer was low because of the frequent chain transfer reactions (alcohol elimination) in the main chain. The formation of a graft copolymer was also suggested with trimethylene carbonate (TMC), a six-membered cyclic carbonate, although transesterification reactions appeared to occur frequently, unlike in the case of the other cyclic esters.

I-4. *Effects of Monomer Concentration*

The graft architectures can also be affected by the monomer concentration. Figure 7A represents the values of grafting density (blue) and grafting length (red) obtained in the copolymerization of CL (0.60 M) and various initial concentrations of EVE ($[\text{EVE}]_0$; 0.30–1.2 M) with the Ti catalysts. In this graph, the grafting density was inversely proportional to $[\text{EVE}]_0$, which is reasonable because more EVE is added between two consecutive AGE events at higher $[\text{EVE}]_0$. By contrast, the grafting length was almost constant regardless of $[\text{EVE}]_0$, which implies that the concentration of EVE does not affect the frequency of the AGE reactions. Figure 7B shows the influences of $[\text{CL}]_0$ on the copolymerization behavior. As expected, the grafting length was proportional to $[\text{CL}]_0$. Notably, the grafting density also increased as $[\text{CL}]_0$ increased. This result suggests that at lower CL concentrations, “meaningless” AGE reactions between the same alkoxy group, which results from the absence of CL propagation from the abstracted alkoxy group, occur frequently, thus resulting in a low grafting density. The effects of monomer concentrations on the copolymerization behavior are schematically summarized in Figure 7C.

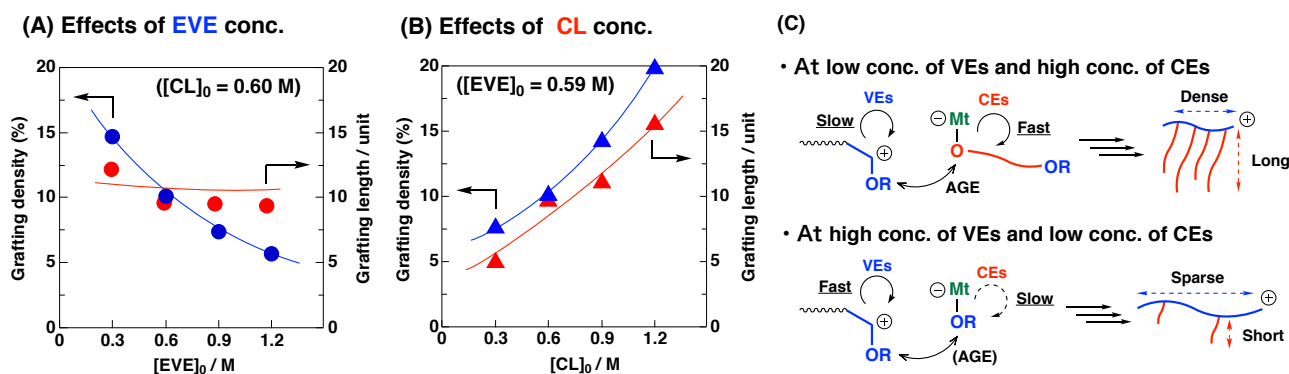


Figure 7. Effects of initial concentrations of (A) EVE and (B) CL on the grafting density and grafting length in the copolymerization of EVE and CL catalyzed by $\text{TiCl}_4/\text{Ti}(\text{OiPr})_4$, and (C) illustrations of graft architectures obtained at different monomer concentrations.

The grafting density and grafting lengths were not constant during polymerization but changed continuously depending on the instantaneous monomer concentrations. Figure 8 shows the time–conversion plots and the instantaneous and accumulative grafting density and grafting length in the copolymerization of EVE and CL with Hf catalysts. Figure 8B indicates that the grafting density was very high in the late stage of polymerization, which is most likely due to a very small amount of remaining EVE monomers. This dependency of the grafting density on the EVE concentration is consistent with the results in Figure 7A to some extent. In addition, the effect of the remaining CL concentration should also be taken into consideration. The decrease in the CL concentration in the late stage will contribute to the decrease in the grafting density due to the “meaningless” AGE reactions (*vide supra*). The balance in the consumption of both monomers is responsible for the grafting density in the late stage. In contrast, the grafting length increased first as the polymerization proceeded, then reached a maximum, and finally decreased. The decrease in the grafting length in the late stage is attributable to the decrease in the relative rate of CL propagation compared to the rate of the AGE reactions. The estimated shape of the graft copolymer based on these analyses is illustrated in Figure 8D (chain transfer of the main chain is neglected).

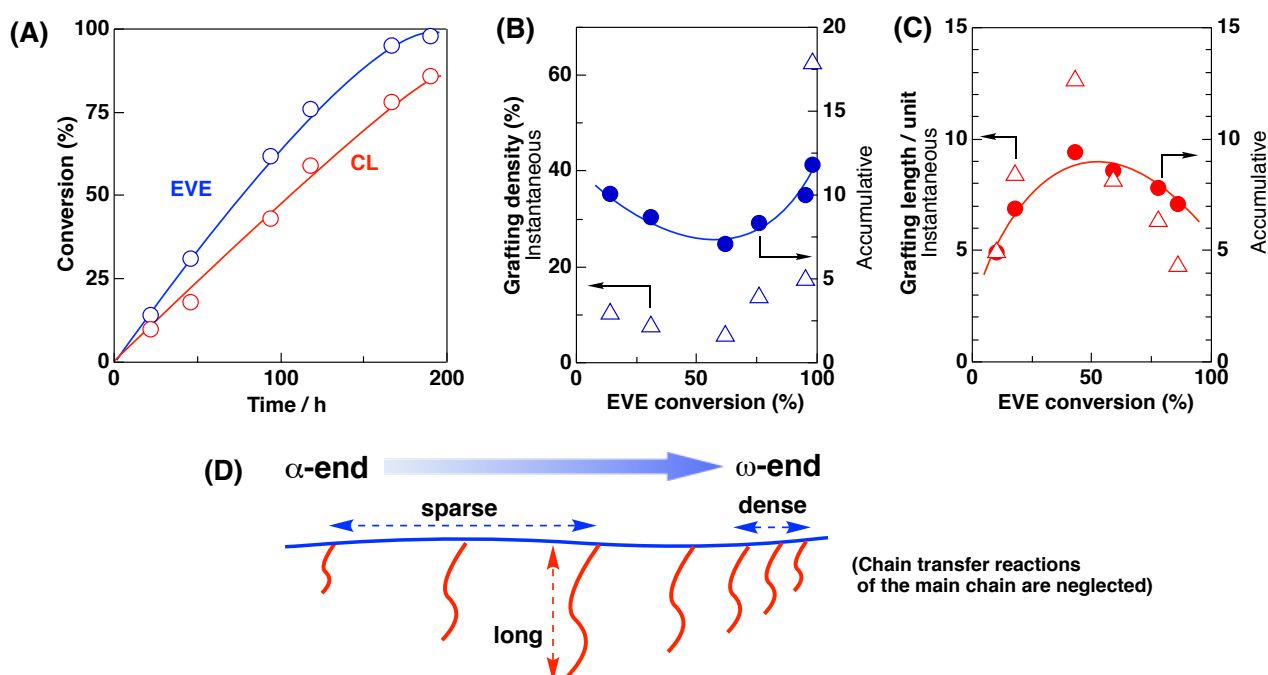


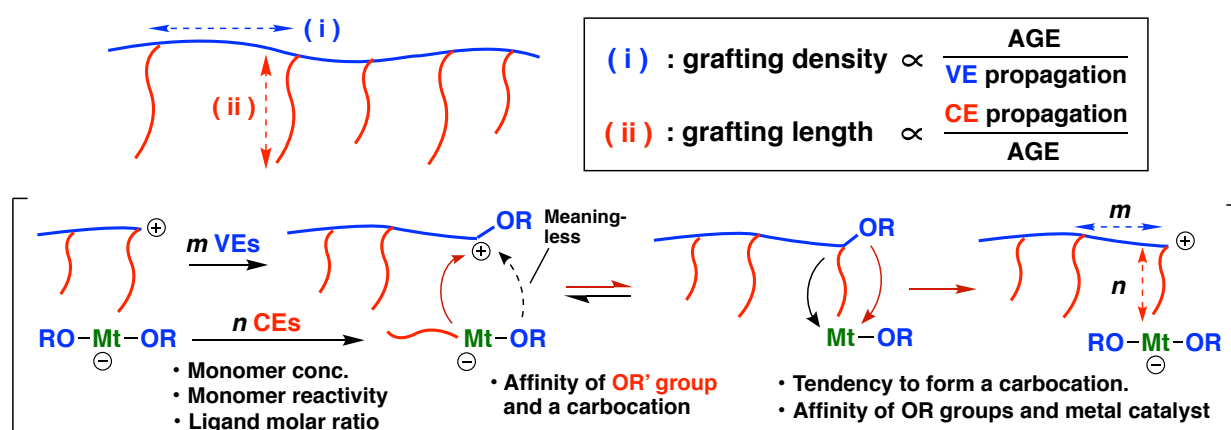
Figure 8. (A) Time–conversion curves for the copolymerization of EVE and CL, (B) the grafting densities and (C) grafting length at different conversion of EVE, and (D) illustration of the architecture of the graft copolymer {polymerization conditions: $[EVE]_0 = 1.52$ M, $[CL]_0 = 1.52$ M, $[HfCl_4]_0 = 12$ mM, $[Hf(OBu)_4]_0 = 10$ mM. in CH_2Cl_2 at 30 °C}.

I-5. Overview and Synthesis of Specific Architectures

Based on the systematic investigations conducted thus far, a principle was proposed for the synthesis of graft architectures by the present mechanisms (Scheme 2). In particular, the control of grafting density and grafting length was feasible by simultaneously controlling the kinetics of the two different propagation reactions and the AGE reaction. The rates of both propagation reactions were tunable by changing the polymerization conditions such as the molar ratio of catalysts, solvent polarity, and monomer concentrations. The rate of the AGE reactions significantly varied depending on the chemical structures of the monomers, which was explained by the following two factors: (a) the tendency to form a VE-type carbocation and (b) the affinity between metal catalysts and alkoxy groups. The kinetics of the two different propagation reactions and the AGE reaction were variable over a wide range; hence, a variety of graft architectures were accessible.

Copolymers with specific shapes were synthesized based on the above guidelines. First, the synthesis of a copolymer with an extremely high grafting density was attempted. For this purpose, MOVE, CL, and $\text{TiCl}_4/\text{Ti}(\text{O}i\text{Pr})_4$ were selected as the optimum monomers and catalysts that most likely induce the AGE reactions most frequently according to the above screening. Moreover, the initial monomer concentrations were set to 0.20 M for MOVE and 1.2 M for CL because a low concentration of VEs and a high concentration of CEs were shown to be effective for achieving a high grafting density (Figure 7A and 7B). Surprisingly, the resultant copolymer had a grafting density of 88% (Figure 9A). The grafting length was approximately 4.2. The results show that the copolymer has a bottlebrush-like polymer structure. In addition, a copolymer having several graft chains with uniform lengths only around the α -end of the backbone, which is regarded as a “broom-like” copolymer, was obtained by the living homopolymerization of CL with $\text{TiCl}_4/\text{Ti}(\text{O}i\text{Pr})_4$ and the subsequent addition of MOVE at the later stage of CL polymerization (Figure 9B).

Scheme 2. Decisive factors for designing various graft architectures



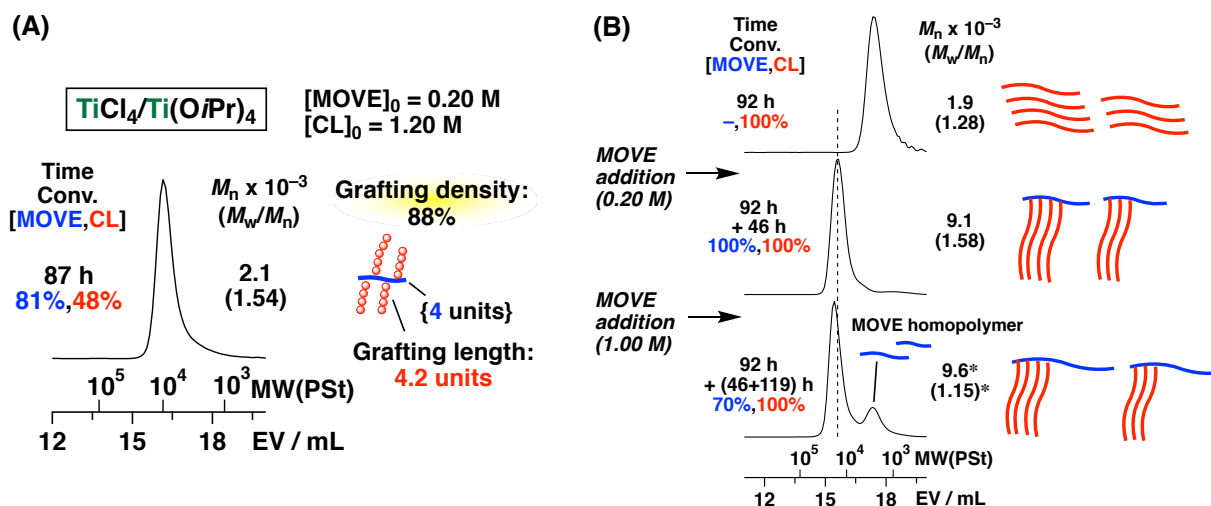


Figure 9. MWD curves of (A) the product obtained by the copolymerization of small amount of MOVE and large amount of CL by $\text{TiCl}_4/\text{Ti}(\text{O}i\text{Pr})_4$ $\{[\text{MOVE}]_0 = 0.20 \text{ M}$, $[\text{CL}]_0 = 1.20 \text{ M}$, $[\text{TiCl}_4]_0 = 16 \text{ mM}$, $[\text{Ti}(\text{O}i\text{Pr})_4]_0 = 6.0 \text{ mM}$, $[\text{IBVE-HCl}]_0 = 12 \text{ mM}$, in CH_2Cl_2 at $20^\circ\text{C}\}$, and (B) the CL homopolymer and poly(MOVE-graft-CL) obtained via the sequential addition of MOVE into the late stage of CL polymerization $\{[\text{MOVE}]_{\text{total}} = 1.00 \text{ M}$, $[\text{CL}]_{\text{total}} = 0.40 \text{ M}$, $[\text{TiCl}_4]_{\text{total}} = 16 \text{ mM}$, $[\text{Ti}(\text{O}i\text{Pr})_4]_{\text{total}} = 10 \text{ mM}$, in toluene at $20^\circ\text{C}\}$; *calculated from the main peak.

II. Thermal Properties and Applications of the Produced Graft Copolymers

DSC measurements were conducted with copolymers having different grafting densities obtained from various VEs and CL (Figure 10). The melting peaks were observed in the cases of all the copolymers except for the copolymer with MOVE. The shapes of the melting peaks and the T_m values were likely related to the grafting length, indicating that the crystalline region is composed of CL homosequences. The absence of melting curves in the case of the copolymer of MOVE and CL is attributable to the short grafting length. In addition, a glass transition was detectable for copolymers of EVE, CEVE, and MOVE. There was a peak due to the glass transition, indicative of the miscibility of the amorphous regions of each segment.

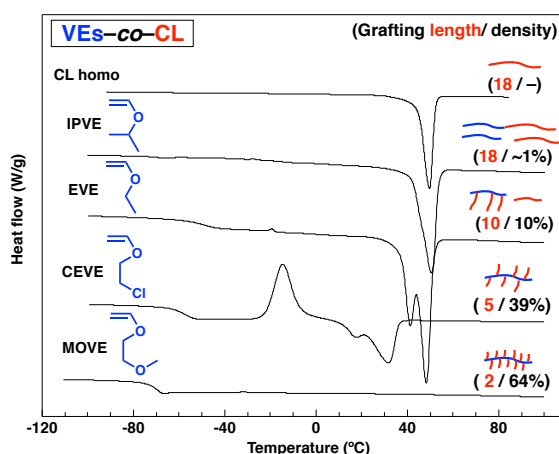


Figure 10. DSC curves for poly(CL) [$M_n(\text{GPC}) = 2.4 \times 10^3$, $M_w/M_n(\text{GPC}) = 1.49$], poly(IPVE-co-CL) (entry 2 in Table 3), poly(EVE-co-CL) (entry 1 in Table 3), poly(CEVE-co-CL) [the same batch as entry 3 in Table 3; obtained at prolonged time (261 h); $M_n(\text{GPC}) = 3.4 \times 10^3$, $M_w/M_n(\text{GPC}) = 3.22$], and poly(MOVE-co-CL) (entry 4 in Table 3).

Table 5. Dispersion of various pigments with polymers via ultrasonification.

entry	pigments	particle size (nm) ^b			
		original	MOVE-graft-CL (3 days later)	MOVE homo	CL homo
1	perylene	990	5–17 (171–192)	–	–
2	Cu phthalocyanine	910	n.d. (317–410)	–	–
3	FeOOH	760/3700	220–320 (285–413)	–	–
4	quinacridone	1400	800–1100 (1200–1400)	–	–
5	TiO ₂	1100	25–35 (43–50)	140	550

^a[pigment] = 0.1 wt%, [polymer] = 0.5 wt% in toluene at 25 °C. ^bDetermined by DLS.

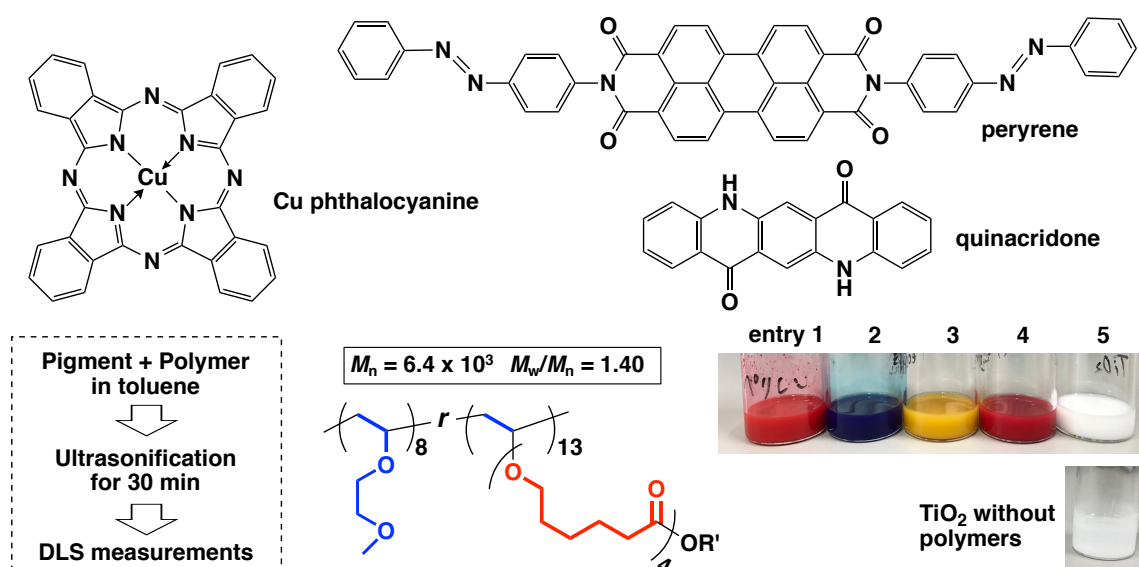


Figure 11. Dispersion of various pigments with poly(MOVE-graft-CL) via ultrasonification.

The obtained graft copolymer of MOVE and CL was employed as a polymeric dispersion agent for several pigments that are generally difficult to disperse (Table 5; Figure 11). The dispersion was carried out via ultrasonification of a mixture of a pigment and the copolymer in toluene for 30 min. The results of DLS measurements conducted soon after ultrasonification suggested that perylene (entry 1 in Table 5) and TiO₂ (entry 5) were dispersed to a very small size, which probably consisted of primary particles.^{20,21} In particular, TiO₂ hardly aggregated in three days, which is indicative of the high dispersion stability. The hydrogen-bonding interaction between the hydroxy groups on the surface of TiO₂ and the side chains of MOVE is possibly responsible for the adsorption, while the graft chains may serve as a steric stabilizer that inhibits aggregation. These two functions of the graft copolymer are likely indispensable for the fine dispersion because the homopolymers of MOVE or CL were not so effective for the dispersion of TiO₂ (Table 5). Well-dispersed TiO₂ has many applications, such as paint, papermaking, cosmetics, and biomedical applications; hence, a facile dispersion method using a graft polymer dispersion agent is highly attractive.

Conclusion

In conclusion, a guideline for creating various graft architectures in the copolymerization of VEs and CEs accompanying AGE reactions was proposed. The grafting density and grafting length of the copolymer were determined by the kinetic balance of the two different propagation reactions and the AGE reactions. The rates of both VE and CE propagation were tunable by changing the molar ratio of the catalysts, the solvent polarity, and the monomer concentrations. The rates of the AGE reactions varied markedly depending on the combinations of monomers and catalysts. In particular, the AGE reactions occurred very frequently when VEs having an ethylenedioxy moiety on the side chain were used in conjunction with $\text{TiCl}_4/\text{Ti}(\text{O}i\text{Pr})_4$, resulting in the formation of a copolymer with a very high grafting density. One of the obtained graft copolymers was highly effective for the dispersion of TiO_2 . The study in this chapter can be a model case for designing primary polymer structures via the simultaneous occurrence of multiple reactions. Moreover, the facile synthesis method for various graft architectures will contribute to the study of the structure-property relationship with special architectures, which will lead to the exploitation of the latent potential of these polymers.

References and Notes

1. Hadjichristidis, N.; Pitsikalis, M.; Iatrou, M.; Drive, P.; Chatzichristi, M.; Sakellariou, G. In *Encyclopedia of Polymer Science and Technology*; Seidel, A.; Wiley, John. Eds.; New York, **2010**.
2. Uhrig, D.; Mays, J. *Polym. Chem.* **2011**, *2*, 69.
3. Lutz, P. J.; Peruch, F. In *Polymer Science: A Comprehensive Reference*; Matyjaszewski, K., Möller, M. Eds.; Elsevier B.V.: Amsterdam, **2012**; Vol. 6.14.
4. Mecerreyes, D.; Moineau, G.; Dubois, P.; Jérôme, R.; Hedrick, L. J.; Hawker, J. C.; Malmström, E. E.; Trollsas, M. *Angew. Chem. Int. Ed.* **1998**, *37*, 1275.
5. Bielawski, C. W.; Louie, J.; Grubbs, R. H. *J. Am. Chem. Soc.* **2000**, *122*, 12872.
6. de Freitas, A. G.; Trindade, S. G.; Murano, P. I.; Schmidt, V.; Satti, A. J.; Villar, M. A.; Ciolino, A. E.; Giacomelli, C. *Macromol. Chem. Phys.* **2013**, *214*, 2336.
7. Simionescu, C. I.; Grigoras, M.; Bicu, E.; Onofrei, G. *Polym. Bull.* **1985**, *14*, 79.
8. Yang, H.; Xu, J.; Pispas, S.; Zhang, G. *Macromolecules* **2012**, *45*, 3312.
9. Kanazawa, A.; Kanaoka, S.; Aoshima, S. *J. Am. Chem. Soc.* **2013**, *135*, 9330.
10. Aoshima, H.; Uchiyama, M.; Satoh, K.; Kamigaito, M. *Angew. Chem. Int. Ed.* **2014**, *53*, 10932.
11. Satoh, K.; Hashimoto, H.; Kumagai, S.; Aoshima, H.; Uchiyama, M.; Ishibashi, R.; Fujiki, Y.; Kamigaito, M. *Polym. Chem.* **2017**, *8*, 5002.
12. Higuchi, M.; Kanazawa, A.; Aoshima, S. *ACS Macro Lett.* **2017**, *6*, 365.
13. Higashimura, T.; Kamigaito, M.; Kato, M.; Hasebe, T.; Sawamoto, M. *Macromolecules* **1993**, *26*, 2670.
14. Mino, T.; Masuda, S.; Nishio, M.; Yamashita, M. *J. Org. Chem.* **1997**, *62*, 2633.
15. (a) Kanazawa, A.; Kanaoka, S.; Aoshima, S. *Macromolecules* **2010**, *43*, 2739. (b) Kanazawa, A.; Kanaoka, S.; Aoshima, S. *J. Polym. Sci., Part A: Polym. Chem.* **2010**, *48*, 2509

16. (a) Kamigaito, M.; Sawamoto, M.; Higashimura, T. *Macromolecules* **1995**, *28*, 5671. (b) Bradley, D. C.; Abd-el Halim, F. M.; Mehrotra, R. C.; Wardlaw, W. J. *Chem. Soc.* **1952**, 4609. (c) Bradley, D. C.; Hancock, D. C.; Wasdlaw, W. J. *Chem. Soc.* **1952**, 2773.
17. The MW of the backbone is too small, although the cationic polymerization is most likely initiated from adventitious water in the reaction mixture, the amount of which is generally not so high (approximately 2 mM). The reason is currently unclear.
18. (a) Silverman, R.; Edington, C.; Elliott, J. D.; Johnson, W. S. *J. Org. Chem.* **1987**, *52*, 180. (b) Denmark, S. E.; Willson, T. M.; Almstead, N. G. *J. Am. Chem. Soc.* **1989**, *111*, 9258. (c) Kobayashi, S.; Arai, K.; Yamakawa, T.; Chen, Y.; Salter, M. M.; Yamashita, Y. *Adv. Synth. Catal.* **2011**, *353*, 1927. (d) Kinugasa, M.; Harada, T.; Egusa, T.; Fujita, K.; Oku, A. *Bull. Chem. Soc. Jpn.* **1996**, *69*, 3639.
19. Galvallo, L.; Del Piero, S.; Decéré J.-M.; Fedele, R.; Melchior, A.; Morini, G.; Piemontesi, F.; Tolazzi, M. *J. Phys. Chem. C* **2007**, *111*, 4412.
20. Farrokhpay, S. *Adv. Colloid Interface Sci.* **2009**, *151*, 24.
21. Klimkevicius, V.; Graule, T.; Makuska, R. *Langmuir* **2015**, *31*, 2074.

Supporting Information

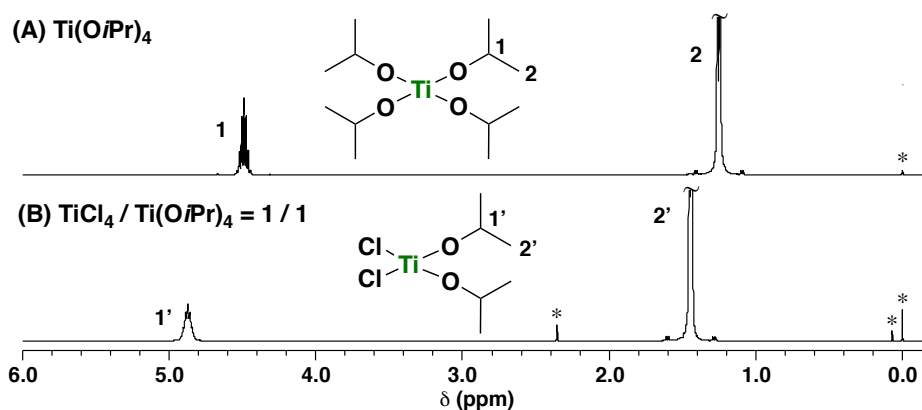


Figure S1. ^1H NMR spectra of (A) $\text{Ti}(\text{O}i\text{Pr})_4$ and (B) the mixture of an equimolar amount of TiCl_4 and $\text{Ti}(\text{O}i\text{Pr})_4$; *TMS, grease, and toluene.

Part II

Synthesis of Alternating Copolymers via Concurrent Unzipping and Scrambling Reactions in Cationic Ring-Opening Copolymerization

Tandem Unzipping and Scrambling Reactions for the Synthesis of Alternating Copolymers by the Cationic Ring-Opening Copolymerization of a Cyclic Acetal and a Cyclic Ester

Introduction

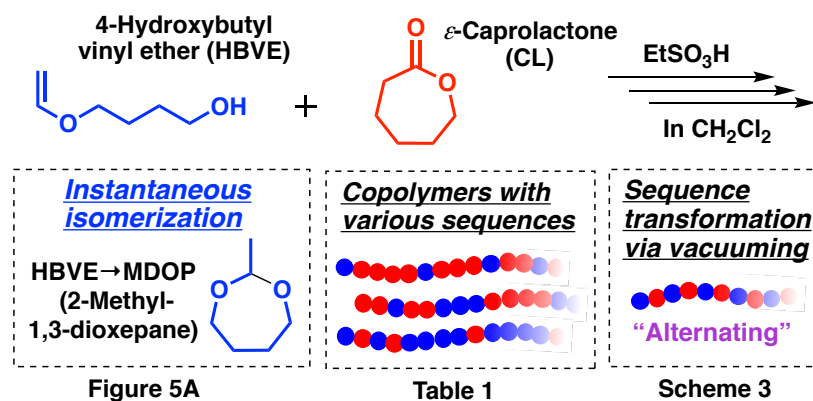
Simultaneous copolymerization via different mechanisms is an intriguing strategy for synthesizing highly functional polymer materials.^{1–12} In particular, copolymers with different types of monomers can be obtained without cumbersome multistep reactions involving purification and isolation. For example, a diblock copolymer of ϵ -caprolactone (CL) and styrene was produced in one pot via simultaneous (but orthogonal) living coordination ring-opening polymerization (ROP) and nitroxide-mediated radical polymerization using a bifunctional initiator with initiating sites for both polymerizations.¹ A specific type of this method in which different mechanisms proceed nonorthogonally has the potential to produce copolymers that are otherwise difficult to obtain. This class of copolymerization includes the copolymerization of vinyl monomers and cyclic monomers via the concurrently occurring vinyl-addition and ring-opening mechanisms^{2–8} and chain- and step-growth copolymerization.^{9,10} These polymerizations are effective for the synthesis of multiblock-type copolymers via two-way crossover reactions. A wider variety of copolymer sequences and architectures can be produced via this type of copolymerization by different intermediates,^{11,12} because the relative rates of both reactions are tuned independently by changing the reaction conditions, such as the amount of catalyst and the solvent polarity.

The sequence of a copolymer chain is determined by several factors depending on the type of polymerization process. When previously formed polymer chains (backbone) do not decompose throughout a copolymerization process, the sequence is exclusively dominated by the selectivity of the addition of each monomer to the active species, which is related to the monomer reactivity ratio in chain-growth polymerization,¹³ or by the selectivity of the reaction between the reactive species in step-growth polymerization.¹⁴ By contrast, when polymer chains decompose via some reactions, additional factors should be taken into consideration. For example, in copolymerization involving depolymerization (equilibrium copolymerization), various parameters, such as equilibrium constants, are responsible for the resulting sequence of copolymer chains.^{15,16} Another example is copolymerization involving random segmental exchanges (scrambling) in main chains, in which copolymer sequences are eventually dominated by a statistical distribution.^{17–19} Many studies have been conducted on this type of polymerization based on reversible exchange reactions of “dynamic covalent bonds”, such as transesterification¹⁸ and radical exchange reactions.¹⁹ Copolymerization involving this type of reaction is generally not suitable for precisely controlling copolymer sequences due to its random nature.

In this study, the author designed a novel nonorthogonal copolymerization system by combining different types of cationically polymerizable monomers, 4-hydroxybutyl vinyl ether (HBVE) and CL, using EtSO₃H as a catalyst (Scheme 1). In general, such copolymerizations via different mechanisms require an astute strategy to avoid interfering with each reaction and to connect different types of polymer chains. The combination of the cationic polyaddition of vinyl ethers with a hydroxyl group on the side chain (OH-VEs)^{20,21} and the ROP of cyclic esters via the activated monomer (AM) mechanism²² can satisfy these demands due to

their mechanistic similarity (Scheme S1 in the Supporting Information). Indeed, copolymers containing HBVE and CL units were successfully produced via simultaneous copolymerization; however, HBVE was quantitatively isomerized to 2-methyl-1,3-dioxepane (MDOP) in the very early stages. Therefore, the reaction devised in this study is essentially equivalent to the cationic ring-opening copolymerization of MDOP and CL, which has also not been reported thus far.^{23,24} In the copolymerization, MDOP was incorporated into polymer chains, even below its equilibrium monomer concentration ($[MDOP]_e$), because depolymerization via unzipping was suppressed due to the generation of MDOP-CL heterosequences. More interestingly, the sequence transformation of a copolymer with no CL homosequences to an “alternating” copolymer was achieved by utilizing unzipping and scrambling reactions during copolymerization.

Scheme 1. Synthesis of poly(HBVE-*co*-CL)s with various sequences via isomerization of HBVE to MDOP and subsequent cationic copolymerization of MDOP and CL



Experimental Section

Materials.

4-Hydroxybutyl vinyl ether (HBVE; Aldrich; >99%), tetrahydrofuran (THF; Wako; >99.5%), butyl acetate (Wako; >98.0%), and butyl butyrate (TCI; >99.0%) were distilled twice over calcium hydride under reduced pressure. Commercially available $EtSO_3H$ (Aldrich; 95%) was used without further purification after preparing a stock solution of this compound in dichloromethane. Other materials were prepared and used as described in the preceding chapters.

Synthesis of 2-Methyl-1,3-Dioxepane (MDOP).

MDOP was synthesized by acetal exchange between diethylacetal and 1,4-butanediol using indium(III) trifluoromethanesulfonate as a catalyst at room temperature.^{25,26} After acetal exchange, the reaction mixture was concentrated to remove ethanol, which was generated as a byproduct. The product was purified by distillation under reduced pressure. See Ref. 26 for the characterization data.

Polymerization Procedure.

The following is a typical polymerization procedure. A glass tube equipped with a three-way stopcock was dried using a heat gun (Ishizaki; PJ-206A; the blowing temperature was ~450 °C) under dry nitrogen. Dichloromethane, HBVE, and CL were sequentially added to the tube using dry syringes. The polymerization was started by the addition of a solution of EtSO₃H in dichloromethane. After a predetermined period, the reaction mixture was quenched with methanol containing a small amount of aqueous ammonia. The quenched mixture was diluted with dichloromethane and then washed with water. The volatiles were removed under reduced pressure to afford the polymer. Monomer conversion was determined by ¹H NMR analysis of the quenched reaction mixture.

Vacuuming Procedure.

The pressure in the glass tube was reduced using a vacuum pump (SATO VAC INC; TSW-50). The vacuum pump was connected to a mercury manometer, a glass trap chilled with liquid nitrogen, and the reaction tube equipped with a three-way stopcock, in this order. The pressure was approximately 2 mmHg throughout the vacuuming process.

Acid Hydrolysis.

The acid hydrolysis of the polymer was conducted in a manner as described in Chapter 2.

Transesterification.

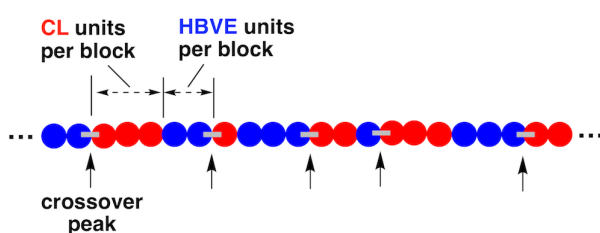
Transesterification was conducted in a manner similar to that described in Chapter 3.

Characterization.

The molecular weight distributions (MWD), ¹H NMR spectra, MALDI-TOS-MS spectra, ESI-MS spectra, and differential scanning calorimetry (DSC) were measured in a manner similar to that described in the preceding chapters.

Methods for the Calculation of HBVE/CL Units Per Block.

The values were determined based on ¹H NMR integral ratios. HBVE units per block were calculated using the peaks of the ether- or hydroxy-adjacent methylenes (3.3–3.8 ppm) against the peaks of the crossover-derived ester methylenes (4.1 ppm). CL units per block were calculated using the peaks of all ester methylenes (4.0–4.2 ppm) against the crossover-derived ester (4.1 ppm). The peaks of the crossover-derived ester methylene and the ester methylene of the CL homosequences partly overlap; hence, HBVE units per block were sometimes calculated to be slightly less than one. In such cases, HBVE units per block were fixed at 1.0 and CL units per block were calculated using the peaks of all ester (4.0–4.2 ppm) against the peaks of the ether- or hydroxyl-adjacent methylenes (3.3–3.8 ppm).



Results and Discussion

The cationic copolymerization of HBVE (0.50 M) and CL (0.50 M) was examined using EtSO₃H (5.0 mM) as a catalyst in toluene at 30 °C, which resulted in a copolymer consisting of both monomer units (entry 1 in Table 1). The number average molecular weight (M_n) of the products increased as the polymerization proceeded (Figure 1) to reach 14.5×10^3 (main peak). Tailing was observed in the low-molecular-weight region of the MWD curves. MALDI-TOF-MS analysis suggested that the main portion of the tailing was composed of cyclic oligomers (Figure 2). The ¹H NMR spectrum of the polymer obtained at 87 h (Figure 3A) had peaks of structures derived from HBVE and CL units and a structure resulting from the crossover reaction from HBVE to CL [peak 12, which is absent in a CL homopolymer (Figure 3C)], suggesting the successful formation of poly(HBVE-*co*-CL). The average numbers of both monomer units per block, calculated from the ratios of ¹H NMR integrals, were 1.0/3.8 and 1.0/5.7 for HBVE/CL at 12 h and 87 h, respectively. These results indicate that a copolymer with negligible HBVE homosequences and multiple HBVE–CL and CL–HBVE heterosequences per chain was successfully produced.

Table 1. Cationic homopolymerization of HBVE and copolymerization of HBVE and CL using EtSO₃H as a catalyst at various monomer concentrations^a

entry	conc. (M)		time (h)	conv. to polymer (%) ^b		$M_n \times 10^{-3}$ ^c	M_w/M_n ^c	units per block ^d	
	HBVE	CL		HBVE	CL			HBVE	CL
1	0.50	0.50	87	19	98	14.5	1.9	1.0	5.7
2 ^e	0.50 (MDOP)	0.50	82	19	99	15.2	1.9	1.0	5.3
3	2.52	1.98	75	51	100	20.8	2.3	1.4	1.8
4	7.20	0.50	22	72	100	8.8	2.7	11	1.0
5	0.50	–	1	0	–	–	–	–	–
6	3.50	–	4	81	–	10.9	2.2	–	–

^a[EtSO₃H]₀ = 5.0 mM, in CH₂Cl₂ (entries 1–3, 5 and 6) or bulk (entry 4) at 30 °C (entries 1–5) or 0 °C (entry 6).

^bDetermined by ¹H NMR analysis of quenched reaction mixtures. Time–concentration plots of entries 5 and 6 are shown in Figure 7. ^cDetermined by GPC (polystyrene standards). The values were calculated from main peaks.

^dDetermined by ¹H NMR analysis. ^eMDOP was used instead of HBVE.

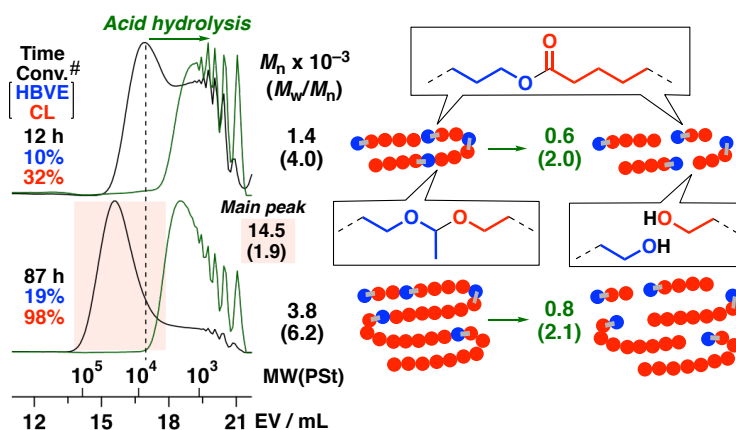


Figure 1. MWD curves of poly(HBVE-*co*-CL)s (black, entry 1 in Table 1) and their acid hydrolysis products (green); #conversion to polymer.

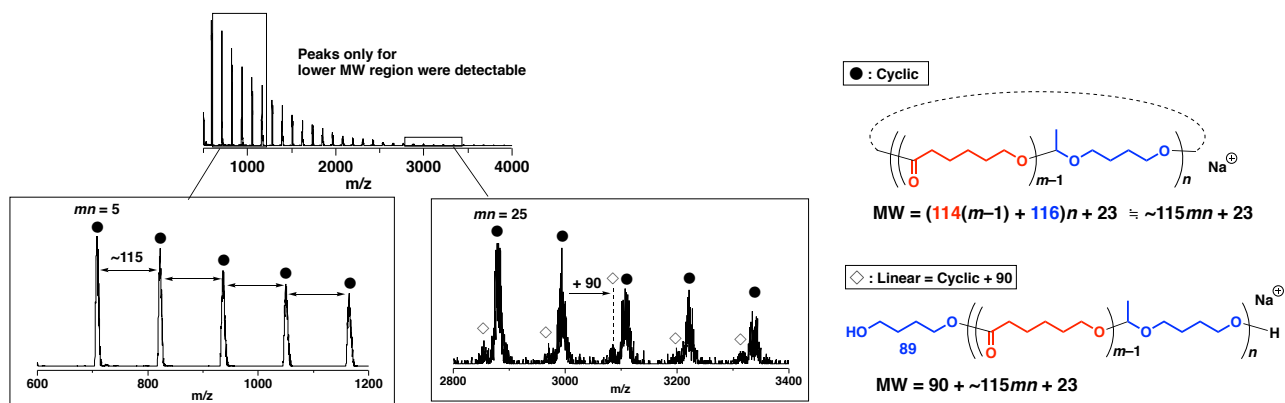


Figure 2. MALDI-TOF-MS spectrum of poly(HBVE-co-CL) (entry 1 in Table 1).

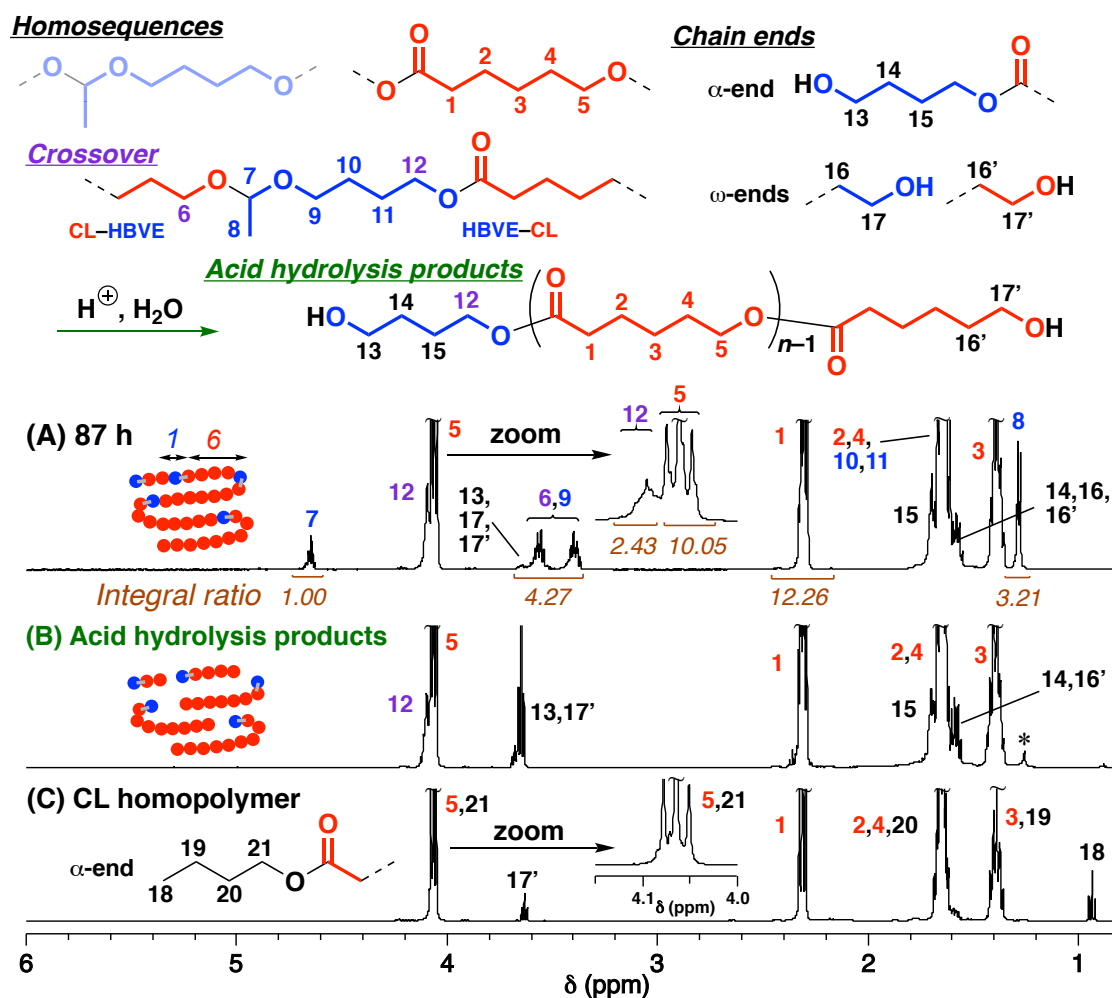


Figure 3. 1H NMR spectra of (A) poly(HBVE-co-CL) obtained at 87 h, (B) its hydrolysis products, and (C) CL homopolymer [M_n (GPC) = 2.4×10^3 , M_w/M_n (GPC) = 1.5] [hydrolysis: 0.5 M HCl in $H_2O/1,2$ -dimethoxyethane (1/1 v/v; 0.5wt% polymer) at r.t. for 3 h; in $CDCl_3$ at 30 °C]; *vaseline.

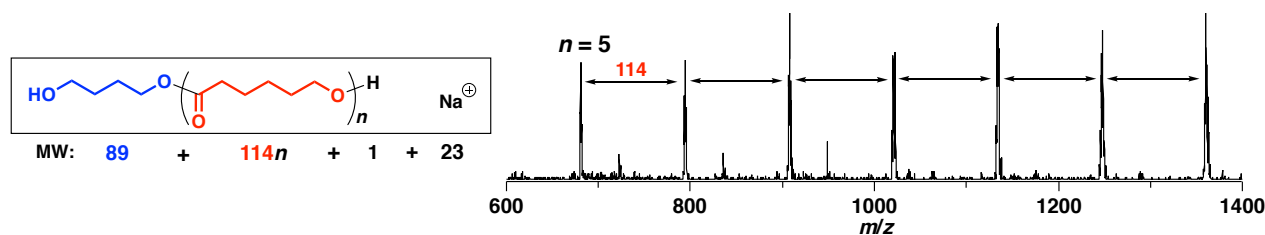


Figure 4. MALDI-TOF-MS spectrum of acid hydrolysis products of the poly(HBVE-co-CL) obtained at 0.50 M monomer concentrations (the sample shown in Figure 3B).

The hydrolysis of the copolymers under acidic conditions was conducted to corroborate the copolymer structure. The ^1H NMR spectrum after hydrolysis (Figure 3B) confirmed the disappearance of the peak of the acetal moiety at 4.6 ppm. The hydrolysis products were composed mainly of CL homosequences with a 4-hydroxybutoxy end group derived from the HBVE moiety, as demonstrated by ^1H NMR (Figure 3B) and MALDI-TOF-MS (Figure 4) analyses. In addition, the clear shift in the MWD curves to the lower region and the significant decrease in M_n values after hydrolysis suggests that the copolymer had not a diblock structure but a multiblock structure with many acetal moieties of CL-HBVE heterosequences. The M_n (GPC) values of the hydrolysis products were 0.6 and 0.8×10^3 at 12 and 87 h, respectively, which is consistent with the above-estimated numbers of units per block.

This copolymerization was found to be essentially identical to the cationic ring-opening copolymerization of MDOP and CL due to the instantaneous isomerization of HBVE to MDOP. Figure 5A presents the changes in the concentrations of HBVE, MDOP, and CL in the copolymerization. HBVE was quantitatively consumed (filled blue circles in Figure 5A), and instead, MDOP was formed (open squares) within 5 min. The generated MDOP was gradually consumed during the copolymerization with CL. In addition, the copolymerization of CL with MDOP instead of HBVE under the same conditions, which was conducted to observe differences, resulted in very similar kinetics, molecular weights, and microstructures (entry 2 in Table 1 and Figure 5B). Cyclic acetals were also generated in previous reports on the cationic polyaddition of OH-VEs in THF,^{20,21} although the cyclic acetals were suggested to be unreactive.²⁷

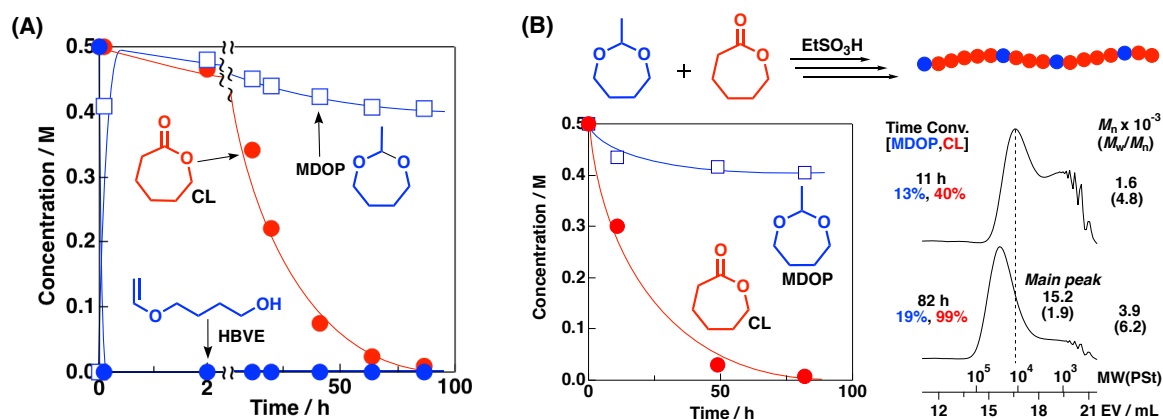


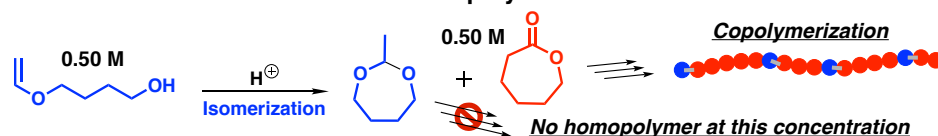
Figure 5. (A) Time-concentration plots for copolymerization of HBVE and CL (entry 1 in Table 1), and (B) Time-concentration plots for copolymerization of MDOP and CL and MWD curves of the obtained products (entry 2).

The propagation reaction of MDOP is considered to proceed mainly via the active chain end (ACE) mechanism at the oxonium chain ends,²⁸ while the propagation of CL probably proceeds only at the hydroxy ends via the AM mechanism (Scheme 2B, left). In addition, intra- and intermolecular chain-end-coupling potentially occurs between the oxonium and hydroxy ends (Scheme 2B, right). The former is likely responsible for the production of a large amount of cyclic oligomers.²⁹ The existence of both oxonium and hydroxy ends is supported by the end-group analysis of HBVE homopolymers (Figure 6). In addition, random segmental exchange via transacetalization^{31,32} (scrambling) was found to occur frequently during the copolymerization (Scheme 2C).³³

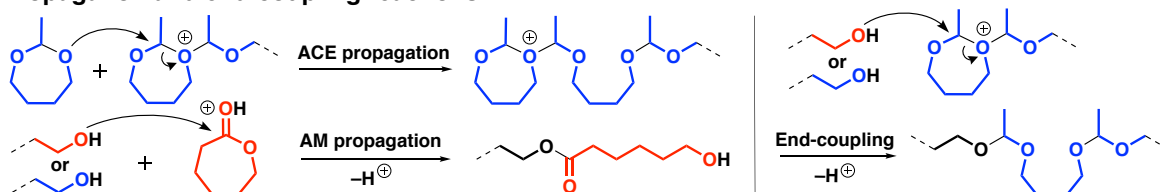
The homopolymerization of HBVE under the same conditions as those used for copolymerization produced only MDOP, and no polymers were obtained (Scheme 2A and Figure 7A), unlike the copolymerization with CL. This result is attributed to the lower monomer concentrations used (0.50 M) compared to [MDOP]_c (2.7 M at 30 °C).^{28,34} HBVE homosequences were also not generated in copolymerization conducted at the same concentration of HBVE (0.50 M; entry 1 in Table 1). Therefore, depolymerization (unzipping) via the backbiting reaction at the oxonium chain end (Scheme 2D, left), which occurs below the equilibrium concentration of MDOP, was most likely suppressed when an ester bond with a CL unit exists next to the oxonium chain end (Scheme 2D, right). This result is partially similar to the copolymerization of nonhomopolymerizable monomers.^{35–39}

Scheme 2. (A) Isomerization of HBVE to MDOP and subsequent cationic copolymerization with CL, (B) propagation and end-coupling reactions, (C) inter- and intramolecular transacetalization in the copolymerization of HBVE and CL (Scheme S2 shows more detailed reaction schemes), and (D) backbiting reactions in the cationic polymerization of HBVE (left) and its suppression in the presence of a CL unit (right)

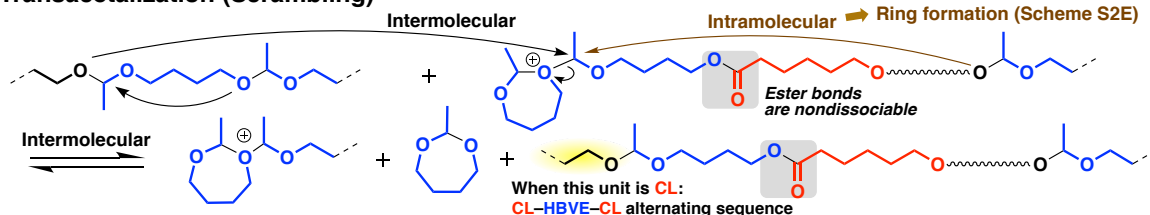
(A) Isomerization of HBVE to MDOP and copolymerization with CL



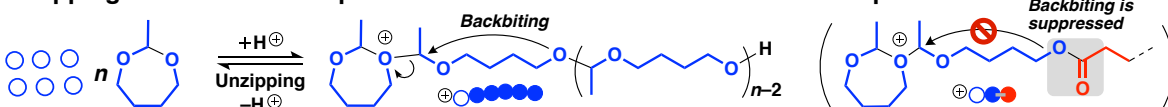
(B) Propagation and end-coupling reactions



(C) Transacetalization (Scrambling)



(D) Unzipping of HBVE homosequences and inertness of HBVE-CL heterosequences



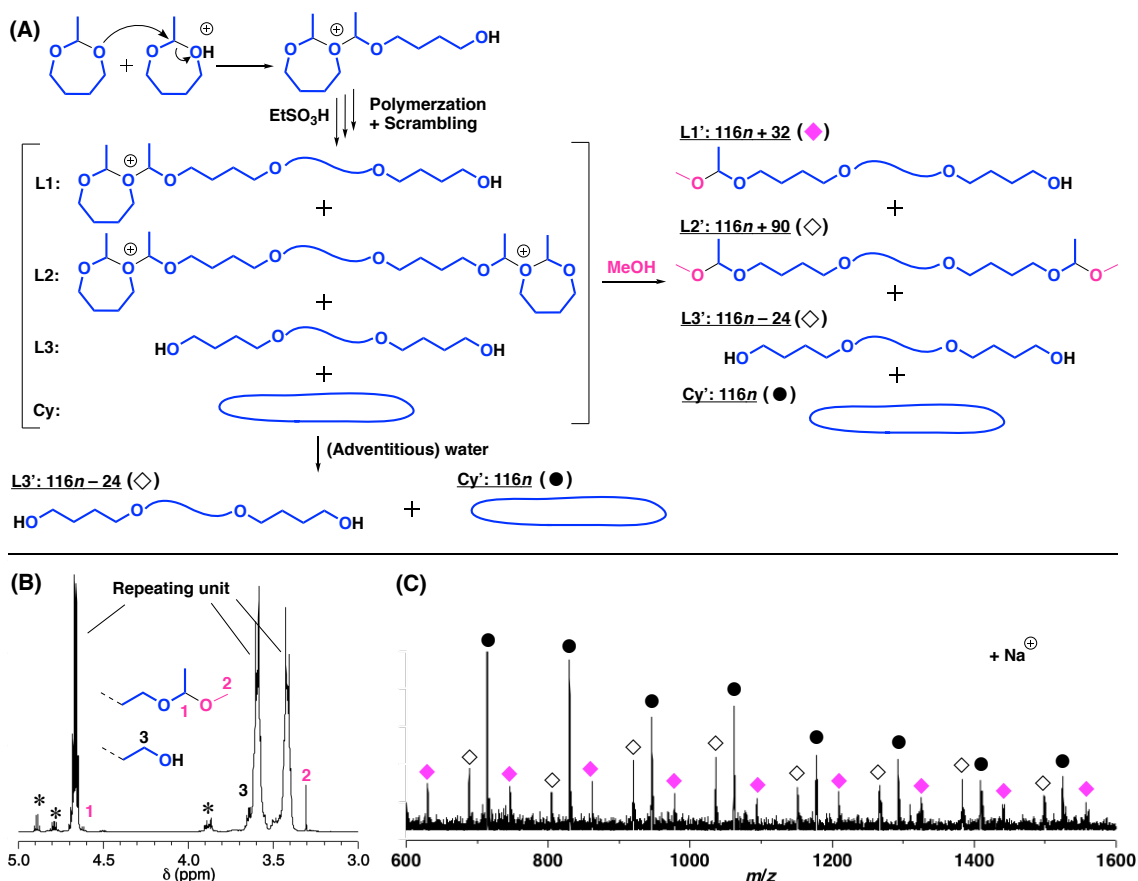


Figure 6. (A) Illustration for the predicted end groups of poly(HBVE) by quenching with MeOH or adventitious water, and (B) ^1H NMR and (C) MALDI-TOF-MS spectra of the poly(HBVE) obtained by quenching with MeOH/ NH_3aq ; *residual MDOP monomer and cyclic dimer. [polymerization conditions: $[\text{HBVE}]_0 = 4.07 \text{ M}$, $[\text{EtSO}_3\text{H}]_0 = 20 \text{ mM}$, in CH_2Cl_2 at 0°C for 43 h: conversion to polymer = 45%, $M_n(\text{GPC}) = 3.2 \times 10^3$, $M_w/M_n(\text{GPC}) = 3.2$].³⁰

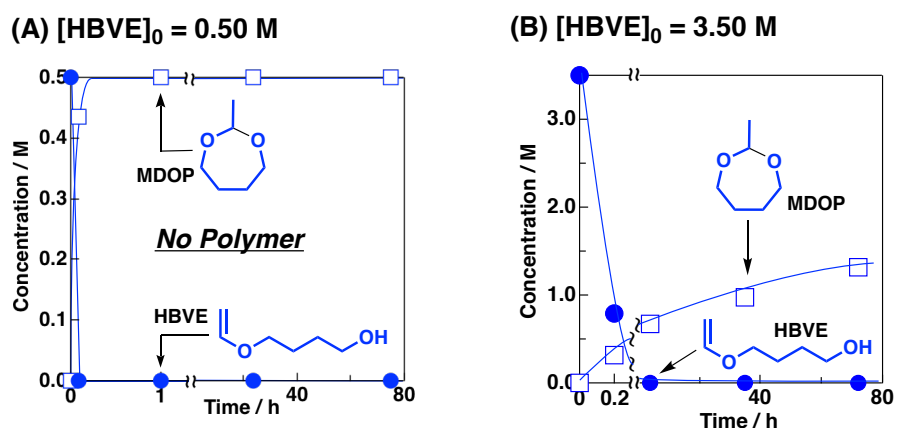
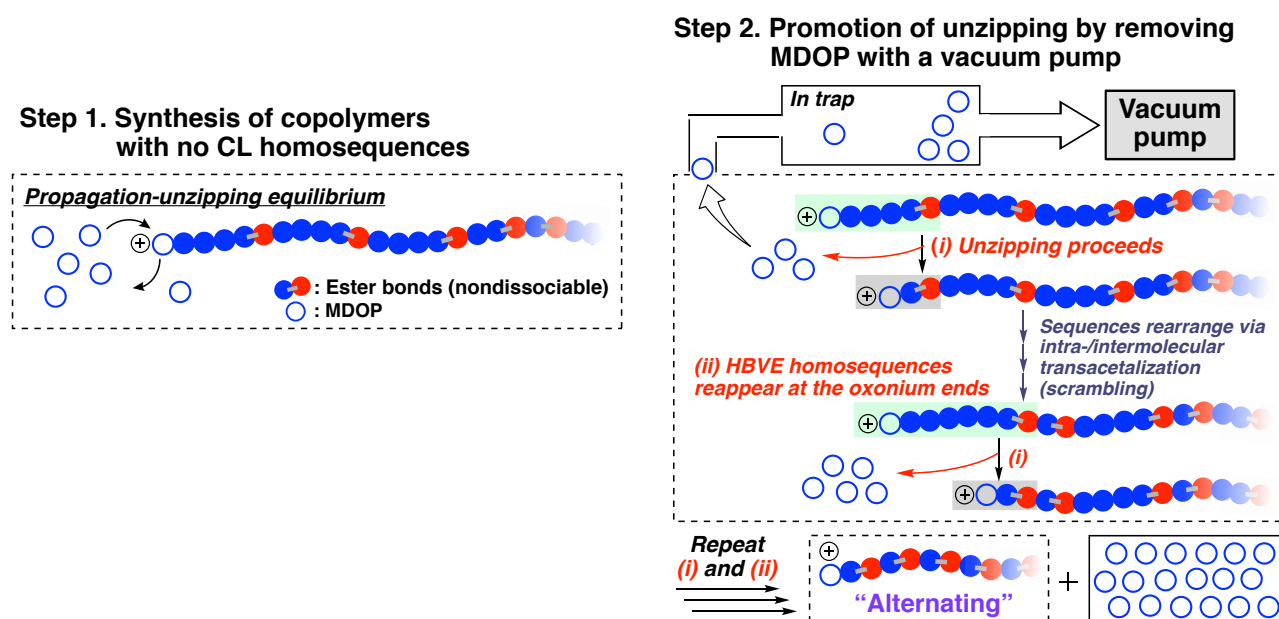


Figure 7. Time–concentration plots for the homopolymerization of HBVE at (A) 0.50 M at 30°C (entry 5 in Table 1), and (B) 3.50 M at 0°C (entry 6).

Copolymers with various types of sequences were obtained by varying the initial monomer concentrations. In contrast to the aforementioned results, HBVE homopolymers were generated at a high HBVE concentration (entry 6 in Table 1 and Figure 7B, 3.50 M; this value is higher than $[\text{MDOP}]_0$), as previously reported.³⁴ This result suggests that copolymers containing HBVE homosequences can also be produced. Indeed, a multiblock-like copolymer of HBVE and CL was generated at high concentrations of both monomers (entry 3). Moreover, even a copolymer with negligible CL homosequences was obtained at a much higher concentration of HBVE compared to that of CL (entry 4).

Based on the characteristic copolymerization behavior, we designed a unique strategy for producing an alternating copolymer as follows: First, the copolymerization is performed at a much smaller concentration of CL than that of HBVE in order to produce a copolymer with no CL homosequences, as in the case of entry 4 in Table 1 (step 1 in Scheme 3). Subsequently, the pressure is reduced using a vacuum pump to remove MDOP (bp 154 °C), which is generated via unzipping reactions, from the system (step 2 in Scheme 3). The decrease in MDOP concentration further moves the position of the propagation–unzipping equilibrium, which promotes the unzipping of HBVE homosequences at the oxonium chain end (Scheme 2D). Unzipping stops when a CL unit emerges next to the chain end (step 2 (i)); however, random sequence redistribution via scrambling occasionally induces the reappearance of HBVE homosequences at the chain end (step 2 (ii)), which leads to unzipping again. The repetition of (i) and (ii) will eventually eliminate all the HBVE homosequences from the polymer chain; hence, a copolymer with “alternating” sequences (acetal and ester units are alternatingly aligned; Scheme S3) will be obtained.

Scheme 3. Strategies for the transformation of poly(HBVE-co-CL) with no CL homosequences to poly(HBVE-alt-CL) by removing MDOP to outside the system using a vacuum pump^a



^a More detailed reaction mechanisms, which include intra- and intermolecular transacetalization and the formation of not head-to-tail but head-to-head sequences, are shown in Scheme S3 and Figure S3A.

An “alternating” copolymer was successfully generated via the above-described method. In step 1, a copolymer with negligible CL homosequences was produced by keeping the instantaneous concentration of CL low (< 0.5 M) via incremental additions of CL (CL was added three times and quantitatively consumed). The ^1H NMR spectrum of the copolymer obtained before vacuuming (Figure 8A(i)) indicates that the peak of CL homosequences (peak 5) is very small, and the average number of units per block was calculated to be 3.7/1.1 for HBVE/CL. Subsequently, vacuuming of the system was conducted, which resulted in a gradual decrease in the volume of the reactants. Accordingly, the average number of HBVE units decreased (Figure 8B), and finally 1.0/1.1 HBVE/CL units per block (Figure 8A(ii)) was reached, suggesting the formation of an “alternating” sequence. The ESI-MS spectrum of the product after vacuuming had peaks with m/z values corresponding to structures consisting of comparable HBVE and CL units, which also supported the “alternating” sequence (Figure 10). The product after vacuuming had a lower M_n value than the original copolymer (Figure 9, black) due to the removal of the HBVE homosequences. In addition, the MDOP removed via vacuuming was recovered in a trap with a purity of $>99.9\%$ (Figure 8A(iii)). DSC measurements showed that the “alternating” copolymer has the T_g value of -70 °C, which is between the values of HBVE and CL homopolymers (Figure 11).

The ester degradation of the obtained copolymer via transesterification reaction with butyl acetate by $\text{Ti}(\text{O}i\text{Bu})_4$ also supported the “alternating” sequence of the copolymer. ^1H NMR analyses of the product obtained by transesterification confirmed the quantitative transformation of the original ester moieties into esters with butyl acetate-derived fragments (Figure S3B). The degradation product had an M_n value much lower than that of the original copolymer (Figure 9, orange). In particular, the low M_n value and narrow MWD of the degradation product (Figure 9, orange, below) corroborated the “alternating” sequence of the copolymer.⁴¹ Structures derived from the “alternating” sequences were detected in the ESI-MS analysis of the transesterification products (Figure S4)

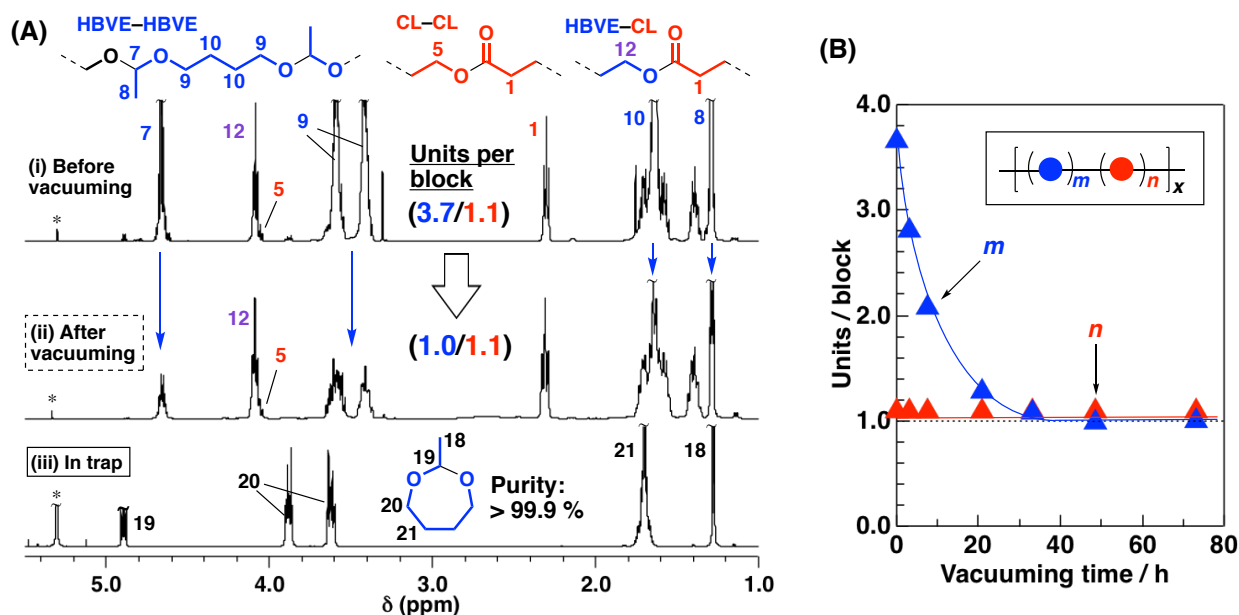


Figure 8. (A) ^1H NMR spectra of (i) poly(HBVE-*co*-CL), (ii) the product obtained after vacuuming, and (iii) the product in the trap in CDCl_3 at 30 °C; * CH_2Cl_2 , (B) vacuuming time–units per block plots for the copolymerization of HBVE and CL (the values were calculated from ^1H NMR integrals).

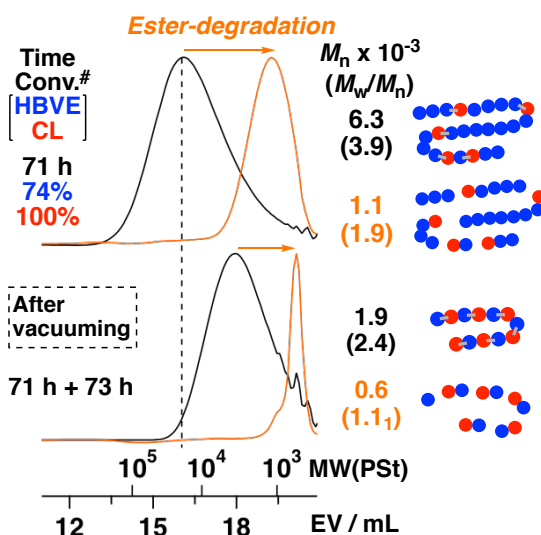


Figure 9. MWD curves of the products before (upper) and after (below) vacuuming (orange: transesterification products); [#]conversion to polymer {polymerization conditions: [HBVE]_{total} = 6.42 M, [CL]_{total} = 1.42 M, [EtSO₃H]_{total} = 10 mM, [CH₂Cl₂]_{total} = 0.40 M, in bulk at 30 °C; transesterification: 25 mM Ti(OBu)₄ in BuOAc/CH₂Cl₂ (8/1 v/v; 0.3 wt% polymer) at 70 °C for 21 h}.

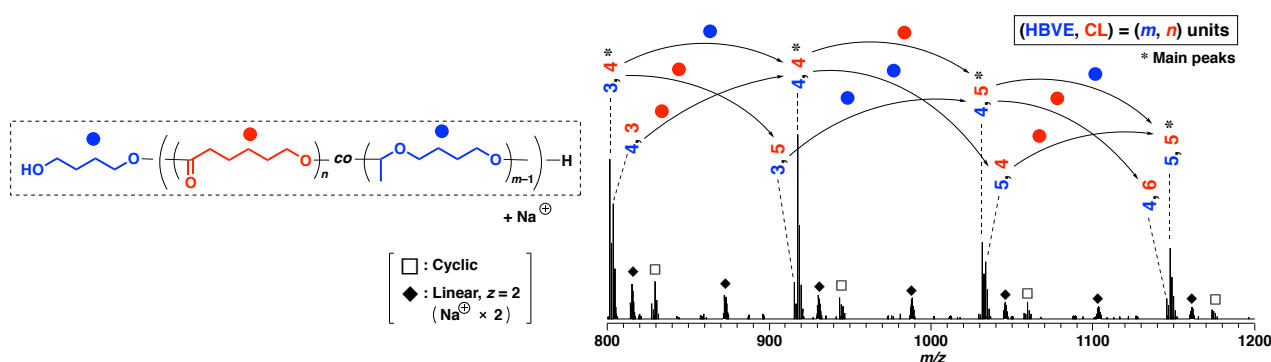


Figure 10. ESI-MS spectrum of poly(HBVE-*alt*-CL) [the sample shown in Figure 8A(ii); Figure 9, black, below].

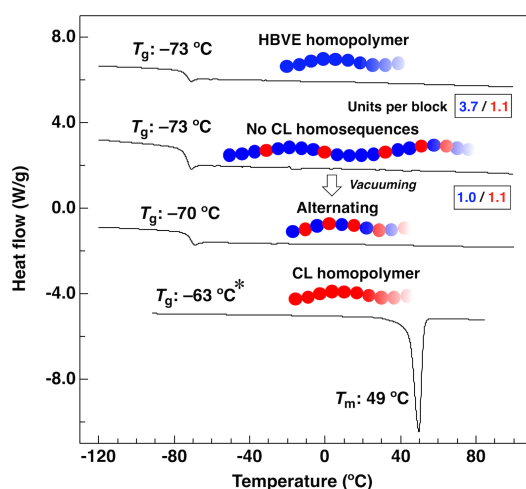


Figure 11. DSC curves for poly(HBVE) [$M_n(\text{GPC}) = 2.3 \times 10^3$, $M_w/M_n(\text{GPC}) = 6.1$], poly(CL) (the sample shown in Figure 3C), poly(HBVE-*co*-CL) (the sample shown in Figure 8A(i)) and the “alternating” copolymer (the sample shown in Figure 8A(ii)); *glass transition was not observed. The described T_g value is from literature.⁴⁰

Conclusion

In conclusion, the copolymerization of HBVE and CL was demonstrated to proceed through the instantaneous isomerization of HBVE to MDOP and the subsequent cationic ring-opening copolymerization of MDOP and CL via concurrently occurring ACE and AM mechanisms. Copolymers with various kinds of sequences were synthesized by changing the initial monomer concentrations. Throughout the copolymerization process, acetal moieties were frequently rearranged via transacetalization and backbiting reactions, while previously formed ester bonds were essentially unchanged. These characteristic reaction behaviors allowed sequence transformation from copolymers with no CL homosequences to “alternating” copolymers by removing MDOP via vacuuming. The removed MDOP, reusable as a monomer, was collected in a trap and had a purity of >99.9%. Using this novel copolymerization system, a variety of poly(acetal-co-ester)s with different monomer structures, composition ratios, and sequences can be easily produced, which will contribute to a systematic understanding of the structure–property relationship. Furthermore, the concept of sequence transformation can be applied to other copolymerization systems with similar reaction behaviors, which will widen the variety of accessible copolymer architectures.

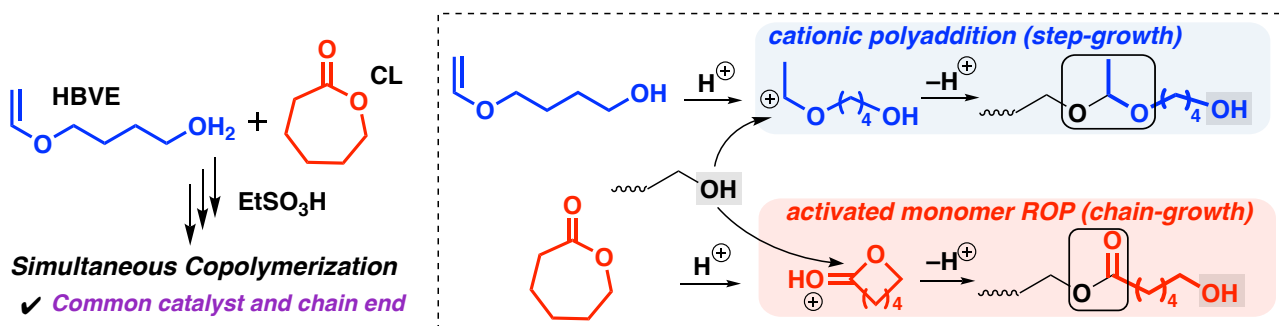
References and Notes

- Mecerreyes, D.; Moineau, G.; Dubois, P.; Jérôme, R.; Hedrick, L. J.; Hawker, J. C.; Malmström, E. E.; Trollsas, M. *Angew. Chem. Int. Ed.* **1998**, *37*, 1274.
- Okada, M.; Yamashita, Y.; Ishii, Y. *Makromol. Chem.* **1966**, *94*, 181.
- Okada, M.; Yamashita, Y. *Makromol. Chem.* **1969**, *126*, 266.
- Simionescu, C. I.; Grigoras, M.; Bicu, E.; Onofrei, G. *Polym. Bull.* **1985**, *14*, 79.
- Rivas, B. L.; Pizarro, G. C.; Canessa, G. S. *Polym. Bull.* **1988**, *19*, 123.
- Hagiwara, T.; Takeda, M.; Hamana, H.; Narita, T. *Macromolecules* **1989**, *22*, 2025.
- Yang, H.; Xu, J.; Pispas, S.; Zhang, G. *Macromolecules* **2012**, *45*, 3312.
- Kanazawa, A.; Kanaoka, S.; Aoshima, S. *J. Am. Chem. Soc.* **2013**, *135*, 9330.
- Mizutani, M.; Satoh, K.; Kamigaito, M. *J. Am. Chem. Soc.* **2010**, *132*, 7498.
- Yang, H.; Zhang, J.; Zuo, Y.; Song, Y.; Huang, W.; Jiang, L.; Jiang, Q.; Xue, X.; Jiang, B. *Macromol. Chem. Phys.* **2019**, *13*, 1900147.
- Aoshima, H.; Uchiyama, M.; Satoh, K.; Kamigaito, M. *Angew. Chem., Int. Ed.* **2014**, *53*, 10932.
- Higuchi, M.; Kanazawa, A.; Aoshima, S. *ACS Macro Lett.* **2017**, *6*, 365.
- Mayo, R. F.; Lewis, M. F. *J. Am. Chem. Soc.* **1944**, *66*, 1594.
- Ueda, M. *Prog. Polym. Sci.* **1999**, *24*, 699.
- Szymanski, R. In *Polymer Science: A Comprehensive Reference*; Matyjaszewski, K., Möller, M. Eds.; Elsevier B.V.: Amsterdam, **2012**; Vol. 4.05.
- Lowry, G. G. *J. Polym. Sci.* **1960**, *42*, 463.
- Maeda, T.; Otsuka, H.; Takahara, A. *Prog. Polym. Sci.* **2009**, *34*, 581.
- Kotliar, M. A. *J. Polym. Sci.: Macromol. Rev.* **1981**, *16*, 367.

19. Otsuka, H.; Aotani, K.; Higaki, Y.; Takahara, A. *Chem. Commun.* **2002**, 23, 2838.
20. Zhang, H.; Ruckenstein, E. *J. Polym. Sci., Part A: Polym. Chem.* **2000**, 38, 3751.
21. Hashimoto, T.; Ishizuka, K.; Umehara, A.; Kodaira, T. *J. Polym. Sci., Part A: Polym. Chem.* **2002**, 40, 4053.
22. Okamoto, Y. *Makromol. Chem., Macromol. Symp.* **1991**, 42, 117.
23. The copolymerization of cyclic acetal and β -lactone was reported in the past study (Ref. 24). However, the β -lactone underwent an alkyl-oxygen scission via the ACE mechanism unlike the present study.
24. Yamashita, Y.; Kondo, S.; Ito, K. *Polym. J.* **1970**, 3, 327.
25. Smith, M. B.; Kubczyk, M. T.; Graham, E. A. *Tetrahedron*, **2012**, 68, 7775.
26. Maruyama, K.; Kanazawa, A.; Aoshima, S. *Polym. Chem.* **2019**, 10, 5304.
27. The results obtained in this study indicate that MDOP is reactive in CH_2Cl_2 in the homopolymerization (Figure 7B) and the copolymerization with CL. The difference likely stems from the solvent used. Indeed, in the homopolymerization of HBVE in THF, which was conducted in this study, the concentration of MDOP was almost steady after the initial stage (Figure S1), which suggested that MDOP was not involved in the polymerization.
28. Kubisa, P.; Vairon, P. J. In *Polymer Science: A Comprehensive Reference*; Matyjaszewski, K., Möller, M. Eds.; Elsevier B.V.: Amsterdam, **2012**; Vol. 4.10.
29. Szymanski, R. In *Polymer Science: A Comprehensive Reference*; Matyjaszewski, K., Möller, M. Eds.; Elsevier B.V.: Amsterdam, **2012**; Vol. 4.04.
30. In some cases of copolymerization in the present chapter, the methoxy groups on acetal moieties were not detected. These results suggest the termination reaction of the oxonium ends and methanol is not quantitative, possibly because the reaction is slow.
31. Franta, F.; Kubisa, P.; Ould Kada, S.; Reibel, L. *Makromol. Chem. Macromol. Symp.* **1992**, 60, 145.
32. Chwialkowska, W.; Kubisa, P.; Penczek, S. *Makromol. Chem.* **1982**, 183, 753.
33. This is corroborated by the experimental result that not diblock-type but multiblock copolymers were produced when a fresh supply of MDOP was added at the later stage of the copolymerization (Figure S2, orange). By contrast, transesterification appeared to negligibly occur under the conditions employed (Figure S2, green).
34. Okada, M.; Yagi, K.; Sumitomo, H. *Makromol. Chem.* **1973**, 163, 225.
35. Ureta, E.; Smid, J.; Szwarc, M. *J. Polym. Sci., Part A-1: Polym. Chem.* **1966**, 4, 2219.
36. Yuki, H.; Hotta, J.; Okamoto, Y.; Murahashi, S. *Bull. Chem. Soc. Jpn.* **1967**, 40, 2659.
37. Inoue, Y.; Koinuma, H.; Tsuruta, T. *J. Polym. Sci., Part B: Polym. Lett.* **1969**, 7, 287.
38. Ishido, Y.; Aburaki, R.; Kanaoka, S.; Aoshima, S. *J. Polym. Sci.: Part A: Polym. Chem.* **2010**, 48, 1838.
39. Hayashi, K.; Kanazawa, A.; Aoshima, S. *Polym. Chem.*, **2019**, 10, 3712.
40. Labet, M.; Thielemans, W. *Chem. Soc. Rev.* **2009**, 38, 3484.
41. Another point to consider in this strategy is the direction of the dialkoxy structures at acetal moieties because “head-to-head” structures can be generated via transacetalization (Figure S3A). The formation of this structure is confirmed with the obtained “alternating” copolymer by detailed analyses (Figures S3B and S4).

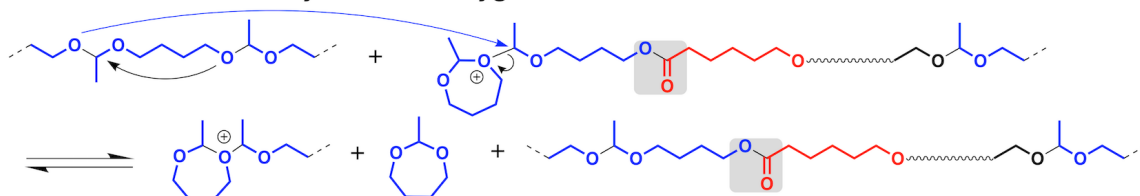
Supporting Information

Scheme S1. Concurrent cationic polyaddition of HBVE and ring-opening polymerization (ROP) of CL via the activated monomer mechanism with a protic acid.

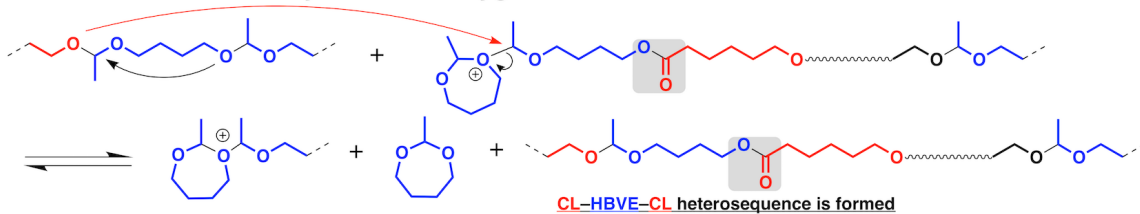


Scheme S2. Different pathways of transacetalization reactions in the copolymerization of HBVE and CL

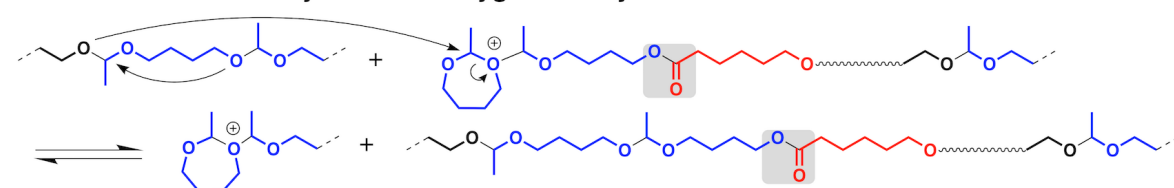
(A) Intermolecular attack by an acetal oxygen derived from HBVE



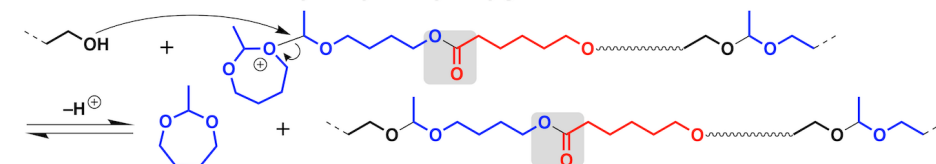
(B) Intermolecular attack by an acetal oxygen derived from CL



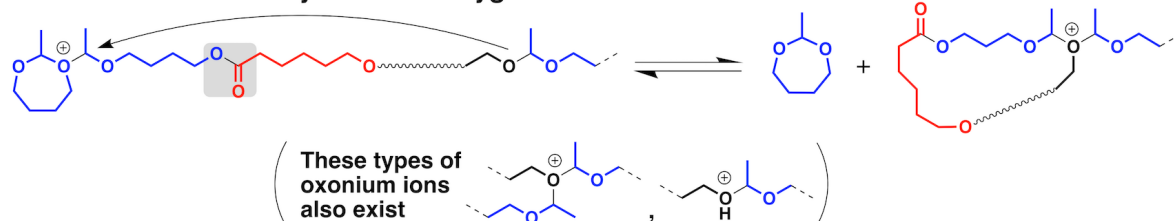
(C) Intermolecular attack by an acetal oxygen to a cyclic acetal carbon



(D) Intermolecular attack by a hydroxy oxygen



(E) Intramolecular attack by an acetal oxygen



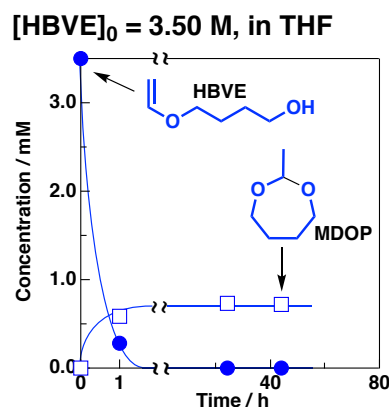


Figure S1. Time–concentration plots for the homopolymerization of HBVE (3.50 M) in THF at 30 °C.

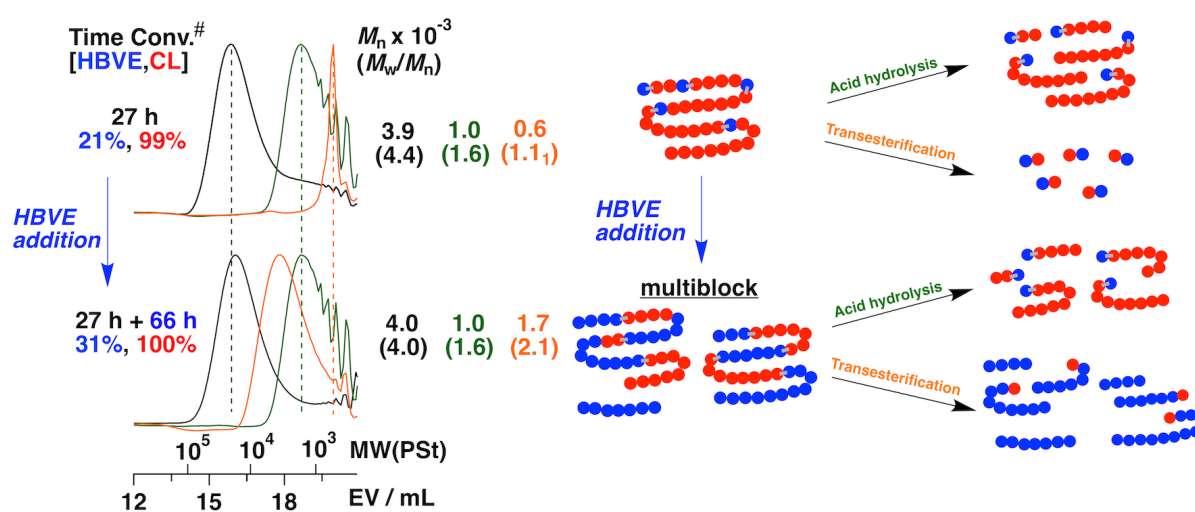


Figure S2. GPC curves of poly(HBVE-*co*-CL)s (black), their acid hydrolysis products (green), and transesterification products (orange) obtained in the HBVE-addition experiment; #conversion to polymer. [polymerization conditions: $[\text{HBVE}]_0 = 0.50 \text{ M}$, $[\text{CL}]_0 = 0.47 \text{ M}$, $[\text{EtSO}_3\text{H}]_0 = 10 \text{ mM}$; $[\text{HBVE}]_{\text{total}} = 3.07 \text{ M}$, $[\text{CL}]_{\text{total}} = 0.32 \text{ M}$, $[\text{EtSO}_3\text{H}]_{\text{total}} = 6.7 \text{ mM}$, in CH_2Cl_2 at 30 °C. Acid hydrolysis: 0.5 M HCl in $\text{H}_2\text{O}/1,2$ -dimethoxyethane (1/1 v/v; 0.5wt% polymer) at r.t. for 3 h. Transesterification: 25 mM $\text{Ti}(\text{O}i\text{Bu})_4$ in $\text{BuOAc}/\text{CH}_2\text{Cl}_2$ (8/1 v/v; 0.3wt% polymer) at 70 °C for 21 h].

Note for Figure S2. The result shown in Figure S2 indicates that the fresh feed of HBVE to the copolymer with no HBVE homosequence generated a multiblock copolymer, instead of a diblock copolymer, most likely via frequent transacetalization (scrambling). This is proved by the fact that the sharp peak, which corresponds to nonsuccessive HBVE units, in the GPC curves of the transesterification product of the original poly(HBVE-*co*-CL) (Figure S2 orange, upper) became negligible after the HBVE addition (Figure S2, orange, below). By contrast, the GPC curves of acid hydrolysis products (Figure S2, green) were almost unchanged before and after the HBVE addition. This means that the rearrangement of CL homosequences via transesterification did not occur under the conditions employed. In addition, after the HBVE addition, the peak top of the GPC curves of poly(HBVE-*co*-CL) (Figure S2, black) slightly shifted to the lower molecular-weight region. This is likely due to dissociation of acetal moieties by acid hydrolysis with adventitious water, as well as the segmental exchange via transacetalization.

Scheme S3. Illustrations of detailed reaction mechanisms for the transformation of a copolymer with no CL homosequences to an “alternating” copolymer using a vacuum pump

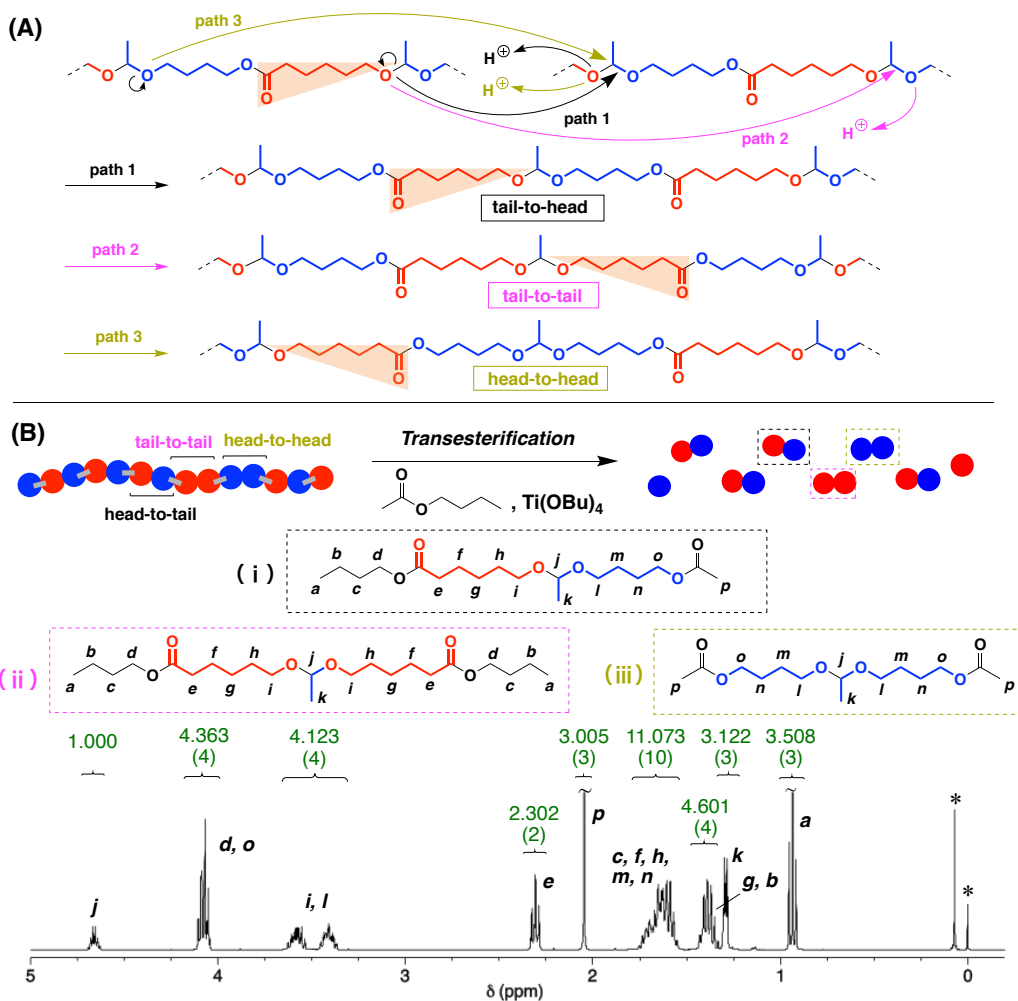
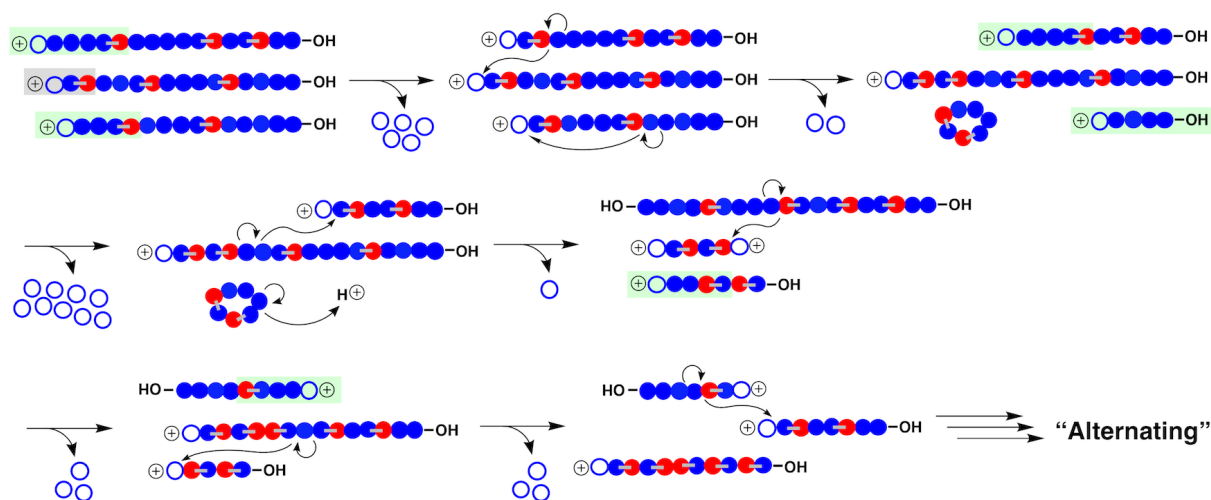
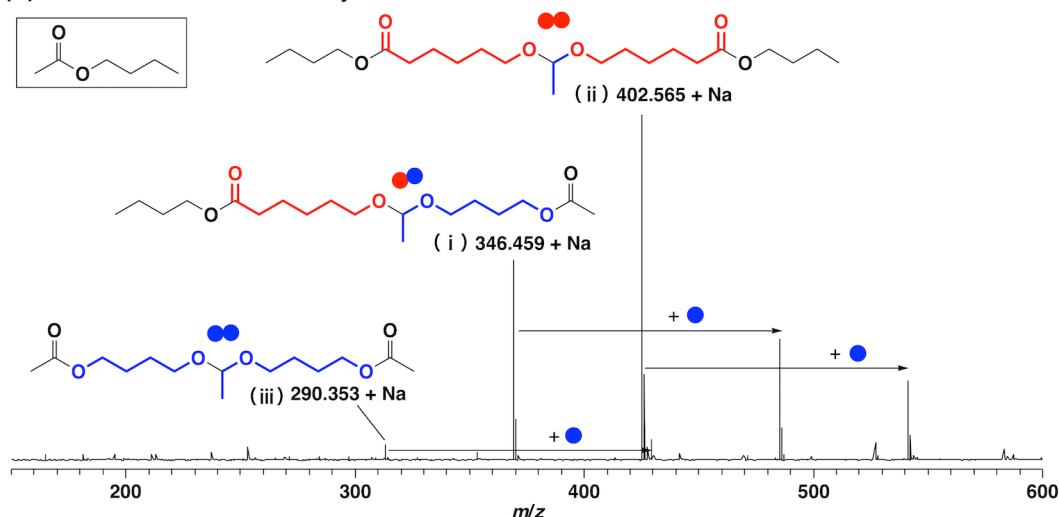


Figure S3. (A) Formation of head-to-tail, tail-to-tail, and head-to-head structures via random scrambling and (B) ^1H NMR spectrum of the transesterification product of the poly(HBVE-*alt*-CL) (in CDCl_3 at 30 °C; the sample shown in Figure 9, below, orange curve); *TMS and grease. Numbers written in green: integral ratios (parenthesis: predicted values for the mixture of (i)/(ii)/(iii) = 2/1/1).

(A) Transesterification with butyl acetate



(B) Transesterification with butyl butyrate

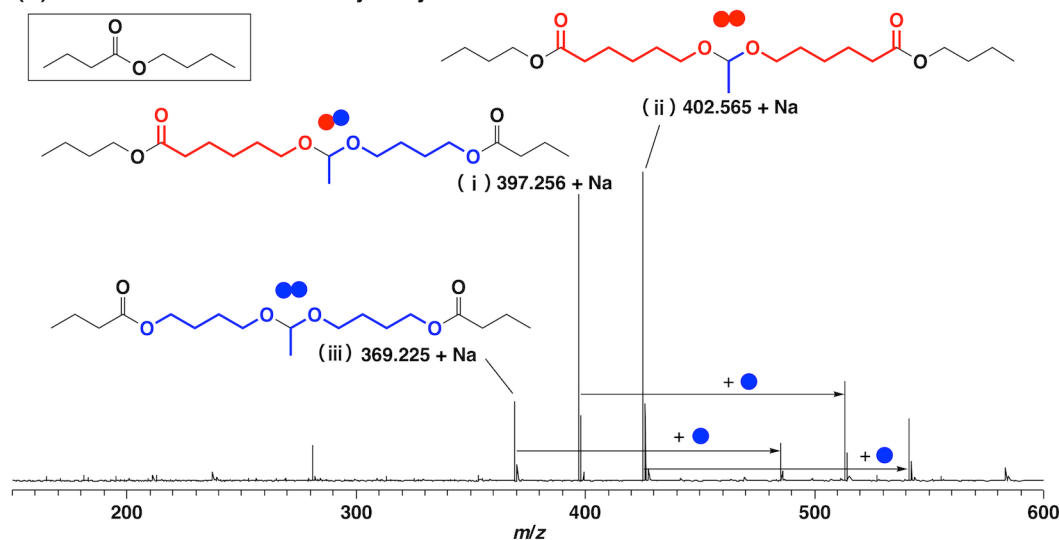


Figure S4. ESI-MS spectra of transesterification products of the poly(HBVE-*alt*-CL) with (A) butyl acetate (the same sample to that shown in Figure S3), and (B) butyl butyrate.

Note for Figures S3 and S4. The peaks of the three kinds of acetal-diester structures were confirmed in the spectrum of the product obtained by transesterification with butyl acetate (Figure S4A); however, the relative peak intensities are completely different from the expectation (1/2/1 for blue-blue/red-blue/red-red circles), considering the random nature of the scrambling reaction (Figure S3B, illustration). The very weak peak intensity of the blue-blue circle is also inconsistent with the ^1H NMR spectrum of the products (Figure S3B): the integral ratio of peak p (2.0 ppm) should be much smaller than the predicted value. This inconsistency is likely due to the non-quantitativity of the ESI-MS measurements. In addition, the relative peak intensities were inconsistent with the expectation and the result of ^1H NMR analysis even when butyl butyrate was used instead of butyl acetate (Figure S4B), although the relative peak intensities changed compared to Figure S4A.

Equilibrium Monomer Concentration-Dependent Sequence Control of Copolymer Chains via Temperature Changes in Cationic Ring-Opening Copolymerization of Cyclic Acetals and Cyclic Esters

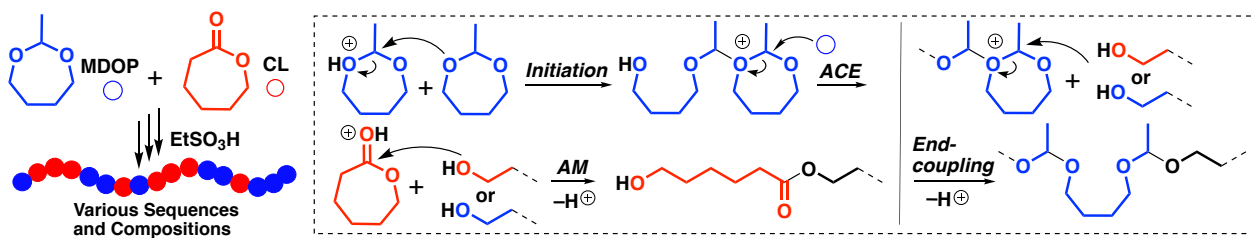
Introduction

The synthesis of copolymers with desired sequences is a remaining challenge in the field of polymer science. In nature, biopolymers, such as proteins and nucleic acids, have strictly controlled sequences, which is the key for their sophisticated functions. In synthetic polymers, various kinds of well-defined diblock (or triblock) copolymers have been synthesized owing to the development of precision polymerization techniques and utilized for many applications, such as drug delivery systems,¹ thermoplastic elastomers,² and lithography.³ By contrast, there are limited examples of copolymers with more complex sequences, e.g., AB-,^{4,5} ABB-,^{6,7} or ABC-type⁸⁻¹⁰ alternating structures, despite the potential high functionalities of these molecules. The difficulty in synthesizing these specific structures is one of the reasons for the insufficient use and studies.

Sequence-regulated copolymers have been synthesized via several methods.¹¹⁻¹⁷ Each method has its inherent advantages and disadvantages. For example, the method of step-by-step monomer addition to a polymer chain (iterative method)^{11, 12} is the most promising strategy for producing the desired sequences, although a considerable amount of time and effort are necessary to generate a long chain. Polymerization of a monomer containing specific sequences of multiple monomer units is also very effective; however, synthesis of such sequence-incorporated monomers usually requires cumbersome procedures.^{13,14} In addition, only a specific sequence is achievable from such types of monomers. Polymerization of monomers with specific reactivities is the most practical method, although the need for very high selectivity in propagation reactions limits the available monomers.^{4-10,15-17} A new strategy and/or hybridization of the existing methods are required for synthesizing a much wider variety of sequence-regulated copolymers in a practical manner.

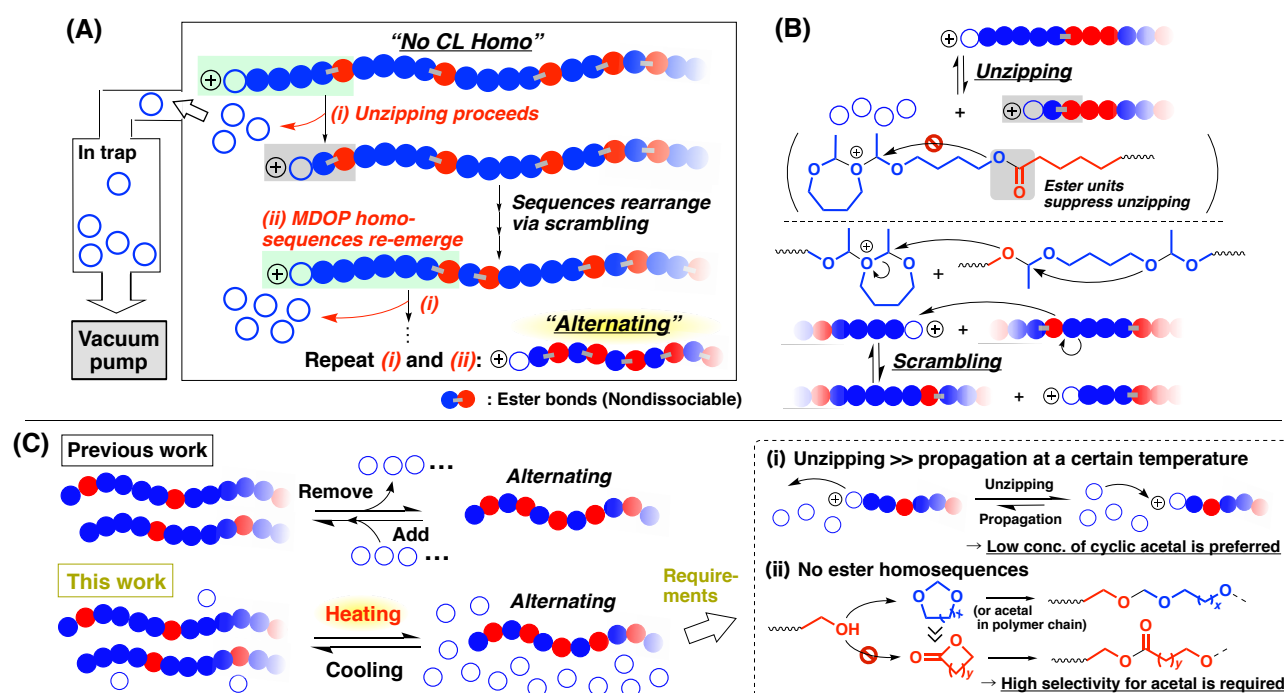
In Chapter 4, the author demonstrated that the cationic ring-opening copolymerization of 2-methyl-1,3-dioxepane (MDOP) [generated via the isomerization of 4-hydroxybutyl vinyl ether (HBVE) in the very early stages of polymerization] and ϵ -caprolactone (CL) with EtSO₃H produced copolymers with a remarkably wide variety of compositions and sequences (Scheme 1).¹⁸ The polymerization was initiated via the reaction of an MDOP monomer and a protonated MDOP, forming a compound with an oxonium group and a hydroxy group at each end. From this compound, the propagations of MDOP and CL proceeded via the active chain end (ACE)¹⁹ and the activated monomer (AM)²⁰ mechanisms, respectively. Intra- and intermolecular coupling reactions between the two ends also occurred. Interestingly, by utilizing the characteristics of this copolymerization, a copolymer with alternating sequences was produced via an unprecedented strategy, as explained in Chapter 4.

Scheme 1. Cationic ring-opening copolymerization of MDOP and CL.

Strategy for the synthesis of alternating copolymers via sequence transformation

In this strategy, an alternating copolymer was synthesized via the preparation of a copolymer with no CL homosequences (prepolyolymer) and the subsequent removal of all the MDOP homosequences by a vacuum pump (Scheme 2A). In this chapter, alternating copolymer synthesis was attempted by changing the polymerization temperature (heating) instead of subjecting the samples to vacuum (Scheme 2C). The temperature-dependent sequence transformation, which does not rely on the removal of cyclic acetals via vacuum, is very attractive because copolymer sequences can be reversibly altered by a change in the temperature. However, this method is more difficult than sequence transformation via vacuum because the unzipping of cyclic acetals needs to proceed predominantly over propagation at the oxonium ends even in the presence of cyclic acetal monomers. Thus, lower concentrations of cyclic acetals are desired; however, the homopropagation of cyclic esters must be prevented at the same time. These demands can be satisfied when the crossover reaction from the cyclic ester-derived hydroxy ends to cyclic acetals is preferred over cyclic ester homopropagation (Scheme 2C, below). Considering these points, systematic investigations were performed with a specific focus on the selectivity in the propagation reaction from the cyclic ester-derived ends.

Scheme 2. (A) Sequence transformation of a copolymer with no CL homosequences to an alternating copolymer using a vacuum pump through tandem reactions of scrambling and unzipping, (B) key reactions for the sequence transformation, and (C) the goal of this chapter and requirements



Experimental

Materials.

1,3-Dioxolane (DOL; TCI; >98.0%), 2-methyl-1,3-dioxolane (MDOL; TCI; >98.0%), β -propiolactone (β -PL; TCI; >95.0%), and δ -valerolactone (δ -VL; TCI; >98.0%) were distilled twice over calcium hydride under reduced pressure. 1,3-Dioxepane (DOP), 2-methyl-1,3-dioxolane (MDOL), and 2,2-dimethyl-1,3-dioxepane (DMDOP) were synthesized according to previously reported procedures.^{21,22} Commercially available PhSO₃H (TCI; >98.0%), Ts₂O (Aldrich; 97%), TfOH (Aldrich; >99.0%), and Tf₂NH (Wako; 98.0+%) were used without further purification after preparing their stock solutions in dichloromethane. C₄F₉SO₃H (TCI; >98.0%) and TsOH·H₂O (TCI; >98.0%) were used without further purification after preparing their stock solutions in dichloromethane (the acids were partly insoluble). HCl (Aldrich; 1.0 M solution in diethyl ether) was used as received. Other materials were prepared and used as described in the preceding chapters.

Polymerization Procedure.

Cationic polymerizations were conducted in a manner similar to that described in Chapter 4.

Acid Hydrolysis

Acid hydrolysis of product copolymers was conducted in a manner similar to that described in the preceding chapters.

Transesterification.

Transesterification of product copolymers was conducted in a manner similar to that described in Chapters 3 and 4.

Characterization.

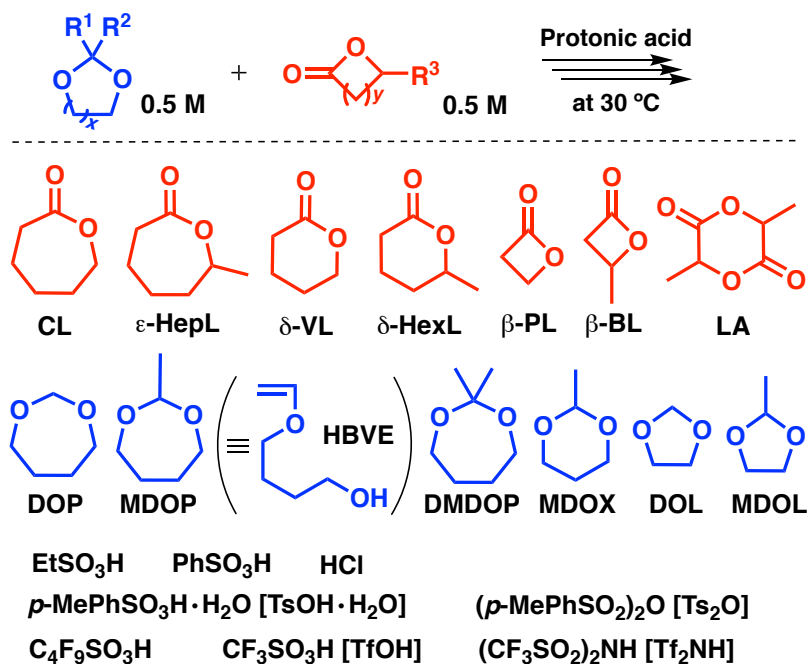
The molecular weight distribution (MWD), ¹H and ¹³C NMR spectra, and differential scanning calorimetry (DSC) data were obtained in a manner similar to that described in the preceding chapters.

Results and Discussion

I. Cationic Copolymerization of Various Cyclic Acetals and Cyclic Esters with a Variety of Protonic Acids: Systematic Investigation of Effective Monomers and Catalysts for Copolymerization.

In this chapter, the author aims to demonstrate the generality of the above-described sequence transformation. First, a series of cyclic esters, cyclic acetals, and protonic acids were examined for copolymerization (Scheme 3) to observe their different kinetics.

Scheme 3. Catalysts and monomers employed in this chapter.

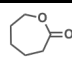
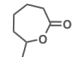
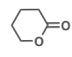
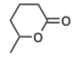
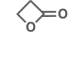
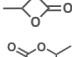
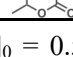


The copolymerization of HBVE (0.50 M) and CL (0.50 M) with EtSO₃H, which was studied in Chapter 4 and treated as a standard system in this chapter, was conducted in dichloromethane at 30 °C. Both monomers were simultaneously consumed to yield a polymer with an M_n value of 3.8×10^3 (Figure 1A, black), and the average number of units per block was calculated to be 1.0/5.7 for HBVE/CL. To achieve the goal of alternating copolymer synthesis upon heating, however, more frequent crossover reactions from cyclic ester to cyclic acetal are necessary desired. Therefore, in this first section, various kinds of monomers and catalysts were examined to determine the conditions needed to generate shorter cyclic ester blocks.

I-1. *Effects of Cyclic Esters*

δ -Valerolactone (δ -VL), a six-membered cyclic ester, was used for copolymerization with HBVE using EtSO₃H in CH₂Cl₂ or toluene (entries 4 and 5 in Table 1). Both monomers were simultaneously consumed in both solvents. The conversion of HBVE to a polymer was relatively high compared to the standard system (entry 1), which suggested that the crossover reactions occurred more frequently. The MWD curve of the product obtained in toluene (entry 5; Figure 1B, black) had a bimodal shape. The main products in the lower-molecular-weight (MW) region were likely cyclic oligomers, as in the case of the copolymerization of HBVE and CL (Figure 1A, black). The ¹H NMR spectrum of the product [Figure 1C(i)] had peaks derived from each monomer unit, and the integral ratio of each unit was calculated to be 1.0/3.4 for HBVE/ δ -VL. Direct evidence for the copolymerization was, however, not provided due to the overlap of crossover-derived peaks with the peaks of CL homosequences (for example, peaks 4 and 11).

Table 1. Cationic Copolymerization of HBVE and Various Cyclic Esters with EtSO₃H^a

entry	cyclic ester	solvent	time (h)	conv. to polymer (%) ^b		$M_n \times 10^{-3}$ ^c	M_w/M_n ^c	units per block ^b	
				HBVE	cyclic ester			HBVE	cyclic ester
1	 CL	CH ₂ Cl ₂	87	19	98	3.8	6.24	1.0	5.7
2	 ε-HepL	CH ₂ Cl ₂	162	8	39	1.3	2.17	n.d.	n.d.
3	ε-HepL	toluene	16	10	38	1.0	3.41	n.d.	n.d.
4	 δ-VL	CH ₂ Cl ₂	141	24	62	1.6	3.97	1.0	3.7
5	δ-VL	toluene	93	35	91	2.0	6.49	1.0	3.4
6	 δ-HexL	toluene	92	0	0	–	–	–	–
7	 β-PL	CH ₂ Cl ₂	358	17	50	1.6	3.97	n.d.	n.d.
8	β-PL	toluene	310	14	54	0.3	2.37	n.d.	n.d.
9	 β-BL	toluene	92	0	0	–	–	–	–
10	 LA	CH ₂ Cl ₂	241	0	0	–	–	–	–

^a[HBVE]₀ = 0.50 M, [cyclic ester]₀ = 0.50 M, [EtSO₃H]₀ = 5.0 (entry 1) or 10 mM (entries 2–10), at 30 °C.

^bDetermined by ¹H NMR analysis. ^cDetermined by GPC (polystyrene standards).

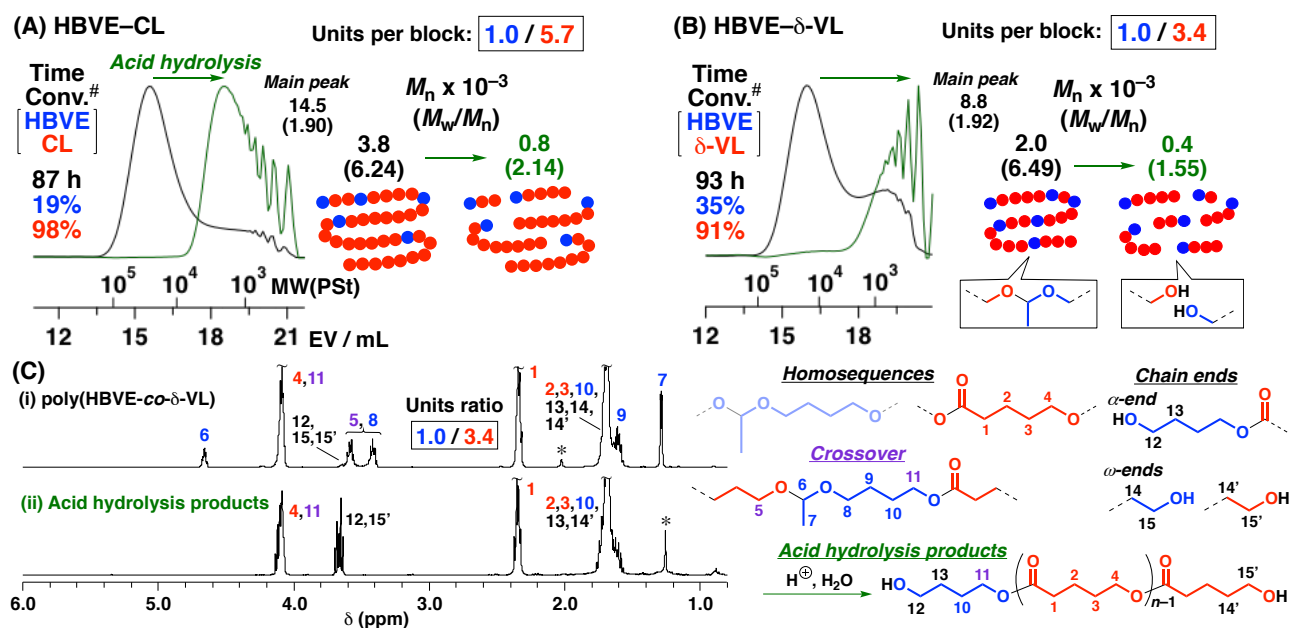
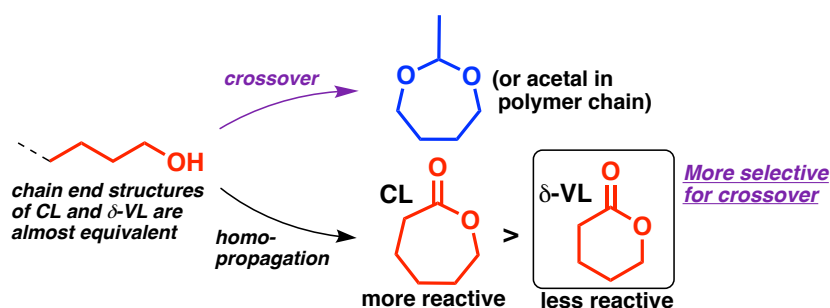


Figure 1. MWD curves of (A) HBVE–CL (entry 1 in Table 1) and (B) HBVE–δ-VL (entry 5) copolymers (black) and their acid hydrolysis products (green); #conversion to polymer. (C) ¹H NMR spectra of (i) HBVE–δ-VL copolymer and (ii) the acid hydrolysis products; *vaseline and toluene; acid hydrolysis: 0.5 M HCl in H₂O/1,2-dimethoxyethane (1/1 v/v; 0.5wt% polymer) at r.t. for 3 h].

Acid hydrolysis of the product revealed the successful formation of the copolymer. The MWD curve significantly shifted to the low-MW region after hydrolysis (Figure 1B, green) due to cleavage of the acetal moieties. The M_n value of the hydrolysis product, which mainly consists of δ -VL homosequences, was 0.4×10^3 . This value is consistent with the copolymer structure having 1.0/3.4 HBVE/ δ -VL units per block (not a unit ratio). The presence of shorter δ -VL blocks in the copolymer than in the CL counterpart indicates that δ -VL has higher selectivity for the crossover reaction in the copolymerization with HBVE than does CL. This is likely due to the lower reactivity of δ -VL than of CL under the condition examined, because the chain end structures derived from each monomer do not have significant differences (Scheme 4).

The other cyclic esters were not effective for copolymerization with HBVE. δ -Hexanolactone (δ -HexL), β -butyrolactone (β -BL), and lactide (LA) were not consumed at all (entries 6, 9, and 10 in Table 1). The copolymerization of ϵ -heptanolactone (ϵ -HepL) or β -propiolactone (β -PL) with HBVE proceeded at slow rates (entries 2, 3, 7, and 8). In these copolymerizations, the rates of HBVE polymerization were relatively high compared to those of the cyclic esters, which implied frequent crossover reactions. Indeed, the ^1H NMR spectra (Figure S1) showed that the peak intensities for the structure derived from cyclic ester-HBVE crossover were relatively strong. However, these copolymerizations suffered from frequent decomposition of the polymer chains throughout the polymerization, likely through acid hydrolysis. This was indicated by their low MW values and the large peak intensities attributed to hydroxy end-derived structures in the ^1H NMR spectra (Figure S1). These cyclic esters would potentially be effective if the decomposition were suppressed, although the reason for the frequent decomposition is currently unclear.

Scheme 4. Selectivity in nucleophilic attack of cyclic ester-derived hydroxy ends




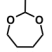
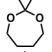
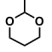
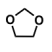
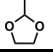
I-2. Effects of Cyclic Acetals

Next, various cyclic acetals were tested in the copolymerization with CL using EtSO_3H in dichloromethane at 30 °C (Table 2). All the cyclic acetals used were copolymerized with CL; however, in comparison with the standard system (entry 1 in Table 1; entry 2 in Table 2), the conversions of cyclic acetals were lower, and the lengths of CL blocks were much longer. The order of the number of CL units per block is as follows: MDOP (5.3) < DMDOP (9.3) < MDOL (23) < DOP (29) < MDOX (52) < DOL (210). This order likely reflects the tendency of homopropagation of CL in the copolymerization. Thus, the crossover proceeded most frequently when MDOP was used. The decrease in the M_n values of the products obtained with DMDOP, MDOX, DOL, and MDOL (entries 3, 4, 5, and 6) after acid hydrolysis was small, which indicated that these polymers had very small amounts of CL-cyclic acetal heterosequences in a single chain. The homosequences of cyclic acetals were not observed except for the case with DOP (entry 1). This result is consistent with the

much higher equilibrium monomer concentrations of these cyclic acetals^{23,24} than the initial concentrations used.

The above-estimated tendency of crossover from the CL-derived hydroxy ends was less correlated to the homopolymerizability of cyclic acetals.²² For example, DOL was least consumed in the copolymerization with CL among the cyclic acetals used, although DOL has high homopolymerizability. The crossover reaction from CL to cyclic acetals is considered to proceed via the nucleophilic attack of a hydroxy end by a protonated cyclic acetal, which corresponds to the AM propagation of cyclic acetals. By contrast, homopolymerization of cyclic acetals probably proceeds mainly via ACE propagation.²⁴ The inconsistency of the DOL homopolymerizability and the copolymerization results likely stemmed from these differences. Further investigation is required for better understanding.

Table 2. Cationic Copolymerization of Various Cyclic Acetals and CL with EtSO₃H^a

entry	cyclic acetal	time (h)	conv. to polymer (%) ^b		$M_n \times 10^{-3}$ ^c (): hydrolysis products	M_w/M_n ^c	units per block ^b		equilibrium monomer conc. at 30 °C (M) ^d
			cyclic acetal	CL			cyclic acetal	CL	
1	 DOP	47	14	100	1.6 (0.6)	3.24	4.1	29	0.84
2	 MDOP	82	19	99	3.9 (0.8)	6.17	1.0	5.3	2.69
3	 DMDOP	28	10	97	2.5 (1.7)	2.20	1.0	9.3	n.d.
4	 MDOX	28	6	89	16.1 (9.8)	1.37	1.0	52	n.d.
5	 DOL	47	6	97	23.3 (20.0)	1.79	1.0	210	2.08
6	 MDOL	28	11	95	10.0 (5.5)	3.10	1.0	23	n.d.

^a[Cyclic acetal]₀ = 0.50 M, [CL]₀ = 0.50 M, [EtSO₃H]₀ = 5.0 (entry 2) or 10 mM (entries 1 and 3–6) in CH₂Cl₂ at 30 °C. ^bDetermined by ¹H NMR analysis. ^cDetermined by GPC (polystyrene standards). ^dCalculated from previously reported ΔH and ΔS values.^{23,24}

I-3. Effects of Protonic Acids

Various kinds of alkyl sulfonic acids were effective for the copolymerization of HBVE and CL (Table 3). The M_n values of the copolymers obtained with these catalysts were comparable,²⁵ whereas the MW of the main peak of the copolymer obtained with EtSO₃H was the highest among those of all the sulfonic acids used. The polymerization rates were obviously different and varied in the order of PhSO₃H > EtSO₃H > TsOH·H₂O > Ts₂O. The concentration of EtSO₃H had little impact on the polymerization behavior (entries 1 and 2). A significant difference in the length of CL blocks was also not observed with these catalysts. By contrast, the other catalysts employed, such as TfOH and HCl (Scheme 3B), showed a possibility to exhibit strong tendency toward crossover. However, the MWs of the products obtained with TfOH and HCl were very low, most likely due to the frequent hydrolysis during polymerization (Figure S2), as in the case with the copolymerization using ϵ -HepL or β -PL.

Table 3. Cationic Copolymerization of HBVE and CL with various catalysts^a

entry	catalyst	(mM)	time (h)	conv. to polymer (%) ^b		$M_n \times 10^{-3}$ ^c	M_w/M_n ^c	$M_n \times 10^{-3}$ (main peak) ^c	units per block ^b	
				HBVE	CL				HBVE	CL
1	EtSO ₃ H	5.0	87	19	98	3.8	6.24	15.5	1.0	5.7
2		10	43	12	67	3.3	5.72	14.3	1.0	5.4
3	PhSO ₃ H	10	19	26	97	3.6	4.46	10.0	1.0	5.4
4	TsOH · H ₂ O	10	111	26	98	4.1	4.31	12.0	1.0	5.1
5	Ts ₂ O	10	112	16	79	2.9	5.33	9.8	1.0	5.5

^a[HBVE]₀ = 0.50 M, [CL]₀ = 0.50 M, in CH₂Cl₂ at 30 °C. ^bDetermined by ¹H NMR analysis. ^cDetermined by GPC (polystyrene standards).

I-4. Overview

The examined cyclic esters and cyclic acetals were categorized into three groups based on their effectiveness in copolymerization (Chart 1). In particular, the monomers satisfying the following three demands were classified as “potentially effective for the synthesis of alternating copolymers via sequence transformation on heating”: (1) high selectivity for the crossover from cyclic ester-derived hydroxy ends to suppress ester homosequences, (2) high equilibrium concentration of cyclic acetals (this is because the unzipping needs to proceed predominantly over the propagation in the presence of cyclic acetal monomers²⁶), and (3) generation of high-MW polymers without frequent hydrolysis during polymerization. By employing these effective monomers and other optimized polymerization conditions, sequence transformation on heating was attempted in the following section.

Chart 1. Effectiveness of Monomers in the Copolymerization

	Potentially Effective for Producing an “Alternating” Copolymer via Sequence Transformation on Heating	Effective for Copolymn.	Ineffective
Cyclic Ester	CL, δ -VL	ϵ -HepL, β -PL	δ -HexL, β -BL, LA
Cyclic Acetal	MDOP (HBVE)	DOP, DMDOP, MDOX, MDOL	DOL

II. Sequence Transformation from a Copolymer with No Ester Homosequences to an Alternating Copolymer upon Heating

Based on the systematic investigations in this study, HBVE, δ -VL, and EtSO₃H were selected as potential monomers and catalysts for the synthesis of alternating copolymers via sequence transformation upon heating. Toluene was used as a solvent because its high boiling point is preferable for heating. To prohibit homopropagation of δ -VL, the initial monomer concentrations were set to 3.00 M for HBVE and 0.50 M for δ -VL.

The copolymerization using the above-described compounds at 30 °C resulted in a copolymer with no δ -VL homosequences, which was subsequently transformed into an alternating-like copolymer upon heating (Figure 2). In three hours, δ -VL was quantitatively consumed. The absence of δ -VL homosequences in the copolymer was suggested from the ¹³C NMR spectrum (Figure 3). The unit ratios of HBVE to δ -VL of the copolymer, which are nearly identical to the HBVE units per block, were 3.8 and 2.8 at 3 h and at 21 h, respectively (Figure 2B). The decrease in HBVE units with reaction time suggested that the rate balance of addition and unzipping at the oxonium ends was approaching equilibrium. Subsequently, the polymerization temperature was increased to 80 °C at 22 h. Soon after heating, the unit ratio dramatically decreased to 1.6 (Figures 2A and 2B), which implied successful sequence transformation. Eventually, the unit ratio reached 1.2 by heating to 100 °C, which suggested the formation of an alternating-like copolymer. Then, the temperature was changed to 30 °C to test the reversibility; however, the unit ratio remained unchanged for some reason, such as the deactivation of the oxonium end. The author is currently optimizing the reaction conditions to achieve reversible transformation by a cycle of heating and cooling. The MWD curves of the product at each temperature (Figure 2C) revealed that the MWs decreased upon heating, although polymers were still obtained at 100 °C. In addition, the conversion of δ -VL also decreased upon heating (Figure 2C), likely through the unzipping of δ -VL ($[\delta\text{-VL}]_e = 0.36 \text{ M}$ at 100 °C).²⁷

The formation of alternating-like copolymers via sequence transformation was supported by the scission of the ester bonds via transesterification with butyl butyrate and Ti(OBu)₄ (Figure 2C, orange). Quantitative degradation was confirmed by ¹H NMR analysis (Figure S4), and the MWD curve clearly shifted to the low-MW region after transesterification (Figure 2C). The structures of the transesterification products correspond to units consisting of HBVEs and one δ -VL in the original copolymer. The transesterification product from the copolymer obtained at 30 °C had a relatively broad MWD and higher MW, which corresponded to the high number of HBVE units per block in the original copolymer. By contrast, the transesterification product from the copolymer obtained at 100 °C had a narrow MWD and low MW. These results confirmed that the HBVE units per block decreased as the polymerization temperature increased and that an alternating-like copolymer was obtained at 100 °C.²⁸

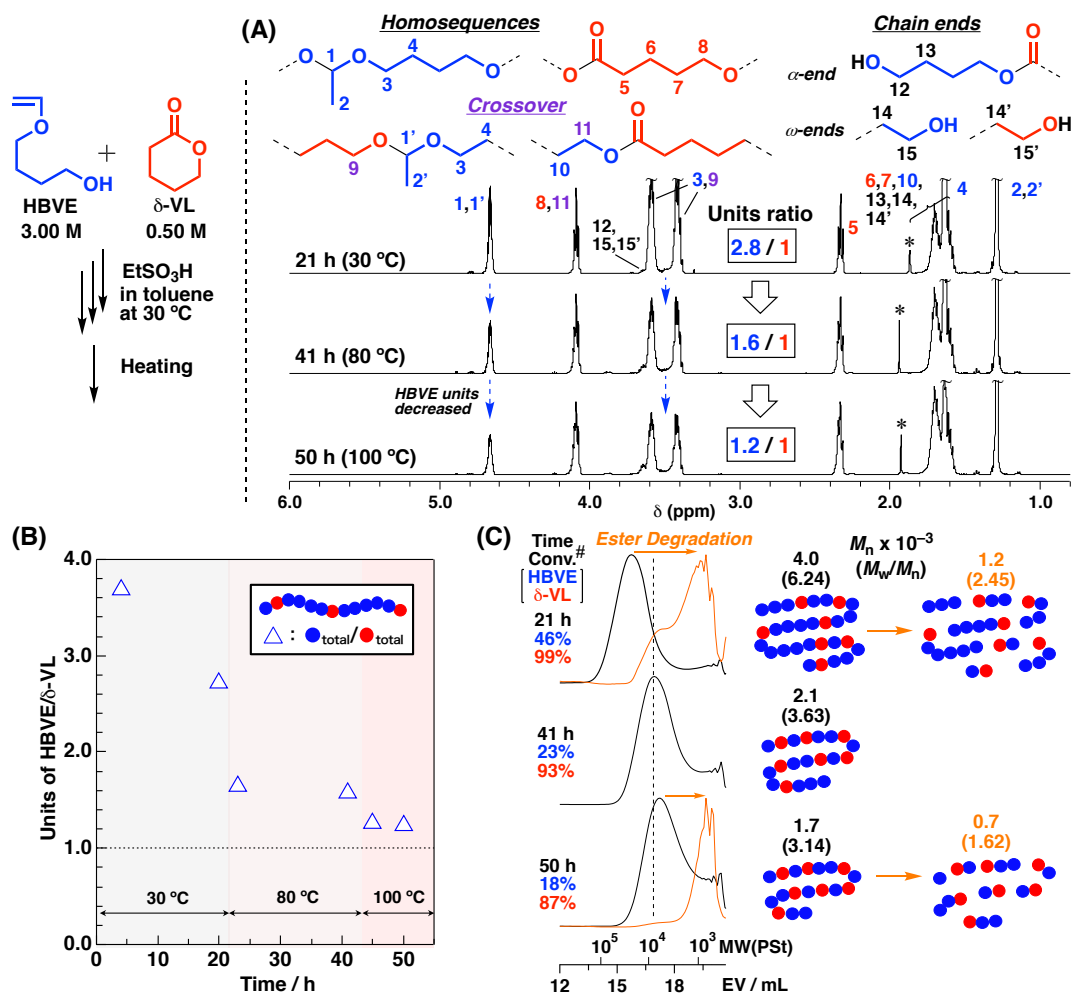


Figure 2. (A) ¹H NMR spectra, (B) the change of HBVE/ δ -VL unit ratios on heating, and (C) MWD curves of poly(HBVE-co- δ -VL)s obtained at different temperature (black) and their transesterification products (orange); #conversion to polymer; polymerization conditions: [HBVE]₀ = 3.00 M, [CL]₀ = 0.50 M, [EtSO₃H]₀ = 10 mM, in toluene at 30–100 °C; transesterification: 25 mM Ti(OBu)₄ in butyl butyrate/CH₂Cl₂ (8/1 v/v; 0.3wt% polymer) at 70 °C for 21 h].

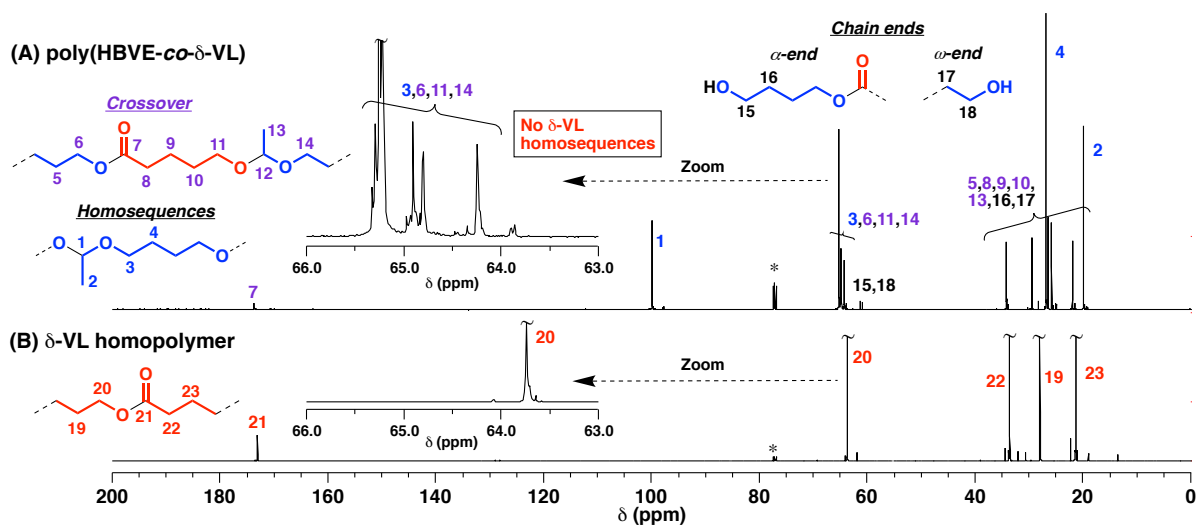


Figure 3. ¹³C NMR spectra of the (A) poly(HBVE-co- δ -VL) obtained at 3 h and (B) δ -VL homopolymer {polymerization conditions: [δ -VL]₀ = 1.00 M, [Ti(OBu)₄]₀ = 10 mM, in toluene at 30 °C.}; 500 MHz in CDCl₃ at 30 °C; *chloroform.

III. Thermal Properties of poly(HBVE-co-CL)s with Various Compositions and Sequences

The differential scanning calorimetry (DSC) measurements of the poly(HBVE-co-CL)s with various compositions and sequences demonstrated that the thermal properties were tunable via the design of primary structures (Figure 3). All the tested poly(HBVE-co-CL)s showed single glass transition peaks, which suggested the miscibility of these amorphous segments. Moreover, the T_g values were tunable based on the compositions of the copolymers between the T_g s of HBVE and CL homopolymers (entries 1 and 3). The melting peaks were observed in the cases of the copolymers having relatively long CL homosequences (entries 3, 4, 5, and 6), and the T_m values depended on the length of the CL block, both of which indicated that the crystalline region was derived from CL homosequences. The copolymers having short CL blocks and alternating sequences (entries 7 and 8) did not exhibit crystallinity, which demonstrated that the crystallinity was affected by the sequences of the copolymer rather than by the compositions.

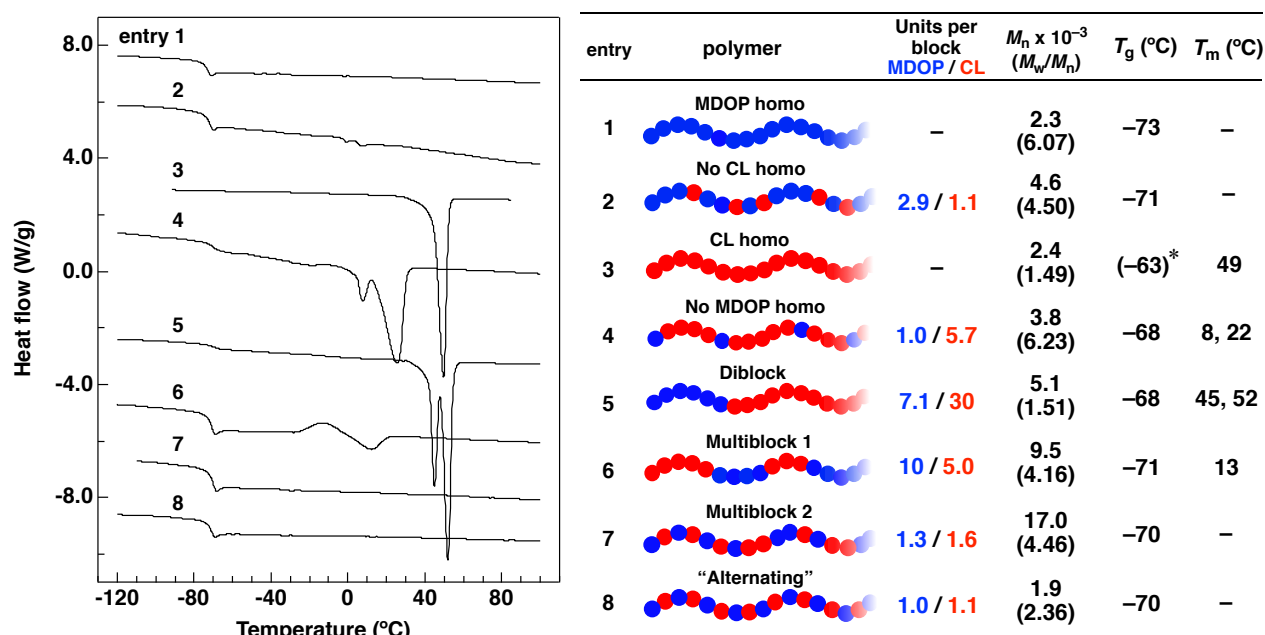


Figure 3. DSC curves of poly(HBVE), poly(CL), and poly(HBVE-co-CL)s with various compositions and sequences. Polymerization conditions and MWD curves are summarized in the Supporting Information. *Glass transition was not clearly observed. The described T_g value is from literature.²⁹

Conclusion

The cationic ring-opening copolymerization of cyclic esters and cyclic acetals was performed using a series of monomers and protonic acids for the purpose of demonstrating the generality of the sequence control method developed in Chapter 4. In particular, reaction conditions that result in the generation of shorter cyclic ester blocks were explored for the synthesis of alternating copolymers upon heating. Cyclic esters with moderate but sufficient reactivities were effective for copolymerization with fewer ester homosequences. The reactivity of cyclic acetals in the copolymerization was not comparable to their homopolymerizability. The MWs, polymerization rate, and tendency to cross-propagate were slightly affected by the kinds of protonic acids. Under the optimum conditions based on these systematic studies, the sequence transformation from a

copolymer with no ester homosequences to an alternating-like copolymer was achieved by changing the polymerization temperatures from 30 °C to 100 °C. For stricter sequence control, further optimization of the reaction conditions is required, which is currently being investigated by Professor Aoshima's group. In addition, the thermal properties of poly(HBVE-*co*-CL)s were tunable by altering the compositions and sequences of the copolymer. These parameters can be widely designed in the devised copolymerization system. Moreover, this sequence transformation concept is potentially applicable to other copolymerization systems involving unzipping and scrambling, which will increase the obtainable sequence-regulated copolymers from various monomer pairs.

References and Notes

1. Kataoka, K.; Harada, A.; Nagasaki, Y. *Adv. Drug, Deliv. Rev.* **2001**, *47*, 113.
2. Chen, Y.-D.; Cohen, R. *J. Appl. Polym. Sci.* **1977**, *21*, 629.
3. Darling, S. B. *Prog. Polym. Sci.* **2007**, *32*, 1152.
4. Huang, J.; Trner, R. *Polymer* **2017**, *116*, 572.
5. Rzaev, V. M. O. *Prog. Polym. Sci.* **2000**, *25*, 163.
6. Satoh, K.; Matsuda, M.; Nagai, K.; Kamigaito, M. *J. Am. Chem. Soc.* **2010**, *132*, 10003.
7. Matsuda, M.; Satoh, K.; Kamigaito, M.; *J. Polym. Sci., Part A: Polym. Chem.* **2013**, *51*, 1774
8. Hsieh, H. L. *J. Macromol. Sci, Part A: Chem.* **1973**, *7*, 1525.
9. Saegusa, T.; Kobayashi, S.; Kimuura, Y. *Macromolecules* **1977**, *10*, 68.
10. Kanazawa, A.; Aoshima, S. *ACS Macro Lett.* **2015**, *4*, 783.
11. Solleder, S. C.; Schneider, R. V.; Lutz, J.-F. *Macromol. Chem. Phys.* **2015**, *216*, 1498.
12. Hill, S. A.; Gerke, C.; Hartmann, L. *Macromolecules. Chem. – Asian J.* **2018**, *13*, 3611.
13. Cho, I.; Hwang, K. M. *J. Polym. Sci., Part A: Polym. Chem.* **1993**, *31*, 1079.
14. Satoh, K.; Ishizuka, K.; Hamada, T.; Handa, M.; Abe, T.; Ozawa, S.; Miyajima, M.; Kamigaito, M. *Macromolecules*, **2019**, *52*, 3327.
15. Rzaev, Z. M. O. *Prog. Polym. Sci.* **2000**, *25*, 163.
16. Klumperman, B. *Polym. Chem.* **2010**, *1*, 558.
17. Lutz, J.-F.; Schmidt, B. V. K. J.; Pfeifer, S. *Macromol. Rapid Commun.* **2011**, *32*, 127.
18. Higuchi, M.; Kanazawa, A.; Aoshima, S. *ACS Macro Lett.* **2020**, *9*, 77.
19. Szymanski, R. In *Polymer Science: A Comprehensive Reference*; Matyjaszewski, K., Möller, M. Eds.; Elsevier B.V.: Amsterdam, **2012**; Vol. 4.04.
20. Okamoto, Y. *Macromol. Chem., Macromol. Symp.* **1991**, *42*, 117.
21. Smith, M. B.; Kubczyk, M. T.; Graham, E. A. *Tetrahedron*, **2012**, *68*, 7775.
22. Maruyama, K.; Kanazawa, A.; Aoshima, S. *Polym. Chem.* **2019**, *10*, 5304.
23. Okada, M.; Yagi, K.; Sumitomo, H. *Makromol. Chem.* **1973**, *163*, 225
24. Kubisa, P.; Vairon, P. J. In *Polymer Science: A Comprehensive Reference*; Matyjaszewski, K., Möller, M. Eds.; Elsevier B.V.: Amsterdam, **2012**; Vol. 4.10.

25. In the previous study on the cationic polyaddition of HBVE in THF, the M_n values were strongly influenced by the employed protonic acid species. Unlike the present study, polymers with high very MW was obtained.
26. Cyclic acetals with no homopolymerizability such as DMDOP were also inappropriate for the copolymerization. However, an alternating copolymer can be potentially obtained from such types of monomers without the sequence transformation.
27. Duda, A. In *Polymer Science: A Comprehensive Reference*; Matyjaszewski, K., Möller, M. Eds.; Elsevier B.V.: Amsterdam, **2012**; Vol. 4.11.
28. Two sharp peaks were observed in the MWD curve of the transesterification product from the copolymer obtained at 100 °C. The peaks were most likely attributed to the structures with one or two units of HBVE and one unit of CL. The number of HBVE units per block calculated by the ^1H NMR spectrum of the transesterification product was 1.6 (Figure S4), which was higher than the value calculated using the ^1H NMR spectrum of the original copolymer (1.2). The vanishment of the lower-MW compound, which consists of single units HBVE and CL, in the vacuum-drying process may be responsible for the difference.
29. Labet, M.; Thielemans, W. *Chem. Soc. Rev.* **2009**, *38*, 3484.

Supporting Information

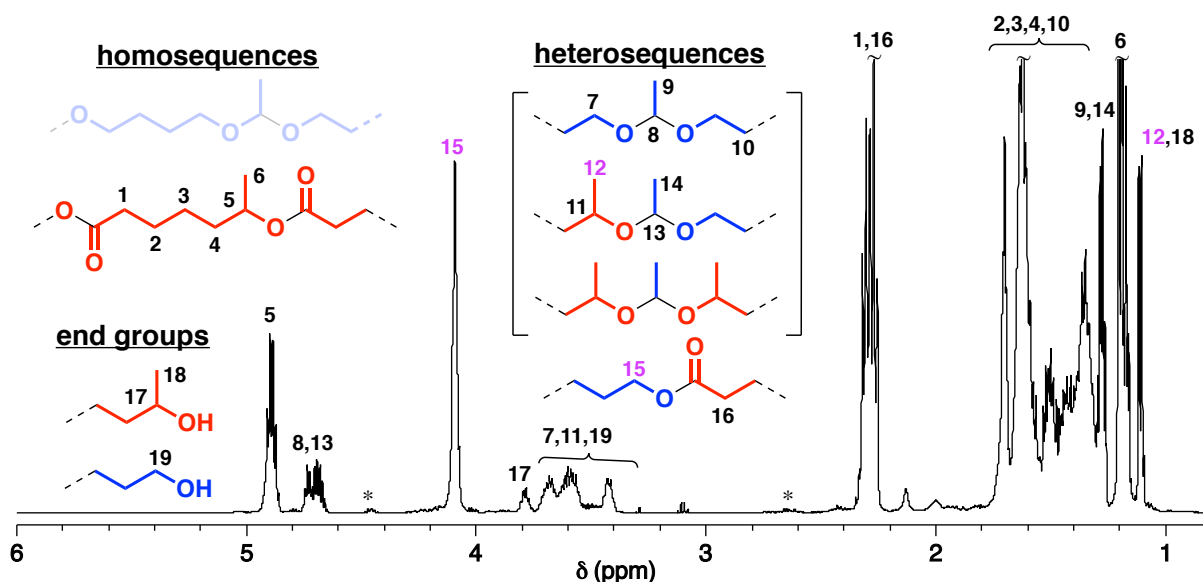


Figure S1. ^1H NMR spectrum of the copolymer obtained in the copolymerization of HBVE and ϵ -HepL; 500 MHz in CDCl_3 at 30 °C; *residual monomer.

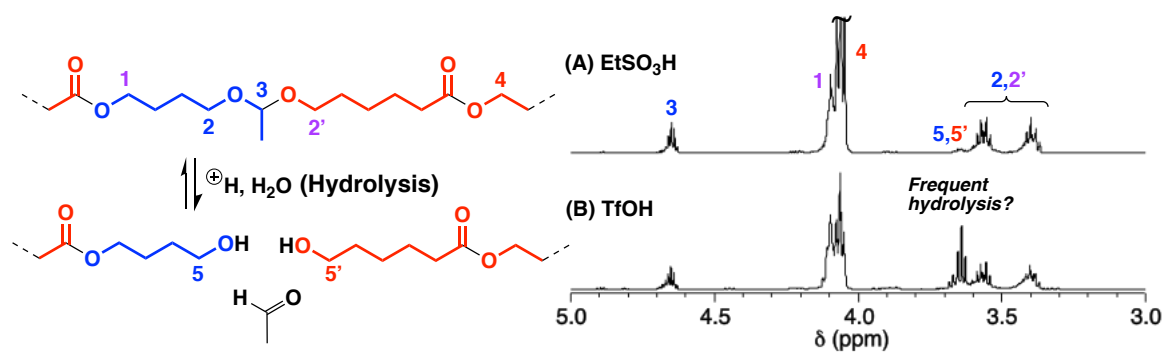


Figure S2. ¹H NMR spectra of poly(HBVE-co-CL) obtained with (A) EtSO₃H (entry 1 in Table 3) and (B) TfOH (entry 5); 500 MHz in CDCl₃ at 30 °C.

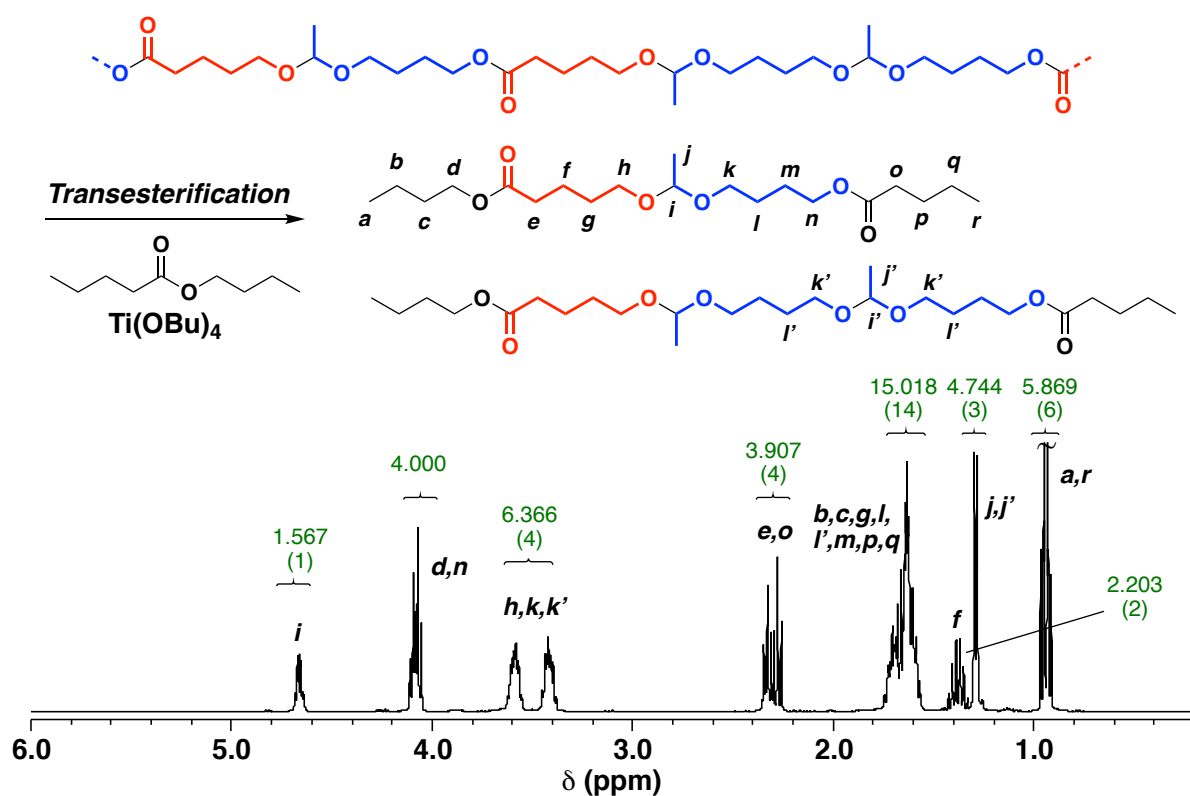


Figure S3. ¹H NMR spectrum of the transesterification products of poly(HBVE-co- δ -VL) obtained at 100 °C (in CDCl₃ at 30 °C; the sample shown in Figure 2A and 2C, below). The number written in green: integral ratio (parenthesis: predicted values for the transesterification product of the completely alternating sequences).

Summary

Copolymers have potentials to exhibit great properties that homopolymer and homopolymer blends cannot achieve, which is based on specific high order structures induced by characteristics of primary structures. In particular, copolymers with specially designed sequences and/or topologies are expected to exert sophisticated properties and functions that are comparable to those of biomacromolecules. However, conventional approaches for the synthesis of such copolymers based on living/controlled polymerization techniques have various intrinsic drawbacks in terms of preciseness, versatility, and facility in synthesis. Considering a huge variety of organic reactions, one can adopt more effective and flexible synthetic methods. Thus, the purpose of this thesis was to develop novel approaches for the synthesis of graft and alternating copolymers by simultaneous copolymerizations via different mechanisms. The acetal exchange reactions, which have many reaction patterns, were employed as the key reaction that provided unconventional copolymerization processes.

Part 1 described a novel strategy for the synthesis of graft copolymers via simultaneously occurring cationic vinyl-addition polymerization of vinyl ethers (VEs), coordination ring-opening polymerization (ROP) of cyclic esters, and the exchange reaction between an alkoxy ligand of the metal catalyst and a VE-derived alkoxy group at the propagating end of poly(VE) (the AGE reactions). Copolymers with a wide variety of grafting density and grafting length were generated in one-shot based on the characteristic polymerization mechanisms

In Chapter 2, concurrent cationic vinyl-addition polymerization of ethyl VE (EVE) and coordination ROP of ϵ -caprolactone (CL) were examined using a mixture of HfCl_4 and $\text{Hf}(\text{O}i\text{Bu})_4$ as catalysts, yielding a graft copolymer consisting of a poly(EVE) main chain with several poly(CL) branched chains via the occurrence of the AGE reactions. An appropriate molar ratio of both catalysts was critical to the simultaneous consumptions of both monomers at comparable rates. By contrast, the copolymerization of isopropyl VE and CL produced a mixture of a diblock copolymer and both homopolymers, instead of a graft copolymer, due to the absence of AGE reactions. These results suggested that the structure of the alkyl side chain of a VE monomer strongly affected the efficiency of the AGE reactions.

In Chapter 3, the author developed a guideline for designing various graft architectures by the mechanisms developed in Chapter 2. The grafting density and grafting length of the copolymers obtained via the mechanisms are determined by the kinetic balances between the two different propagations and the AGE reactions; hence, it was crucial to reveal the factors that are responsible for each reaction rate. The systematic investigations of monomers and catalysts demonstrated that the rates of both propagations strongly depended on the molar ratio of a catalyst mixture, as well as the kinds and concentrations of monomers. By contrast, the frequency of AGE reaction was affected by the tendency to form a VE-type carbocation from the acetal

propagating end and the affinity between alkoxy groups and a metal catalyst. In particular, the AGE reaction occurred very frequently when 2-methoxyethyl VE (MOVE) was used with Ti catalysts. A copolymer with the grafting density of 88% was achieved at a maximum under the optimized conditions. In addition, the obtained poly(MOVE-*graft*-CL) functioned as a very effective dispersing agent for TiO₂ in toluene.

Part 2 dealt with the design of various sequences by the cationic ring-opening copolymerization of cyclic acetals and cyclic esters. In particular, a unique method for the synthesis of an alternating copolymer was developed by utilizing tandem reactions of unzipping and scrambling.

In Chapter 4, the cationic ring-opening copolymerization of 2-methyl-1,3-dioxepane (MDOP), which was formed via the isomerization of 4-hydroxybutyl VE (HBVE) in the early stages of polymerization, and CL was examined using EtSO₃H as a catalyst. MDOP was copolymerized with CL even below the equilibrium monomer concentration of MDOP, which indicated that the unzipping of MDOP was suppressed when the ester bond of a CL unit existed next to the oxonium chain end. Copolymers with various sequences, such as a copolymer with no HBVE homosequences, no CL homosequences, and multiblock sequences, were obtained by manipulating the initial monomer concentrations. More interestingly, a copolymer with no CL homosequences was transformed into an “alternating” copolymer, by removing MDOP monomers from the system using a vacuum pump. The concurrently occurring unzipping and scrambling of the acetal moieties were responsible for the unprecedented sequence transformation.

Chapter 5 demonstrated the generality of the sequence transformation concept developed in Chapter 4. In particular, the sequence transformation to an alternating copolymer was attempted on heating, instead of removing cyclic acetal monomers from the system using a vacuum pump. To this end, crossover reactions were required to occur frequently from cyclic esters to cyclic acetals. Screening of monomers and catalysts demonstrated that the combination of HBVE, δ -valerolactone (δ -VL), and EtSO₃H met the requirement. The copolymerization of HBVE (3.50 M) and δ -valerolactone (δ -VL; 0.50 M) with EtSO₃H at 30 °C yielded a copolymer with no δ -VL homosequences, which was successfully transformed into an alternating-like copolymer on heating to 100 °C.

In conclusion, this thesis developed novel approaches for the synthesis of graft and alternating copolymers by utilizing simultaneous polymerizations with different mechanisms and acetal exchange reactions. The facile and versatile design of copolymer structures was achieved by simultaneously controlling multiple reactions. The author hopes that the research conducted in this thesis will be a clue for the development of future-generation smart polymerization techniques.

List of Publications

1. Motoki Higuchi, Arihiro Kanazawa, Sadahito Aoshima
“Concurrent Cationic Vinyl-Addition and Coordination Ring-Opening Copolymerization via Orthogonal Propagation and Transient Merging at the Propagating Chain End”
ACS Macro Lett. **2017**, *6*, 365–369.
(Corresponding to Chapter 2)
2. Motoki Higuchi, Arihiro Kanazawa, Sadahito Aoshima
“Design of Graft Architectures via Simultaneous Kinetic Control of Cationic Vinyl-Addition Polymerization of Vinyl Ethers, Coordination Ring-Opening Polymerization of Cyclic Ester, and Merging at the Propagating Chain End”
to be submitted.
(Corresponding to Chapter 3)
3. Motoki Higuchi, Arihiro Kanazawa, Sadahito Aoshima
“Tandem Unzipping and Scrambling Reactions for the Synthesis of Alternating Copolymers by the Cationic Ring-Opening Copolymerization of a Cyclic Acetal and a Cyclic Ester”
ACS Macro Lett. **2020**, *9*, 77–83.
(Corresponding to Chapter 4)
4. Motoki Higuchi, Arihiro Kanazawa, Sadahito Aoshima
“Equilibrium Monomer Concentration-Dependent Sequence Control of Copolymer Chains via Temperature Changes in Cationic Ring-Opening Copolymerization of Cyclic Acetal and Cyclic Esters”
to be submitted.
(Corresponding to Chapter 5)

